

Proxy Reconstruction of Cenozoic Arctic Ocean Sea-Ice History – from IRD to IP₂₅ –*

by Ruediger Stein¹, Kirsten Fahl¹ and Juliane Müller¹

Abstract: This review paper focusses on reconstructions of the long- and short-term history of past Arctic Ocean sea-ice cover. Based on commonly used sedimentological, geochemical and micropaleontological proxies (ice-rafted debris (IRD), mineralogical composition of terrigenous sediment fraction, and abundances of specific diatoms and foraminifers), three examples of reconstructions of glacial history, sea-ice cover and surface-water characteristics are presented and discussed: (1) the onset Arctic Ocean sea-ice cover near 47 Ma and its long-term variability through Cenozoic times; (2) the Quaternary glacial/interglacial variability in Arctic Ocean ice-rafting and its relationship to sea-ice and ice-sheet history; and (3) Last Glacial Maximum (LGM), Deglacial to Holocene changes in Arctic Ocean sea-ice cover and ice-sheet decay.

In the second part of this paper we concentrate on Arctic Ocean sea-ice reconstructions, using a recently developed biomarker approach that is based on the determination of sea-ice diatom-specific highly-branched isoprenoids with 25 carbon atoms (IP₂₅) and IP₂₅ in combination with phytoplankton biomarkers (PIP₂₅). The diene/ IP₂₅ ratio might give additional information about sea-surface temperature (SST) in the low temperature Arctic environment. The high potential of these novel biomarker proxies to improve reconstructions of paleo-sea-ice cover and its variability through time is demonstrated in three examples: (a) the sea-ice variability in Fram Strait over the last 30 ka, (b) the deglacial/Holocene variability of central Arctic sea-ice cover with special emphasis on the Younger Dryas Cooling Event, and (c) a comparison of historical sea-ice observations off northern Iceland over the last millennium and a corresponding high-resolution IP₂₅ record.

In a pilot study carried out in a sediment core from the Barents Sea continental slope we were able to prove for the first time that IP₂₅ is even preserved in Arctic Ocean sediments as old as 130 to 150 ka (MIS 6), i.e., IP₂₅ can be used for reconstruction of sea-ice variability during older glacial/interglacial intervals (MIS 6/MIS 5).

In order to establish the IP₂₅ approach as a key proxy for reconstruction of past Arctic Ocean sea-ice conditions, more basic information about production, degradation and preservation/burial of the IP₂₅ signal is still needed. Furthermore, the hypothesis that the diene/IP₂₅ ratio might be used as reliable proxy for SST reconstructions in the low temperature Arctic environments has to be verified by a ground-truth study including the IP₂₅ and diene data as well as independent SST proxies like alkenone-derived SST. All these data should be obtained in future investigations of sea-ice, water column, and sediment-trap samples as well as surface sediments and sediment cores with large spatial coverage from different environments of the entire Arctic Ocean.

Zusammenfassung: Meereis ist ein wichtiges Charakteristikum des Arktischen Ozeans und von großer Bedeutung für das globale Klimasystem. Um die Veränderungen der Meereisdecke in jüngster Vergangenheit besser verstehen zu können, ist die Untersuchung der Meerausdehnung in der geologischen Vergangenheit und seiner zeitlichen Variabilität mittels meeresgeologischer Stellvertreterdaten (Proxys) von großem Nutzen. In drei Beispielen werden im ersten Teil Rekonstruktionen der Meereisverteilung und deren zeitliche Änderungen (1) im Verlauf des Känozoikums, (2) im Spätquartär und (3) für den Zeitabschnitt vom Letzten Glazialen Maximum bis heute vorgestellt, die auf der Anwendung herkömmlicher sedimentologischer und mineralogischer Proxys basiert. Hierbei ist insbesondere der Gehalt an eistransportierter Grobfraction – “ice-rafted debris” oder “IRD” – als Basisparameter hervorzuheben. Im zweiten Teil dieser Arbeit werden neue Biomarkerproxys für Meereis (IP₂₅ und PIP₂₅) und Temperatur des Oberflächenwassers (Dien/IP₂₅-Verhältnis) in drei Beispielen diskutiert: (a) die Meereisverteilung und Meer eisvariabilität in der Framstraße während der letzten 30 ka; (b) die postglaziale Meereisva-

riabilität im zentralen Arktischen Ozean vom Bølling-Allerød über Jüngere Dryas bis Heute und (c) ein Vergleich der Meereisbeobachtungen für den historischen Zeitabschnitt 800–1950.

In einer Pilotstudie wird erstmals IP₂₅ in arktischen Sedimenten mit einem Alter >30 ka (MIS 6–MIS 1 oder 150–0 ka) nachgewiesen. Um diese neuen Biomarkerproxys als verlässliche Parameter für die quantitative Rekonstruktion von Meereisverbreitung (und Oberflächenwassertemperatur) im Arktischen Ozean zu etablieren, müssen weitere grundlegende Datensätze mit großer räumlicher Verteilung und unter Einbezug von Untersuchungen an Meereisproben, Sedimentfallen, Oberflächensedimenten und Sedimentkernen gewonnen werden.

INTRODUCTION AND BACKGROUND

One of the most important characteristics of the modern Arctic Ocean is the sea-ice cover with its strong seasonal variability in the marginal (shelf) seas (Fig. 1). Satellite data have shown that the area of sea ice decreases from roughly 14–15 million km² in March to 6–7 million km² in September, as much of the first-year ice melts during the summer (GLOERSEN et al. 1992, CAVALIERI et al. 1997, JOHANNESSEN et al. 2004). The area of multi-year sea ice, mostly over the Arctic Ocean basins and the Canadian polar shelf, is about 4 to 5 million km² (e.g., JOHANNESSEN et al. 1999, NGHIEM et al. 2007). In the geological past, changes in sea-ice cover may have been even more extreme ranging from totally ice-free to permanently ice-covered conditions. These variations occurred on very long time scales (e.g., the Paleogene Greenhouse/Icehouse transition) as well as glacial/interglacial and shorter time scales, and were often coinciding with the waxing and waning of circum-Arctic ice sheets (Fig. 1, e.g., SVENDSEN et al. 2004, for reviews see STEIN 2008, POLYAK et al. 2010).

Sea ice, the main focus of this paper, has a large influence on the environment of the Arctic Ocean itself, the Earth system on a global scale, and climate change. Sea-ice formation is strongly controlled by freshwater supply. Freshwater is essential for the maintenance of the low-salinity layer of the central Arctic Ocean and, thus, contributes significantly to the strong stratification of the near-surface water masses, encouraging sea-ice formation (e.g., AAGAARD & CARMACK 1989, MACDONALD et al. 2004). Changes in the freshwater balance would influence the extent of sea-ice cover. The melting and freezing of sea ice results in distinct changes in the surface albedo, the energy balance, and the temperature and salinity structure of the upper water masses. The albedo of open water is as low as 0.10, whereas the sea-ice albedo ranges between 0.6 and 0.8 (Fig. 2, BARRY 1996). Therefore, up to eight times as much of the incoming shortwave radiation is reflected from the ice surfaces as compared to open water, resulting in lower surface temperatures. Furthermore, the sea-ice cover strongly affects the biological productivity, as a more closed sea-ice cover restricts primary production due to low light influx in

* Extended version of an oral presentation at the “20 year North Pole anniversary symposium” 7 September 2011 at IfM-GEOMAR, Kiel.

¹ Alfred Wegener Institute for Polar and Marine Research, Am Alten Hafen 26, D-27568 Bremerhaven, Germany.

Manuscript received 11 April 2012, accepted in revised form 13 July 2012.

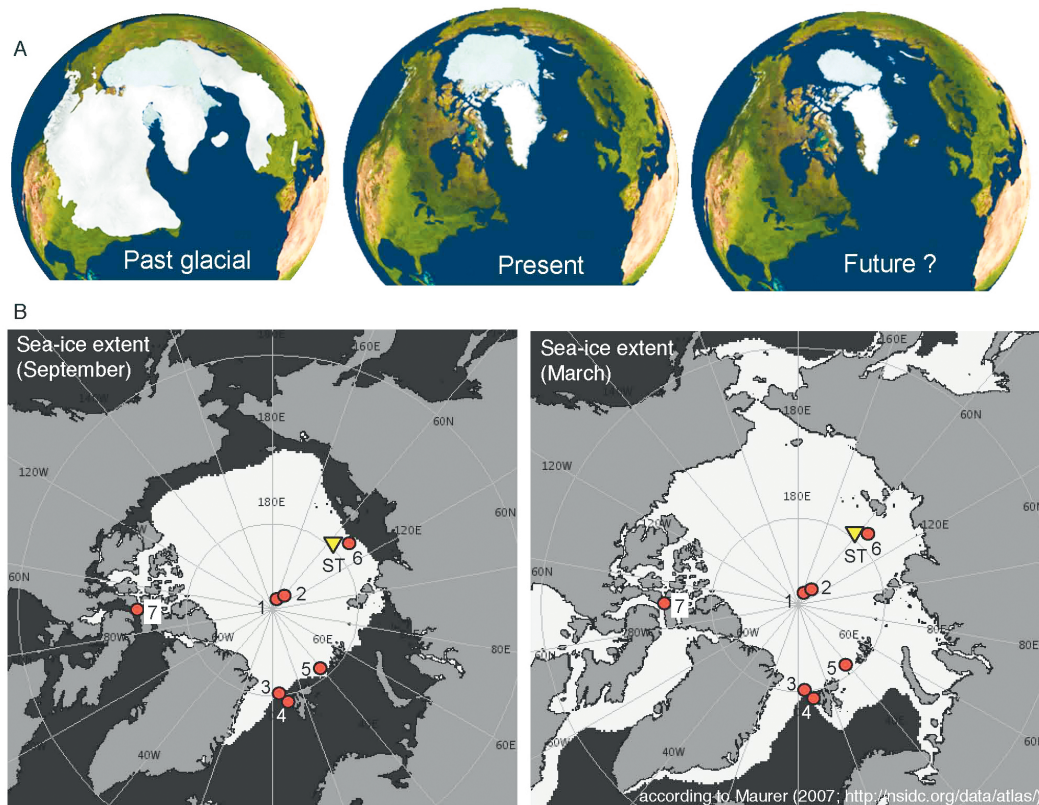


Fig. 1: (A): Distribution of Northern Hemisphere ice sheets and sea ice during past glacials (left), Present (middle) and a possible scenario of the future (right); (Courtesy Martin Jakobsson, Stockholm University, 2012). (B): Maps showing the average distribution of sea ice in the Arctic Ocean in September 1979–2004 (left) and March 1979–2005 (right). Numbers and letters indicate site locations of sediment traps and sediment cores presented and discussed in the text: ST = sediment trap LOMO-2; 1 = IODP-ACEX drill site; 2 = core PS2185; 3 = PS2837-2; 4 = MSM5/5-723-2; 5 = PS2138-1; 6 = PS2458-4; 7 = core ARC-3.

Abb. 1: (A): Verteilung von Meereis und Eisschilden während quartärer Eiszeiten (links), heute (Mitte) und mögliches Szenario in der Zukunft (rechts). (B links): Mittlere minimaler Meereisausbreitung im Spätsommer (September 1979–2004); (B rechts): mittlere maximale Meereisverbreitung im Spätwinter (März) der Jahre 1979–2005). ST und Ziffern 1 bis 6 = im Text diskutierte Lokationen.

the surface waters (Fig. 2). Owing to its light limitation and sea-ice cover, the central Arctic Ocean is the least productive region of the world's oceans, whereas in the marginal ice zone high primary productivity may be reached (SAKSHAUG 2004, WASSMANN et al. 2004, WASSMANN 2011).

Freshwater and sea ice are exported from the Arctic Ocean through the Fram Strait into the North Atlantic. The interplay of the cold Arctic freshwater-rich surface-water layer and its ice cover with the relatively warm and saline Atlantic water is important for the renewal of deep waters driving the global thermohaline circulation (THC) (e.g., BROECKER 1997, 2006, CLARK et al. 2002). Because factors such as the global THC, sea-ice cover and Earth's albedo have a strong influence on the earth's climate system, climate change in the Arctic could cause major perturbations to the global environment.

Over the last decades, the extent and thickness of Arctic sea ice has changed dramatically (Fig. 3) (e.g., JOHANNESSEN et al. 2004, ACIA 2004, 2005, FRANCIS et al. 2005, SERREZE et al. 2007, STROEVE et al. 2007). According to STROEVE et al. (2007), the reduction in the extent of Arctic sea ice observed from 1953 to 2006 is -7.8 ± 0.6 % per decade, three times larger than the multi-model mean trend of -2.5 ± 0.2 % per decade. For the shorter, yet more reliable period of observations based on modern satellite records (1979–2006), both the observed (-9.1 ± 1.5 % per decade) and multi-model mean trend (-4.3

± 0.3 % per decade) are larger. The reduction of future sea-ice, however, may be even more rapid. A record-low in minimum sea-ice cover was observed in September 2007, which is about 40 % less than that of 1979, the start of sea-ice observation by satellites (Fig. 3, KERR 2007). Such a minimum was forecasted by modelling to occur in the middle of this century (Fig. 3, JOHANNESSEN et al. 2004, STROEVE et al. 2007).

Observed changes not only included a reduction in total area covered by sea ice (MASLANIK et al. 1996, JOHANNESSEN et al. 1999, 2004, PARKINSON et al. 1999, VINNIKOV et al. 1999, LEVI 2000), but also an increase in the length of the ice melt season (SMITH 1998, STABENO & OVERLAND 2001, RIGOR et al. 2002), a loss of multiyear ice (NGHIEM et al. 2007) and a general decrease in the thickness of ice over the central Arctic Ocean (ROTHROCK et al. 1999, KWOK & ROTHROCK 2009).

Although there is a general consensus that polar regions – and especially the Arctic Ocean and surrounding areas – are (in real time) and were (over historic and geologic time scales) subject to rapid and dramatic change, the causes of the recent changes are a subject of intense scientific and environmental debate. As outlined by JOHANNESSEN et al. (2004), it remains open to debate whether the warming in recent decades is an enhanced greenhouse-warming signal or (at least partly) natural decadal and multidecadal climate variability (POLYAKOV & JOHNSON 2000, POLYAKOV et al. 2002). Here, high-resolution paleo-

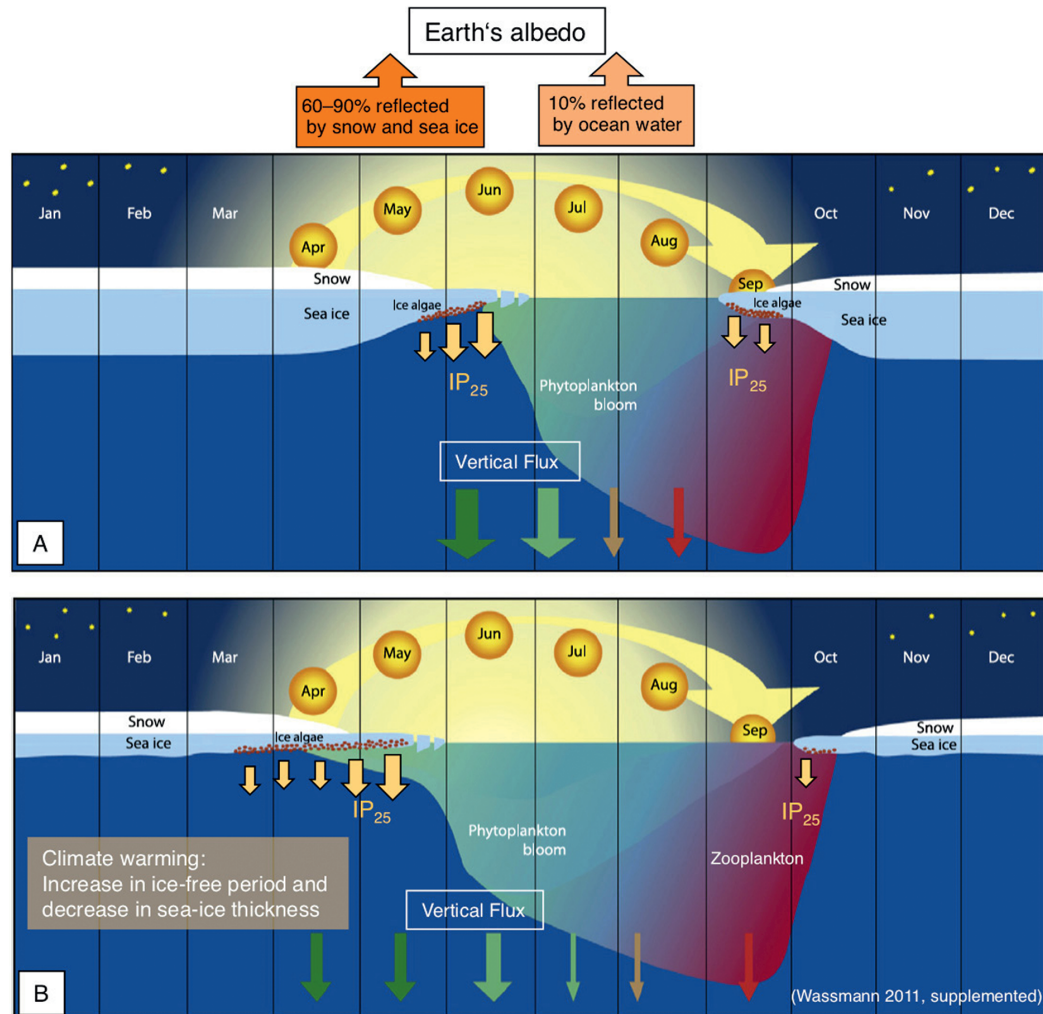


Fig. 2: (A) Schematic illustration of principal processes controlling productivity and carbon flux in the seasonal ice zone. The dark period, height of the sun and changing thickness of snow and ice over the year as well as phytoplankton, zooplankton, and sea-ice algae productivity are indicated. Arrows indicate the changing dominance of autotrophic (green) and heterotrophic (red) processes in the euphotic zone. Flux of sea-ice algae and IP₂₅ are indicated by yellow arrows. In addition, Earth's albedo values for snow and sea-ice as well as open ocean conditions are shown (BARRY 1996). (B) Climate warming may result in an increase of the ice-free period and a decrease in sea-ice thickness. Sea-ice algae can start to grow already from mid March, provided that snow cover is not too thick.

Abb. 2: (A) Schematische Darstellung der grundlegenden Prozesse, welche Produktion und Flux von Phytoplankton, Zooplankton und Eisalgen mit Eisalgenproxy "IP₂₅" im jahreszeitlichen Gang von Licht und Meereis beeinflussen. Zusätzlich sind Albedo-Werte für Schnee und Eis gegenüber denen von eisfreier Ozeanoberfläche angegeben (BARRY 1996). (B) Zeigt mögliche Auswirkungen und Veränderungen einer Klimaerwärmung mit verminderter Eisausdehnung und Eisdicke.

climatic records going back beyond the timescale of direct measurements can help reduce some of the uncertainties in the debate of recent climate change. In this context, however, not only high-resolution studies of the most recent (Holocene) climate history are of importance, but also detailed studies of the earlier Earth history characterized by a much warmer (Greenhouse-type) global climate.

The instrumental records of temperature, salinity, precipitation and other environmental observations span only a very short interval (<150 years) of Earth's climate history and provide an inadequate perspective of natural climate variability, as they are biased by an unknown amplitude of anthropogenic forcing. Generally, paleoclimate records document the natural climate, rates of change and variability prior to anthropogenic influence. Paleoclimate reconstructions can be used to assess the sensitivity of the Earth's climate system to changes of different forcing parameters (e.g. CO₂) and to test the reliability of climate models by evaluating their performance under condi-

tions very different from the modern climate. Precise knowledge of past rates and scales of climate change are the only means to separate natural and anthropogenic forcings and will enable us to further increase the reliability of prediction of future climate change. Thus, understanding the mechanisms of natural climate change is one of the major challenges for mankind in the coming years. In this context, the polar regions certainly play a key role, and detailed climate records from the Arctic Ocean spanning time intervals from the Paleogene Greenhouse world to the Neogene-Quaternary Icehouse world (Fig. 4) will give new insight into the functioning of the Arctic Ocean within the global climate system. Here, especially the synchronous versus asynchronous histories of ice-sheet and sea-ice development in the north- and southpolar regions are of special interest.

This paper deals with proxy reconstructions of the long- and short-term history of past circum-Arctic ice sheets and sea-ice cover – with a focus on the latter. Starting with examples of

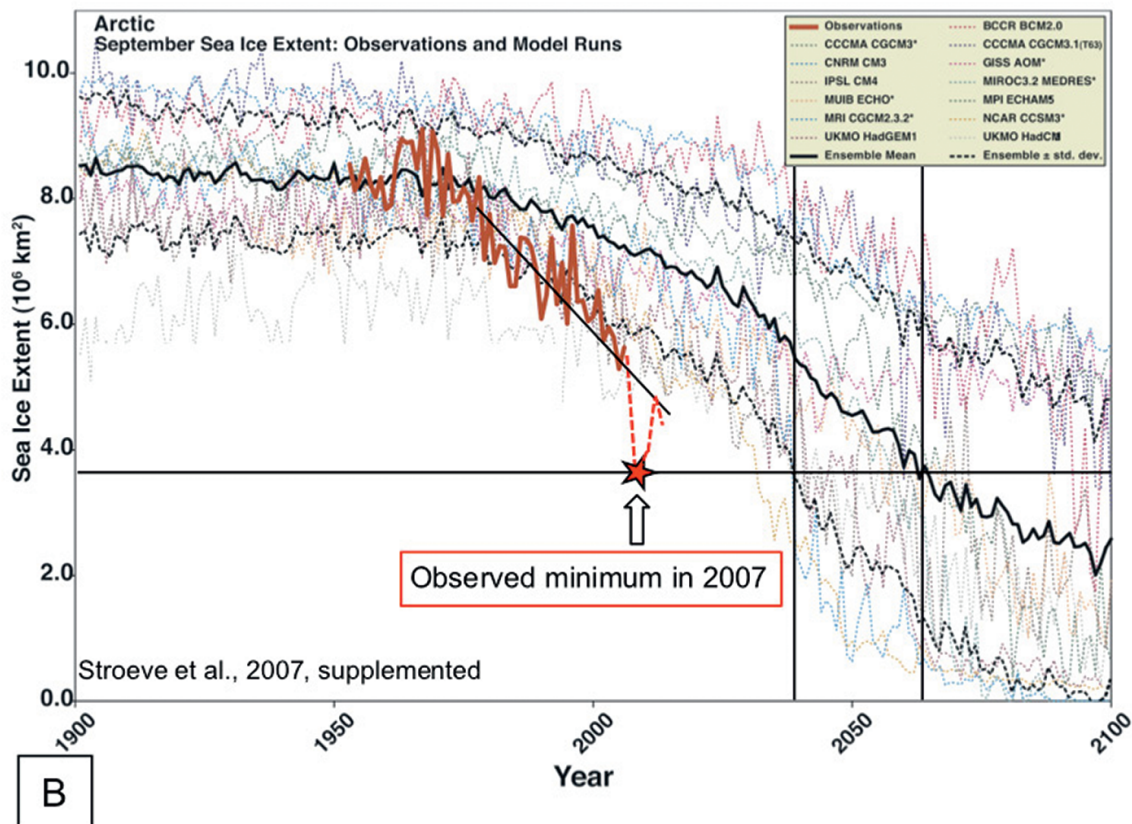
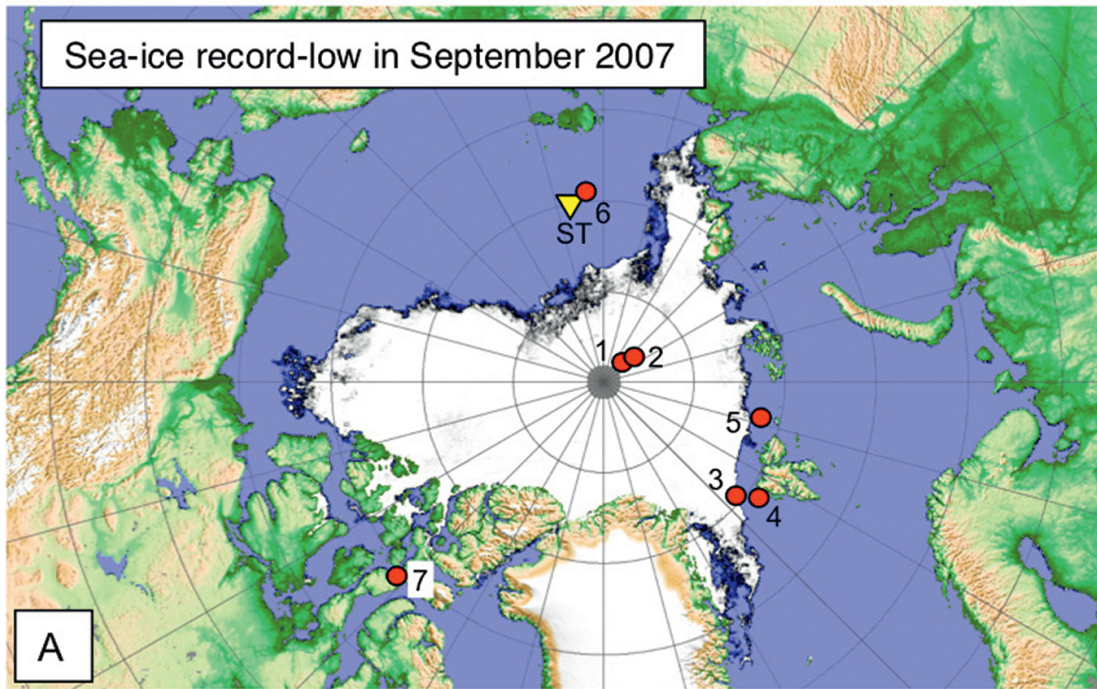
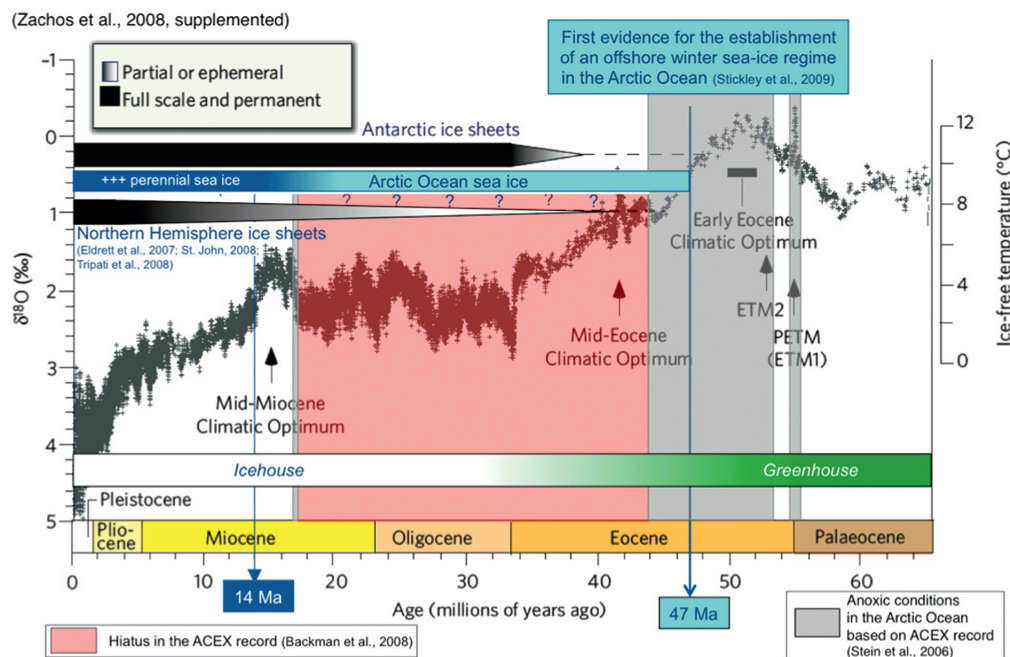


Fig. 3: (A): Distribution of sea-ice cover in the Arctic Ocean on September 12, 2007 (<<http://iup.physik.uni-bremen.de:8084/amsr/amsre.html>>) and site locations discussed in the text: ST = Sediment trap LOMO-2; sediment cores: 1 = IODP-ACEX drill site; 2 = core PS2185-6; 3 = core PS2837-2; 4 = core MSM5/5-723-2; 5 = core PS2138-1; 6 = core PS2458-4; 7 = core ARC-3. (B) Arctic September sea-ice extent ($\times 10^6 \text{ km}^2$) from observations (thick red line) and 13 IPCC AR4 climate models together with the multi-model ensemble mean (solid black line) and standard deviation (dotted black lines). The absolute minimum of 2007 is highlighted by asterisk.

Abb. 3: (A): Meereisverbreitung im Arktischen Ozean im September 2007 (<<http://iup.physik.uni-bremen.de:8084/amsr/amsre.html>>) und Lokationen der im Text diskutierten Sedimentfallen und Sedimentkerne: ST = Sedimentfalle LOMO-2. Sedimentkerne: 1 = IODP-ACEX Bohrlokation, 2 = PS2185-6, 3 = PS2837-2, 4 = MSM5/5-723-2, 5 = PS2138-1, 6 = PS2458-4, 7 = ARC-3. (B) Meereisausdehnung im Arktischen Ozean für September (10^6 km^2) für die Zeit 1900 bis 2100, d.h. Beobachtungen und Messwerte (Kurve rot), Mittelwert der Ergebnisse unterschiedlicher Klimamodelle (Kurve fett schwarz) mit Standardabweichung (punktierter schwarze Kurven).

Fig. 4: Smoothed global benthic foraminifer $\delta^{18}\text{O}$ time series showing the long-term cooling and the Greenhouse/Icehouse transition through Cenozoic times. The occurrence of Cenozoic ice sheets on the Northern and Southern Hemisphere and Arctic sea-ice are shown. The hiatus in the ACEX record is indicated by a red bar as based on the age model by BACKMAN et al. 2008 (for alternate age model see Fig. 5); periods with anoxic water mass conditions are highlighted by grey bars (STEIN et al. 2006).

Abb. 4: Globale $\delta^{18}\text{O}$ -Kurve von benthischen Foraminiferen, welche die langzeitliche Abkühlung und den Wechsel von Treibhaus- zu Eishausbedingungen im Verlauf des Känozoikums anzeigen. Die Ausbreitung von Eisschilden auf der Nord- und Südhemisphäre sowie das Vorkommen von Meereis und anoxischen Bedingungen im Arktischen Ozean sind markiert.



paleoenvironmental reconstructions based on more commonly used sedimentological, micropaleontological and geochemical proxies, the second part of the paper highlights recently developed novel biomarker proxies indicative for modern and past changes in sea-ice cover. These new proxies may allow a more quantitative reconstruction of sea-ice cover and potentially may provide some information about past sea-ice thicknesses.

LONG- AND SHORT-TERM CHANGES IN SEA-ICE COVER: RECONSTRUCTIONS FROM COMMON GEO-PROXIES

Sediment-laden or “dirty” sea ice is a common phenomenon in the Arctic Ocean and its marginal seas and an important transport agent for terrigenous sediments (e.g., PFIRMAN et al. 1989, REIMNITZ et al. 1993b, NÜRNBERG et al. 1994, EICKEN et al. 1997, 2005, DETHLEFF et al. 2000). In areas of sea-ice melting, sediment particles are released and deposited at the sea floor, contributing significantly to the present and past Arctic Ocean sedimentary budget. This sea-ice sediment – or “ice-rafted debris (IRD)” – mainly consists of terrigenous material with clay minerals, quartz, and feldspars as the main components (NÜRNBERG et al. 1994). The mineralogy of sea-ice sediments may be very variable in time and space. Thus, studies of the mineralogical composition may allow the identification of source areas for sea-ice transported sediments and, based on these data, the reconstruction of past and present transport pathways (e.g. NÜRNBERG et al. 1994, WAHSNER et al. 1999, DARBY 2003, STEIN 2008 for review). IRD however, can also be transported by icebergs. If IRD is related to iceberg transport and not sea ice, the IRD proxy record records the existence of extended continental ice sheets reaching the shelf-break. Therefore, a method of distinguishing between sea-ice and iceberg transport is required for paleoenvironmental reconstructions based on the analysis of IRD.

A first-order proxy to discriminate between sea-ice and iceberg-rafted deep-sea sediments is the grain-size distribu-

tion. It is generally accepted that very coarse-grained material $>250\ \mu\text{m}$ (coarse-sand-, very-coarse-sand-, gravel- and pebble-sized particles), are mainly restricted to iceberg transport whereas the dominance of finer-grained (silt and clay sized) sediments are more typical for sea-ice transport (e.g., CLARK & HANSEN 1983, NØRGAARD-PEDERSEN et al. 1998, SPIELHAGEN et al. 2004, DETHLEFF 2005). Grain-size distribution by itself, however, has to be interpreted with caution as other processes (e.g., ocean currents) may overprint the ice-rafted distribution (MANIGHETTI & MCCAVE 1995, HASS 2002).

A large number of studies on the paleodistribution of sea ice are commonly based on sedimentological, mineralogical, and geochemical data (e.g., SPIELHAGEN et al. 1997, 2004, KNIES et al. 2001, DARBY 2003, NØRGAARD-PEDERSEN et al. 2003, POLYAK et al. 2010) and microfossils such as diatoms, dinoflagellates, ostracods, and foraminifers (e.g., CARSTENS & WEFER 1992, KOC et al. 1993, MATTHIESSEN et al. 2001, CRONIN et al. 2010, for most recent review see POLYAK et al. 2010). In particular, sea-ice associated organisms like pennate ice diatoms, are frequently used for reconstructing present and past sea-ice conditions (e.g., KOC et al. 1993, STICKLEY et al. 2009). However, it has also been shown that the preservation of fragile siliceous diatom frustules can be relatively poor in surface sediments from the Arctic realm and the same is also true (if not worse) for calcareous-walled microfossils, thus limiting their applicability (STEINSUND & HALD 1994, SCHLÜTER & SAUTER 2000, MATTHIESSEN et al. 2001). In contrast, radiolarians might be better preserved than diatoms but few data have been published yet (e.g., KRUGLIKOVA et al. 2009). A multi-proxy approach, considering sediment texture in combination with lithology and sediment provenance as well as micropaleontological and geochemical data indicative for surface-water characteristics certainly provides a much sounder interpretation of sea-ice versus iceberg rafting and reconstruction of past sea-ice conditions.

As complimentary approach to reconstructions from marine sediment cores, past sea-ice conditions may also be inferred

from driftwood found on Arctic beaches (e.g., DYKE et al. 1997, BENNIKE 2004, ENGLAND et al. 2008, FUNDER et al. 2009). This approach is based on the assumptions that (1) ice is essential for long-distance transport of the wood, which otherwise becomes water-logged and sinks after about a year, and (2) ice-free coastal areas exist to allow the driftwood to strand. JAKOBSSON et al. (2010) have summarized results from different approaches (including results from marine sediment core as well as driftwood studies) to provide a more holistic picture of past Arctic sea-ice conditions during the last about 15 Cal. kyrs. BP (see Fig. 21 and discussion below).

In the following, three example reconstructions of the glacial history, sea-ice cover and surface-water characteristics are presented using common sedimentological, mineralogical, geochemical and micropaleontological proxies. These are:

- Onset and long-term variability of Cenozoic Arctic Ocean ice-rafting: sea-ice versus iceberg transport
- Quaternary glacial / interglacial variability in Arctic Ocean ice-rafting
- LGM, deglacial to Holocene changes in Arctic Ocean sea-ice cover and ice-sheet decay.

Onset and long-term variability of Cenozoic Arctic Ocean ice-rafting: sea-ice versus iceberg transport

During the Arctic Coring Expedition “ACEX” (IODP Expedition 302), the first scientific drilling was carried out successfully in the permanently ice-covered central Arctic Ocean. During ACEX, 428 m of Quaternary, Neogene, Paleogene, and Campanian sediments were penetrated on the crest of Lomonosov Ridge close to the North Pole (Fig. 5, BACKMAN et al. 2006, 2008, MORAN et al. 2006). Numerous outstanding results dealing with the Arctic Ocean climate history came out of studies of ACEX material (BACKMAN & MORAN 2008). Unfortunately, the ACEX record contains a large hiatus, probably spanning the time interval from late Eocene to middle Miocene (Fig. 5, BACKMAN et al. 2008, O’REGAN 2011). This is a critical time interval, as it spans the time when prominent changes in global climate took place during the transition from the early Cenozoic Greenhouse world to the late Cenozoic Icehouse world (FIG. 4; ZACHOS et al. 2008).

Throughout the upper about 195 m of Miocene-Pleistocene siliclastic silty clays of the ACEX sequence, isolated pebbles and granules interpreted as IRD or “dropstones”, were found together with sand lenses, but unexpectedly also in ~50 m of the underlying middle Eocene biosiliceous silty clays and oozes (Fig. 6, BACKMAN et al. 2006). The deepest dropstone, a gneiss of 1 cm in diameter, was found at about 240 m

composite depth (mcd). This dropstone was recovered from an undisturbed section of core and was not reworked or moved downward from higher in the sedimentary section. The location of the ACEX site during this time period, although probably in shallow water (~200 m), was distal from the Siberian continental coast and isolated from it by the Gakkel Ridge, suggesting ice transport as the most probable process (MORAN et al. 2006). This dropstone was suggested to represent the onset of Northern Hemisphere glaciation at about 46 million years BP (Ma) (MORAN et al. 2006, using the revised biostratigraphically-derived age model of BACKMAN et al. 2008), i.e., sea-ice formation and/or iceberg transport took place ~30 my earlier than previously thought. When using the alternate chronology based on osmium isotopes (POIRIER & HILLAIRE-MARCEL 2011), the age of the occurrence of the first dropstone at 240 mcd would become about three million years younger (~43 Ma, Fig. 5).

Eocene-age dropstones in the ACEX record provided strong direct evidence for the presence of ice, but are stratigraphically discontinuous, and only about 60 granules and pebbles of ~0.2 to 3.0 cm in diameter were visually identified between 0–240 mcd (BACKMAN et al. 2006). In order to get a more continuous record of the ice-rafting history of the central Arctic Ocean, ST. JOHN (2008) studied the terrigenous coarse (IRD) fractions >150 and >250 μm throughout the entire depth interval 0–275 mcd of the ACEX sequence in much more detail (Fig. 6). Along with information on grain size, composition, and mass accumulation rates of IRD, SEM imaging of represen-

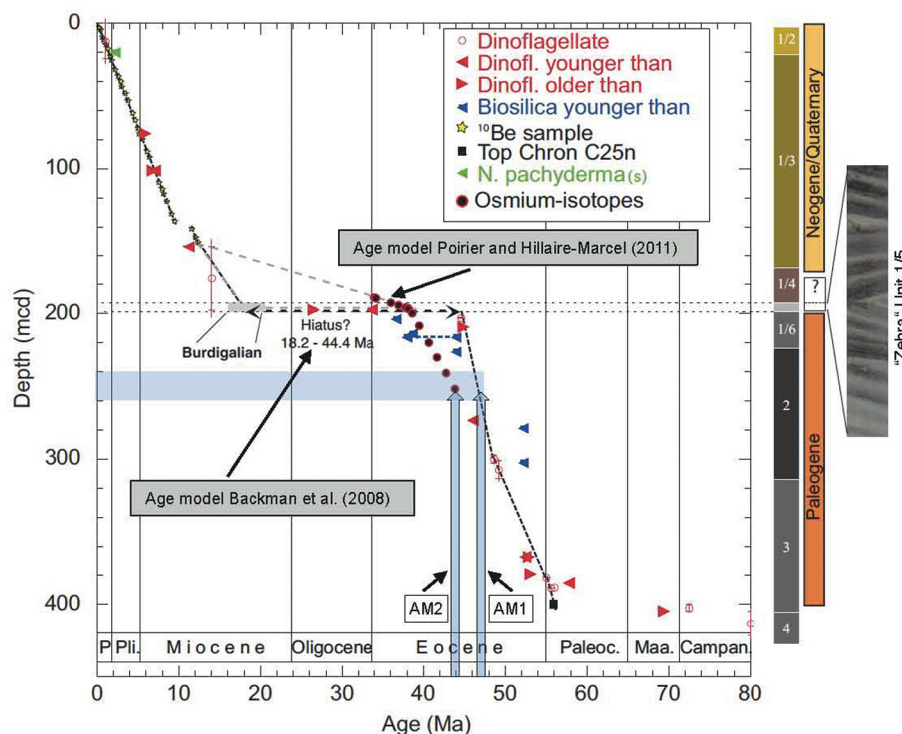


Fig. 5: Age-depth diagram and main lithological units of the ACEX section, based on the biostratigraphic age model AM1 by BACKMAN et al. (2008). Included is chronology AM2 based on osmium isotopes (POIRIER & HILLAIRE-MARCEL 2011). First occurrences of IRD at 240–260 mcd are marked as light blue horizontal bar. Different ages of first occurrence of IRD, obtained by age models AM1 and AM2 are indicated by light blue arrows (from O’REGAN 2011, supplemented).

Abb. 5: Alters-Tiefen-Diagramm AM1 (BACKMAN et al. 2008) und lithologische Einheiten der ACEX-Bohrung. Beigefügt das Altersmodell AM2 nach POIRIER & HILLAIRE-MARCEL (2011). Hellblaue Pfeile = erstes Einsetzen von IRD zwischen 240–260 mcd (ergänzt nach O’REGAN 2011).

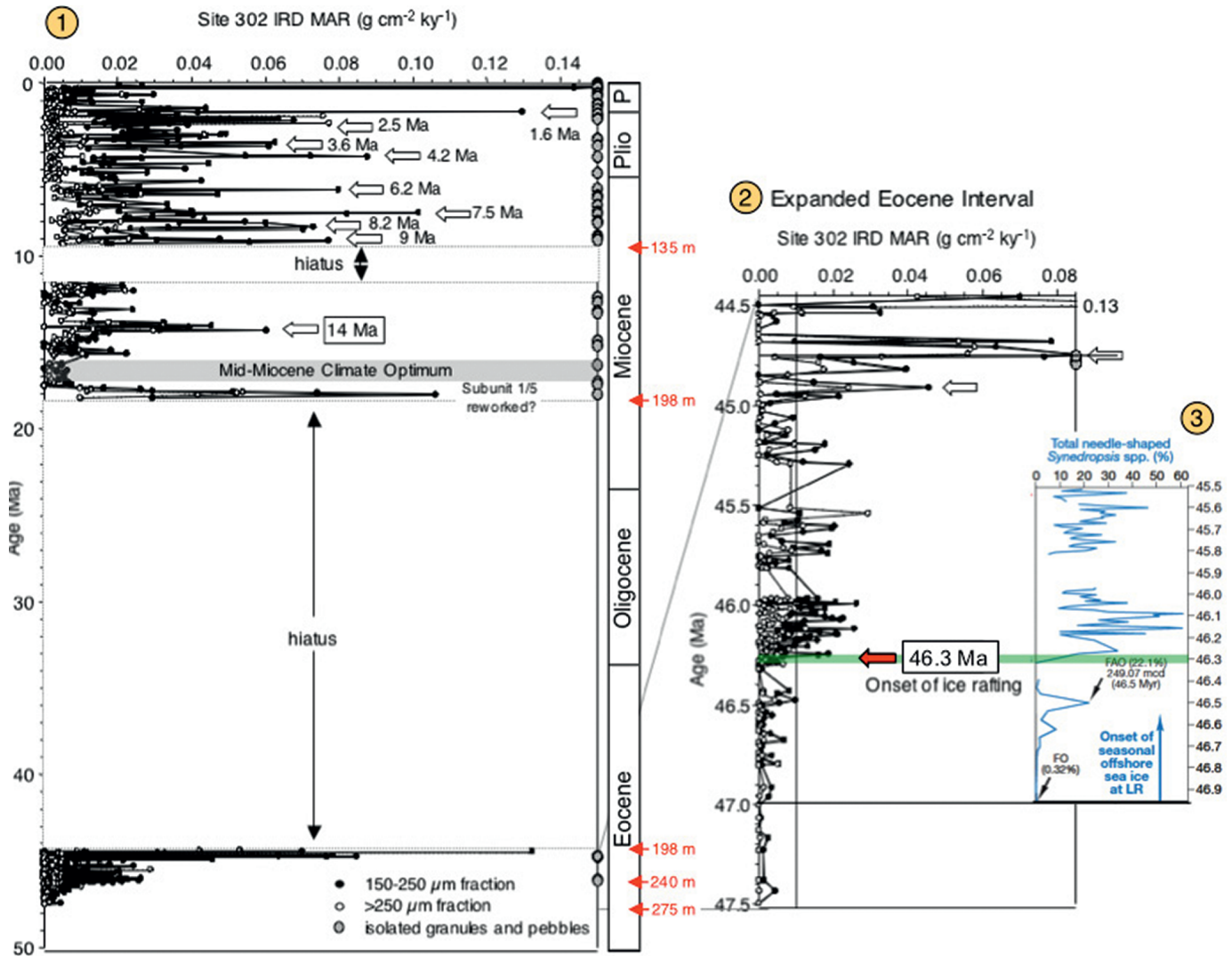


Fig. 6: (1) = IRD mass accumulation rates ($\text{g cm}^{-2} \text{ky}^{-1}$) in the $>250 \mu\text{m}$ (open circles) and $150\text{--}250 \mu\text{m}$ (solid circles) size fractions of the Eocene to Pleistocene (275 to 0 mcd) section of the IODP-ACEX record (ST. JOHN 2008, supplemented), along with isolated granules and pebbles (large grey circles) (from BACKMAN et al. 2006) versus age (Ma). Open arrows indicate major pulses of IRD input. The Mid-Miocene Climate Optimum (e.g., FLOWER & KENNET 1995, ZACHOS et al. 2001) is marked as horizontal grey bar. Red numbers indicate "meters composite depth (mcd)". (2) = blow-up of the middle Eocene interval (44.5–47.5 Ma) of this dataset and (3) = concentrations of needle-shaped sea-ice diatom *Synedropsis* spp. (STICKLEY et al. 2009).

Abb. 6: (1) Akkumulationsraten der terrigenen Grobfraction $>250 \mu\text{m}$ und $150\text{--}250 \mu\text{m}$ im eoziänen-pleistozänen Kernabschnitt (0–275 m bzw. 0–50 Ma) der IODP-ACEX-Bohrung (ST. JOHN 2008). Offene Pfeile heben Maxima mit erhöhtem Eintrag terrigener Grobfraction = eistransportiertes Material ("ice-rafted debris" = IRD) hervor. Das "Mittel-Miozäne Klimaoptimum" (e.g., FLOWER & KENNET 1995, ZACHOS et al. 2001) ist als grauer Balken hervorgehoben. Rote Zahlen zeigen Kernteufen an. (2) = Kernabschnitt 47.5–44.5 Ma mit Akkumulationsraten von IRD und (3) = vergrößert dargestellt die Häufigkeit der Meereis-Diatomee *Synedropsis* spp. (nach STICKLEY et al. 2009).

tative quartz grains was used to distinguish between sea-ice and iceberg transport. As outlined by ST. JOHN (2008), surface features of iceberg-transported grains are dominated by those produced by mechanical breakage (e.g., angular edges, high relief, and step-fractures), whereas surface features of sea-ice transported grains show more rounded edges and chemical features, such as silica-dissolution and precipitation (for further information and references see ST. JOHN 2008).

The results from ST. JOHN's (2008) study (Fig. 6) confirm the pebble-based interpretation made by the IODP 302 Scientific Party (BACKMAN et al. 2006, MORAN et al. 2006) that ice initiated in the Arctic in the middle Eocene near 46.3 Ma. At that time, IRD ($150\text{--}250 \mu\text{m}$) percentages and accumulation rates reached values $>1 \%$ and $0.02 \text{ g cm}^{-2} \text{ky}^{-1}$, respectively. Quali-

tatively, the IRD coarse fraction $>250 \mu\text{m}$ mainly composed of quartz, looks very similar in samples from the middle Eocene and from the Pleistocene.

Contemporaneously with the onset of IRD near 46.3 Ma, the abundance of weakly silicified needle-shaped pennate diatoms *Synedropsis* spp. significantly increased, indicating the presence of sea ice and silica-enriched waters (STICKLEY et al. 2009). As the fossil *Synedropsis* spp. found in the ACEX record are uniquely associated with the IRD peaks from the same cores, these authors interpret the IRD being predominantly derived from sea ice (STICKLEY et al. 2009). The first occurrence of these sea-ice related diatoms was at about 47 Ma (or ~ 43 Ma when using the alternate chronology of POIRIER & HILLAIRE-MARCEL 2011), at times when IRD grains

were found in the ACEX section, albeit in low abundance, suggesting the onset of seasonally paced offshore sea-ice formation at that time (Fig. 6). These sedimentological and micropaleontological data are a strong indication for sea-ice formation in the middle Eocene. Iceberg transport, however, was probably also present in the middle Eocene, as indicated by mechanical surface-texture features on quartz grains from this interval (ST. JOHN 2008).

With the first occurrence of significant amounts of IRD near 46.3 Ma, the alkenone-based sea-surface temperature (SST) estimate in the ACEX record dropped by about 7.5 °C, and temperatures of 10–17 °C were determined for the time interval 46.3–44.8 Ma (WELLER & STEIN 2008). Such SSTs do not seem unrealistic. Assuming that the alkenone SST represents summer SST and considering the strong seasonal temperature variability of >10 °C during the early-middle Eocene (STEIN 2008, WELLER & STEIN 2008), favourable conditions for sea-ice formation may have occurred during wintertime. This could have been a situation similar to that observed in the modern Baltic Sea where summer SSTs of >15 °C and winter SSTs <1 °C with sea-ice formation are typical (WÜST & BROGMUS 1955, KRAUSE 1969).

The records from ACEX (BACKMAN et al. 2006, MORAN et al. 2006, ST. JOHN 2008) as well as similar IRD records from the Greenland Basin ODP Site 913 (ELDRETT et al. 2007, TRIPATI et al. 2008) prove an early onset / intensification of Northern Hemisphere glaciations during Eocene times, as was proposed from changes in oxygen-isotope composition across the Eocene / Oligocene boundary and in late Eocene records from the tropical Pacific and South Atlantic (COXALL et al. 2005, TRIPATI et al. 2005). Furthermore, the increase in IRD in the ACEX and ODP Site 913 records coincided with major decreases in atmospheric CO₂ concentrations (PEARSON & PALMER 2000, PAGANI et al. 2006, LOWENSTEIN & DEMICCO 2006, THOMAS 2008). These data suggest that the Arctic and Antarctic Cenozoic climate evolutions are more closely timed, i.e., the Earth's transition from the "greenhouse" to the "icehouse" world was bipolar (Fig. 4), which points to greater control of global cooling linked to changes in greenhouse gases in contrast to tectonic forcing (MORAN et al. 2006). The decline of atmospheric concentrations of CO₂ in the middle Eocene may have driven both poles across the temperature threshold that enabled the nucleation of glaciers on land and partial freezing of the surface Arctic Ocean, especially during times of low insolation (ST. JOHN 2008).

The ACEX record also provided information about the variability of Northern Hemisphere icesheets and/or sea-ice cover during Neogene times. Between about 17.5 and 16 Ma a distinct minimum in ice-rafting in the central Arctic was found (Fig. 6), which may correspond to the Middle Miocene climate optimum (FLOWER & KENNETT 1995, ZACHOS et al. 2001, MORAN et al. 2006), suggesting minimal ice conditions in the Arctic during this period (ST. JOHN 2008). Between about 15 and 14 Ma, IRD accumulation in the ACEX record distinctly increased, contemporaneously with similar IRD maxima in the Greenland Sea (WOLF-WELLING et al. 1996), the existence of glacially eroded material in sediments recovered at Fram Strait Site 909 (KNIES & GAINA 2008), and the onset of cooling in Baffin Bay (STEIN 1991). This may suggest a shift to larger-scale or permanent sea ice in the Northern Hemisphere high latitudes, which is consis-

tent in timing to the onset of the global mid-Miocene cooling (Fig. 4, ZACHOS et al. 2008), the establishment of more extensive ice sheets in Antarctica and greater Antarctic Bottom Water formation (WRIGHT et al. 1992, FLOWER & KENNETT 1995), and a corresponding eustatic sea-level regression (MILLER et al. 1998). The late Cenozoic maxima in IRD mass accumulation rates found in the ACEX record probably indicate further expansion of sea ice or growth of ice sheets shedding icebergs into the Arctic Ocean (Fig. 6, ST. JOHN 2008), and most of them co-occurred with either initial or intensified ice-rafting events at sub-Arctic sites (WOLF & THIEDE 1991, STEIN 1991, FRONVAL & JANSEN 1996, WOLF-WELLING et al. 1996, THIEDE et al. 1998, 2011, ST. JOHN & KRISSEK 2002). That means ST. JOHN's (2008) data provide a long-term pattern of Arctic ice expansion and decay, on the order of those determined for the sub-Arctic oceans.

A major shift in the composition of heavy minerals in the IRD of the ACEX record is seen at about 13–14 Ma (Fig. 7, KRYLOV et al. 2008). The low-resolution record shows high clinopyroxene (Cpx) and low hornblende (Hbl) (amphibole) (high Cpx/Hbl ratios) below 14 Ma, and low clinopyroxene and high hornblende (amphibole) values (low Cpx/Hbl ratios) above 14 Ma. Considering that sea-ice is the main transport agent for the heavy minerals, this points to the western Laptev Sea and Kara Sea as major IRD source prior to about 14 Ma and the eastern Laptev Sea and East Siberian Sea as major IRD source area after 14 Ma, assuming a Transpolar Drift system similar to that of today (KRYLOV et al. 2008). Due to the fact that the distance between the Hornblende (amphibole) source region in the eastern Laptev Sea and East Siberian Sea and the ACEX drill site requires a drift time that exceeds one year when assuming present-day drift trajectories and velocities (Fig. 7), KRYLOV et al. (2008) proposed that the sea-ice transporting this material must have survived a melting season. If this assumption is correct, it may point to the development of a perennial sea-ice cover in the Arctic Ocean at about 13–14 Ma, contemporaneously with the global mid-Miocene cooling (Fig. 4). DARBY (2008) who studied the composition of Fe oxide grains in the ACEX section, came to a similar conclusion that during the last 14 Ma a significant amount of IRD was derived from the northern Canadian islands and Ellesmere Island (Fig. 7), with additional sources in the Eurasian Arctic, and proposed a perennial sea-ice cover since at least about 14 Ma.

The dominance of smectite in the lower part of the ACEX record (Fig. 7) supports the heavy-mineral data, i.e., it indicates a terrigenous sediment input from the western Laptev Sea and Kara Sea. The changes in the clay- and heavy-mineral assemblages, however, do not occur exactly in phase. The decrease in smectite (and increase in illite) already occurred within Unit 1/5, i.e., a few million years earlier (Fig. 7). As outlined by KRYLOV et al. (2008), the reason for this discrepancy could be related to climate-driven changes in weathering conditions in the source regions, that is important for formation of clay in soils, or to different mechanisms of clay- and heavy-minerals transportation.

Concerning the onset of perennial sea-ice cover, there are still some discrepancies that have to be solved. As stated by MATTHIESSEN et al. (2009), a year-round (perennial) sea-ice cover as proposed by DARBY (2008) and KRYLOV et al. (2008) being predominant in the central Arctic Ocean since the

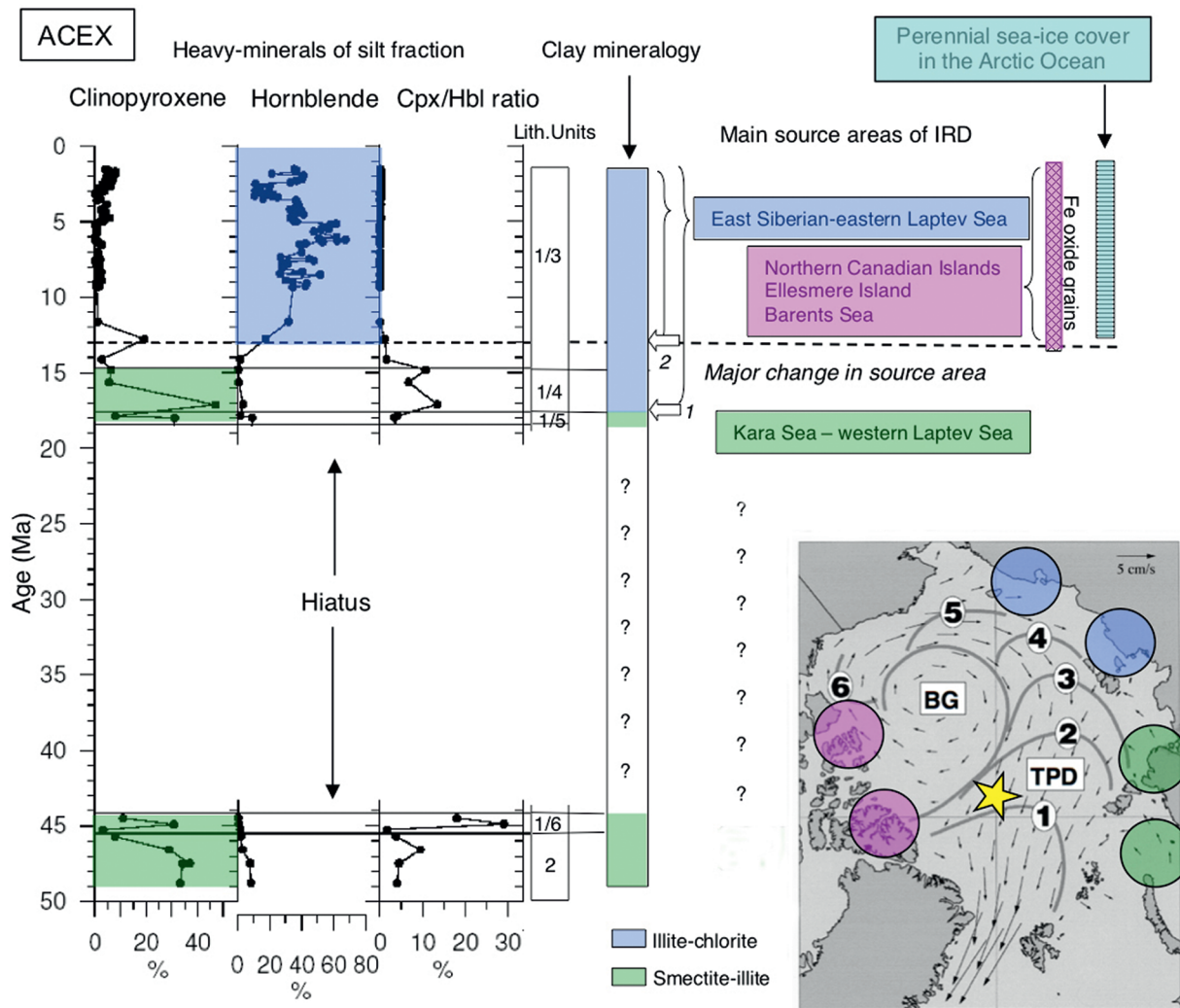


Fig. 7: Percentages of clinopyroxene and hornblende in the heavy mineral silt fraction as well as the clinopyroxene/hornblende (cpx/hbl) ratio, determined in the IODP-ACEX core (KRYLOV et al. 2008), and interpretation in terms of source areas of the terrigenous (IRD) fraction and sea-ice cover. Source-area identification based on Fe-oxide grains (DARBY 2008) and clay-mineral assemblages (KRYLOV et al. 2008) is indicated at right-hand side. Figure from Stein (2008). Inset map (bottom right) shows mean fields of ice drift in the Arctic Ocean derived from buoy drift between 1979 and 1994 (from HOVLAND 2001, supplemented, based on COLONY & THORNDIKE 1985, THORNDIKE 1986, PFIRMAN et al. 1997). Velocities indicated by arrows. Numbered lines indicate the average number of years required for ice in this location to exit the Arctic through the Fram Strait. BG = Beaufort Gyre, TPD = Transpolar Drift. Colour code highlights source areas (pink = Northern Canada, blue = East Siberia/eastern Laptev Sea, green = western Laptev Sea/Kara Sea). Yellow star = location of the ACEX drill site.

Abb. 7: Gehalte an Clinopyroxen und Hornblende in der Schwermineral-Siltfraktion sowie das Clinopyroxen/Hornblende-Verhältnis im eoänen-pleistozänen Kernabschnitt (0-50 Ma) des IODP-ACEX-Kerns (KRYLOV et al. 2008) und Interpretation in Hinblick auf potentielle Liefergebiete der terrigenen (IRD) Sedimentfraktion. Zusätzlich sind Tonmineral- (KRYLOV et al. 2008) und Fe-Oxid-Daten (DARBY 2008) als Anzeiger für Liefergebiete dargestellt. Inset-Karte (unten rechts) zeigt mittlere Driftraten von Meereis im Beaufort-Wirbel (BG) und in der Transpolar-Drift (TPD). Ziffern 1-5 geben die Zeit in Jahren wieder, die Eis an der Position braucht, bis es den Arktischen Ozean durch die Framstraße verlässt (ergänzt aus HOVLAND 2001, nach COLONY & THORNDIKE 1985, THORNDIKE 1986, PFIRMAN et al. 1997).

Middle Miocene, can be ruled out because this would have led to an extremely low production as in the modern Arctic Ocean (e.g., WHEELER et al. 1996) leading to low abundances or absence of aquatic palynomorphs in the sediments. In contrast to this, the co-occurrence of *Nematosphaeropsis* spp. and *Impagidinium* spp. found in the Neogene part of the ACEX sequence, points to seasonally open waters (MATTHIESSEN et al. 2009). Abundance maxima of agglutinated foraminifers in the Early Pleistocene ACEX section also support seasonally ice-free conditions during that time (CRONIN et al. 2008).

On one hand, the discrepancies to Darby's and Krylov et al.'s reconstructions may be explained by their lower temporal resolution. The study by DARBY (2008) has an average

sampling interval of about 0.17 Ma whereas MATTHIESSEN et al. (2009) used samples at an average sample interval of 60 cm in the Late Miocene corresponding to a temporal resolution of approximately 0.04 Ma (based on the age model of FRANK et al. 2008). According to MATTHIESSEN et al. (2009), therefore periods with a reduced seasonal extent of the sea-ice cover (interglacials?) may have alternated with periods of a year-round sea-ice cover (glacials?). On the other hand, applying modern mean drift speeds to argue for perennial ice in the past – as done by DARBY (2008) and KRYLOV et al. (2008) – might also be dangerous, as i) thinner ice may drift faster ii) wind-driven circulation may have been stronger, and iii) there is no modern analysis on how significant mean speeds are (cf. O'REGAN et al. 2010, O'REGAN 2011).

Concerning the variability of IRD during the Neogene, another prominent phenomenon is the distinct reduction in the amount of IRD in the ACEX record in the early Pleistocene (Fig. 8, O'REGAN et al. 2010, POLYAK et al. 2010). The IRD numbers remain low until a core depth of about 6 mcd. These low IRD values might be explained by (i) a rather stable ice pack, that would reduce the transport and melting of debris-laden sea ice and icebergs across the central Arctic, (ii) a decrease in IRD deposition due to lower inflow of Atlantic-derived intermediate water, that would reduce basal melting of sea ice, or (iii) less icebergs entering the Transpolar Drift from the Eurasian margin (O'REGAN et al. 2010, POLYAK et al. 2010). At 6 mcd, i.e., with the onset of the MIS 6 (Saalian) glaciation, IRD increased significantly in the ACEX record as well as in the neighbouring cores PS2185-6 and 96/12-1PC (Fig. 8, JAKOBSSON et al. 2000, 2001, SPIELHAGEN et al. 2004, O'REGAN et al. 2008, 2010). These distinct maxima in IRD recorded on Lomonosov Ridge are related to advances and retreats of the Barents-Kara Sea Ice Sheet during the last 200 ka (e.g.

SVENDSEN et al. 2004, see discussion below). Whereas the Lomonosov Ridge cores display a signal related to the Eurasian ice sheets and IRD input via the Transpolar Drift, started to increase with the onset of MIS 6, a pronounced increase in IRD abundances was recorded in the western Arctic Ocean (Amerasian Basin) significantly earlier than on the Lomonosov Ridge, i.e., probably already during glacial MIS16 at about 650 ka (Fig. 8, POLYAK et al. 2009, STEIN et al. 2010a, 2010b). As outlined by POLYAK et al. (2009), the western Arctic is largely controlled by the Beaufort Gyre circulation system and sediment input from the North American margin. That means, these sedimentary records reflect primarily the history of the Laurentide Ice Sheet and possibly different sea-ice conditions than in the eastern Arctic.

From the discussion above, it is clearly obvious that for the reconstruction of a more complete history of perennial versus seasonal sea ice and ice-free intervals during the past several million years additional well-dated proxy records distributed throughout the Arctic Ocean, are needed (POLYAK et al. 2010, O'REGAN et al. 2010, STEIN et al. 2010b). These proxy records have to be obtained by multidisciplinary studies of long sedimentary sections that can only be recovered by future drilling campaigns to be carried out hopefully within the new phase of IODP (STEIN 2011).

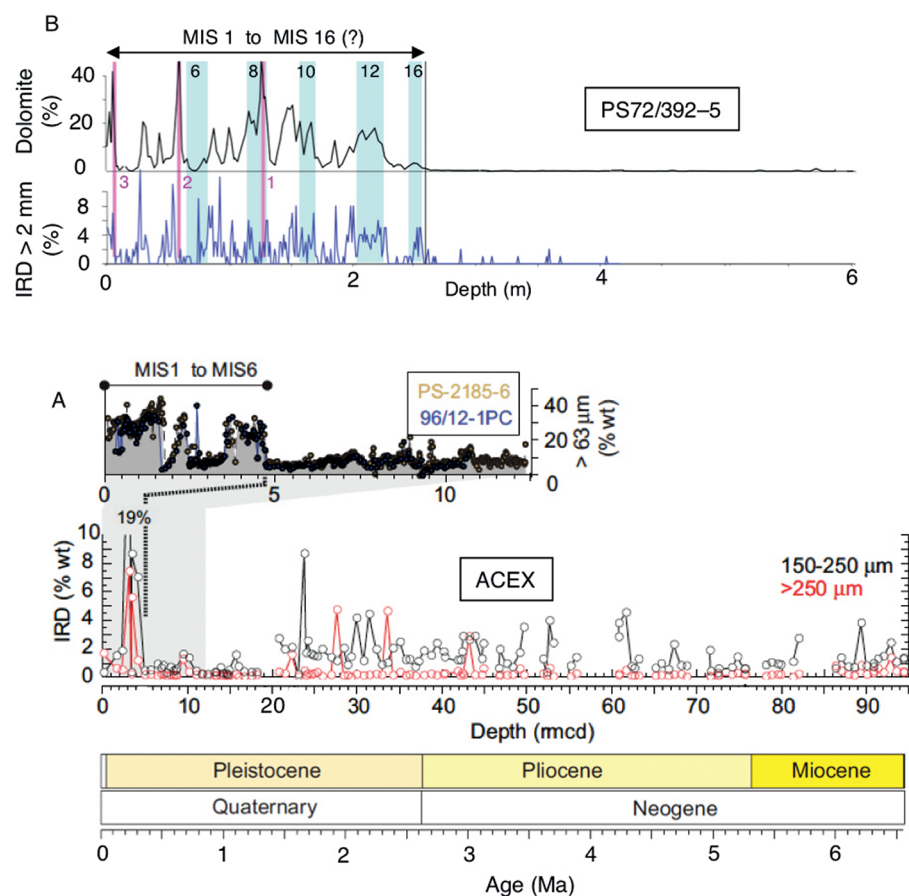


Fig. 8: A = Stratigraphically aligned coarse fraction contents from cores PS-2185-6 and 96/12-1PC shown on the ACEX revised composite depth scale, and the ACEX terrigenous IRD record of the upper 95 mcd (ST. JOHN 2008). Age model based on beryllium stratigraphy (FRANK et al. 2008) (modified after O'REGAN et al. 2010). B = Number of IRD grains >2 mm and content of dolomite (%) determined by XRD and inorganic carbon content, from core PS72/392-5 (for location see Fig. 10; Figure from STEIN et al. 2010a). More sandy intervals are marked by horizontal light blue bars, probably correlating with periods of maximum ice-sheet extend during glacials MIS 6, MIS 8, MIS 10, MIS 12, MIS 16. Main pink-white (1 = PW1 and 2 = PW2) and white (3 = W3) layers are indicated by pink bars.

Abb. 8: A = Gehalte von terrigener Grobfraction (IRD >63 μm) der Kerne PS2185-6 und 96/12-1PC (Lokationen siehe Fig. 10) und der oberen 95 mcd der ACEX-Abfolge (150-250 μm und >250 μm), aufgetragen gegen revidierte ACEX-Teufenskala (aus O'REGAN et al. 2010, abgeändert). B = Gehalte von IRD >2 mm und Dolomit (Bestimmung mittels Röntgendiffraktometrie und Elementanalyse) von Kern PS72/392-5. Mehr sandige Intervalle sind durch blaue Balken angezeigt, rosa Balken markieren "pink-white layers" (aus STEIN et al. 2010a).

Quaternary glacial / interglacial variability in Arctic Ocean ice-rafting: The last 200 ka

The glacial / interglacial variability in Arctic Ocean ice-rafting may be controlled by different but interrelated factors, i.e., the waxing and waning of circum-Arctic ice sheets, changes in sea-ice cover and changes in oceanic circulation patterns. In detail, however, the interrelationships and the timing of these processes are not fully understood yet (e.g., POLYAK et al. 2004, 2009, STEIN 2008, O'REGAN et al. 2010, O'REGAN 2011). Especially the probably different evolution of ice sheets and sea-ice distribution in the western and eastern Arctic is still a matter of discussion and further studies are needed (see previous chapter). In the following, we will concentrate of the climatic evolution of the last 200 ka.

As shown in several sediment cores from the Eurasian Basin as well as the Amerasian Basin, records of both IRD input and foraminifer abundances from the last 200 thousand years BP (200 ka) clearly demonstrate that sedimentary environments in the central Arctic Ocean were strongly variable. In most of these Arctic Ocean sediment

cores, IRD content and abundances of planktonic foraminifers display a general anticorrelation (DARBY et al. 1997, SPIELHAGEN et al. 1997, 2004, NØRGAARD-PEDERSEN et al. 1998, 2003, 2007, POLYAK et al. 2004). As an example, records from core PS2185-6 recovered from Lomonosov Ridge are shown in Figure 9. The foraminifer-rich intervals likely reflect times with an inflow of Atlantic Water of variable strength, temperature, and regional extension, at least a seasonally reduced sea-ice cover (i.e., more open-water conditions), and some increased surface-water productivity (e.g., HEBBELN et al. 1994, NØRGAARD-PEDERSEN et al. 2003, SPIELHAGEN et al. 2004). In core PS2185-6, for example, most prominent peaks in planktonic foraminifer abundance occur in substages MIS 5.5, 5.3, and 5.1 and in the <50 ka interval (Fig. 9, SPIELHAGEN et al. 2004).

Coarse-grained IRD layers contain very few or no foraminifers and are mainly related to iceberg transport of terrigenous material. Distinct maxima in IRD were recorded in uppermost MIS 7 to MIS 6 (190 to 130 ka), upper part of MIS 5 (substage 5.2, about 90 to 80 ka), near the MIS 5/4 boundary (around 75 ka), and in the late MIS 4 to early MIS 3 time interval (65 to 50 ka) (Fig. 9, SPIELHAGEN et al. 2004), indicating major continental glaciations during those times. The central Arctic Ocean sediments from <50 ka show an upward decrease of

IRD content and a minimum in the deposits from the LGM around 20 ka (NØRGAARD-PEDERSEN et al. 1998, 2003, SPIELHAGEN et al. 2004). In general, Holocene deep-sea sediments from the Eurasian Arctic Ocean have a low coarse-fraction content (<10 wt.%, NØRGAARD-PEDERSEN et al. 1998, 2003), which reflects the scarcity of icebergs in the modern Arctic.

Concerning the provenance of the IRD and its variability through time in the Eurasian Arctic, bulk-, clay-, and heavy-mineral associations of core PS2185-6 were used to identify source areas of the terrigenous (IRD) fractions (Fig. 10, e.g., WAHSNER et al. 1999, BEHRENDTS et al. 1999, SPIELHAGEN et al. 1997, 2004, STEIN 2008). Here, elevated smectite and kaolinite concentrations as well as high clinopyroxene / amphibole ratios during MIS 6, upper MIS 5, and late MIS 4 early MIS 3, mostly coinciding with IRD maxima (Fig. 9), serve as a tracer for an IRD origin from the area of western Laptev Sea, southeastern Kara Sea, Franz Josef Land and the area of central Barents Sea respectively. High smectite concentrations, however, do not always coincide with high coarse fraction content. In some intervals, e.g. in the uppermost and lowermost MIS 5 (5.1 and 5.5), smectite enrichments correlate with very low terrigenous coarse fraction which may suggest transport by sea ice (or currents) rather than icebergs. Furthermore, the IRD-rich intervals are enriched in quartz, reaching

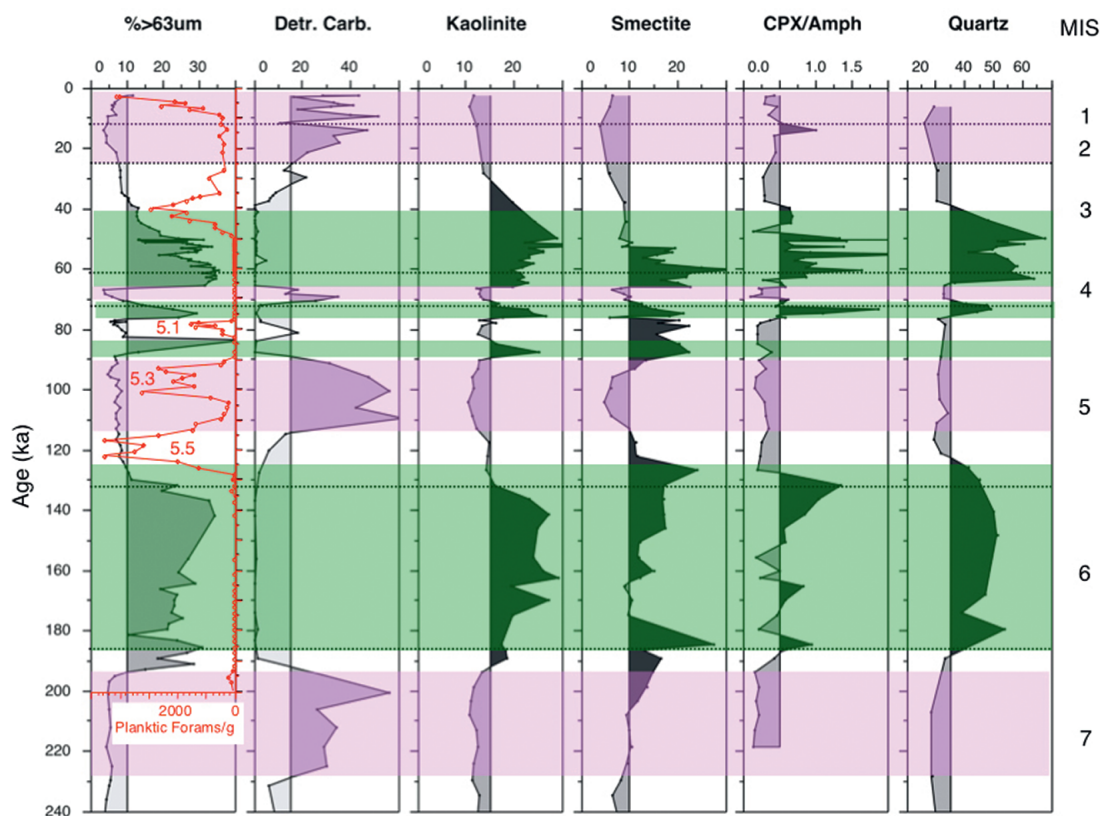


Fig. 9: Summary plots showing coarse-fraction content >63 μm (wt.%), detrital carbonate (% of coarse fraction >500 μm), and kaolinite and smectite (% of clay minerals in the clay fraction <2 μm) (data from SPIELHAGEN et al. 1997) as well as the clinopyroxene/amphibole (CPX/Amph) ratio (data from BEHRENDTS 1999) and quartz content (data from VOGT 1997, 2004) in core PS2185 for the last 240 ka (MIS 7 to MIS 1), using the age model of SPIELHAGEN et al. (2004). Marine isotope stages MIS 1 to MIS 7 are indicated. In addition, the concentration of planktic foraminifers per gram sediment is shown (data from SPIELHAGEN et al. 2004). Green and pink bars indicate sediment source areas in Eurasia and northern Canada, respectively. Figure from STEIN (2008).

Abb. 9: Gehalte an Grobfraktion >63 μm , detritischem Karbonat, Kaolinit und Smektit (Daten aus SPIELHAGEN et al. 1997), Verhältnis Clinopyroxen/Amphibol (Daten aus BEHRENDTS 1999) und Quarzgehalte (Daten aus VOGT 1997) im Zeitintervall der letzten 240,000 Jahre v.H. (240 ka, MIS 7 bis MIS 1) (Altersmodell nach SPIELHAGEN et al. 2004). Zusätzlich wird der Gehalt an planktischen Foraminiferen gezeigt (Daten aus SPIELHAGEN et al. 2004). Grüne bzw. rosa Balken heben Herkunftsgebiete in Eurasien bzw. Kanada hervor. Abbildung aus STEIN (2008).

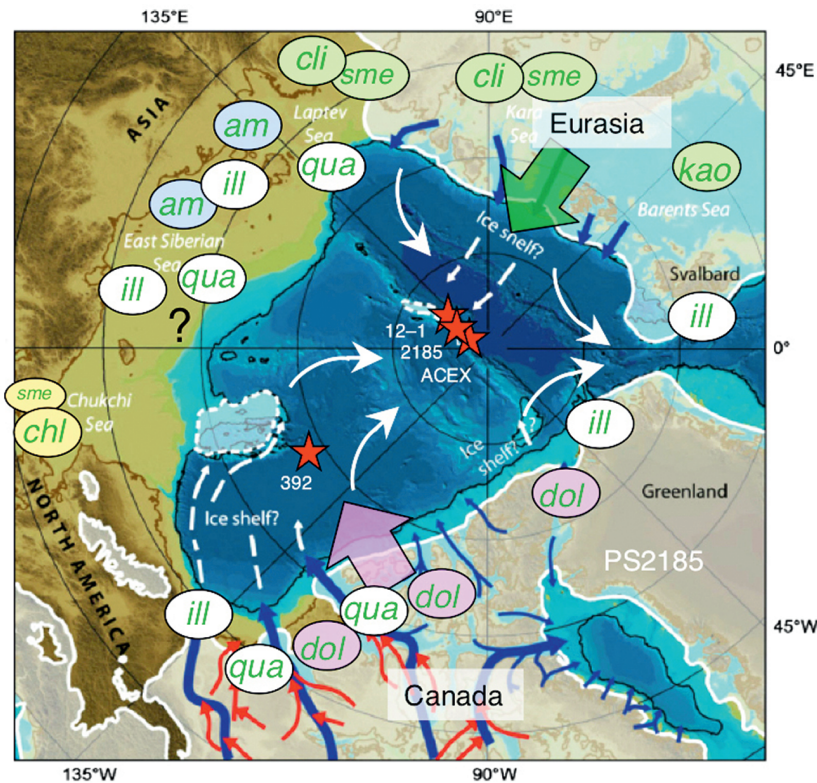


Fig. 10: Bathymetric map of the Arctic Ocean modified to showing lowered sea level of 120 m during LGM maximum glaciation. Limits of the Eurasian and North American ice sheets according to SVENDSEN et al. (2004) and DYKE et al. (2002), respectively; main ice streams (blue arrows) according to DE ANGELES & KLEMAN (2005) and KLEMAN & GLASSER (2007). Red arrows show ice stream tributaries and episodic diversions of ice stream drainage within main ice stream corridors. Projected flow lines of ice shelves and limits of ice rises are mapped based on interpretation of observed glaciogenic seafloor bedforms (figure from JAKOBSSON et al. 2008, supplemented). Main source areas of specific minerals are shown (from STEIN 2008, STEIN et al. 2010 and references therein): qua = quartz; dol = dolomite; ill = illite; sme = smectite; chl = chlorite; kao = kaolinite; am = amphibole; cli = clinopyroxene. Colour codes mark source region: green = western Laptev Sea, Kara Sea, Barents Sea; blue = eastern Laptev Sea, East Siberian Sea; orange = Bering Strait; pink = Canada, northern Greenland; white = no specific source area. Red stars indicate core locations on Lomonosov Ridge and Canada Basin; large green and pink arrows indicate sediment input from the Eurasian and northern Canadian ice sheets, respectively.

Abb. 10: Modifizierte bathymetrische Karte des Arktischen Ozeans zur Zeit des letzten glazialen Maximums mit einem 120 m abgesenkten Meeresspiegel. Ausdehnung der eurasischen und nordamerikanischen Eisschilde nach SVENDSEN et al. (2004) bzw. DYKE et al. (2002), Eisströme (blaue Pfeile) nach DE ANGELES & KLEMAN (2005) und KLEMAN & GLASSER (2007). Abbildung ergänzt nach JAKOBSSON et al. 2008. Liefergebiete bestimmter Minerale nach STEIN (2008) und STEIN et al. (2010).

values of $>50\%$ (Fig. 9). This is also consistent with an Eurasian source, although quartz alone is not specific enough for a source identification because it also occurs in major abundance in the Canadian Arctic (Fig. 10).

During interglacials, i.e., MIS 7 and the middle part of MIS 5 as well as during the last about 20 ka, increased amounts of detrital carbonate (dolomite) were determined in the record of core PS2185-6, coinciding with very low amounts of terrigenous coarse fraction (Fig. 9). Detrital carbonate, especially dolomite, is related to a sediment source in the Canadian Arctic (Fig. 10, e.g., BISCHOF et al. 1996, PHILLIPS & GRANTZ 2001) whereas the fine-grained terrigenous material points to a transport by sea ice (or currents) rather than icebergs. This may suggest substantial sediment transport towards the Eurasia Basin by sea ice in an extended Beaufort Gyre at those (mainly interglacial) time intervals.

LGM, Deglacial to Holocene changes in Arctic Ocean sea-ice cover and ice sheet decay

In order to reconstruct the Arctic Ocean sea-ice distribution and other surface-water characteristics, NØRGAARD-PEDERSEN et al. (2003) carried out a very detailed study on a large number of well-dated sediment cores from the Eurasian sector of the Arctic Ocean, representing the MIS 2/1 time interval. Based on sedimentological, micropaleontological, and stable isotope data, these authors were able to characterize and map regions of different paleoceanographic conditions for the Last Glacial Maximum (LGM) time slice (18.0–21.5 Cal. kyrs. BP according to GLAMAP (SARNTHEIN et al. 2003b)). This reconstruction is based on (1) the spatial distribution of $\delta^{18}\text{O}$ values as proxy for the distribution of Atlantic and polar water masses, (2) flux records of planktic foraminifers as productivity proxy reflecting nutrient supply and degree of ice cover (e.g., HEBBELN & WEFER 1991, HEBBELN et al. 1994), and (3) the IRD content $>500\ \mu\text{m}$ as a proxy to estimate the input of terrigenous sediments transported by icebergs derived from continental ice sheets calving into the Arctic Ocean. As a result, NØRGAARD-PEDERSEN et al. (2003) could separate three areas characterized by different sedimentation regimes and surface ocean properties during the LGM (Fig. 11):

- Area (1), the eastern Fram Strait and the northern Barents Sea margin;
- Area (2), the western Fram Strait and the southwestern Eurasian Basin up to about 84–85° N, and
- Area (3), the central Arctic Ocean (north of 85° N in the Eurasian Basin).

In summary, these areas have the following characteristics (Fig. 11, detailed discussion see NØRGAARD-PEDERSEN et al. 2003):

Area (1), the eastern Fram Strait and the northern Barents Sea margin area, is characterized by high sedimentation rates of 2–10 cm ky^{-1} and high abundances of planktic foraminifers (about 4000–6000 specimens g^{-1} sediment). Today, such environments are found in areas of seasonally changing ice cover like the central Fram Strait (HEBBELN & WEFER 1991). The high $\delta^{18}\text{O}$ values of *N. pachyderma* (sin.) of 4.5–4.8 ‰ and the estimates of summer sea-surface temperatures (SST) of about 1.6–3.0 °C (PFLAUMANN et al. 2003) suggest a strong inflow of Atlantic Water. The high abundances of planktic foraminifers (and fluxes of 10–35 10^3 specimens $\text{cm}^{-2} \text{ky}^{-1}$, NØRGAARD-PEDERSEN et al. 2003) correspond to the glacial “high productive zones” (HPZ) first reported from the eastern Fram Strait and the Norwegian Sea by HEBBELN et al. (1994) and DOKKEN & HALD (1996).

Area (2), the western Fram Strait and the southwestern Eurasian Basin up to about 84–85° N, is characterized by lower sedimentation rates of 1–2 cm ky^{-1} and moderately high abundances and fluxes of planktic foraminifers, high $\delta^{18}\text{O}$ values of *N. pachyderma* (sin.), and summer SST estimates slightly lower than in Area (1). This region may have been characterized by the pres-

ence of ice cover with some open leads in summer, similar to the present interior Arctic Ocean. NØRGAARD-PEDERSEN et al. (2003) suppose that Area 2 was under the steady influence of Atlantic subsurface waters advected from Area (1). The impact of recirculating saline and relatively warm Atlantic Water over a large area of the southwestern Eurasian Basin was the decisive factor causing a break-up of the ice cover, relatively high sedimentation rates and a comparatively high planktic foraminifer flux (about $5-10 \times 10^3$ specimens $\text{cm}^{-2} \text{ky}^{-1}$, Fig. 11, NØRGAARD-PEDERSEN et al. 2003).

Area (3), the central Arctic Ocean north of 85°N in the Eurasian Basin, is characterized by extremely low sedimentation rates (dominantly $<1 \text{ cm ky}^{-1}$), low abundances and fluxes

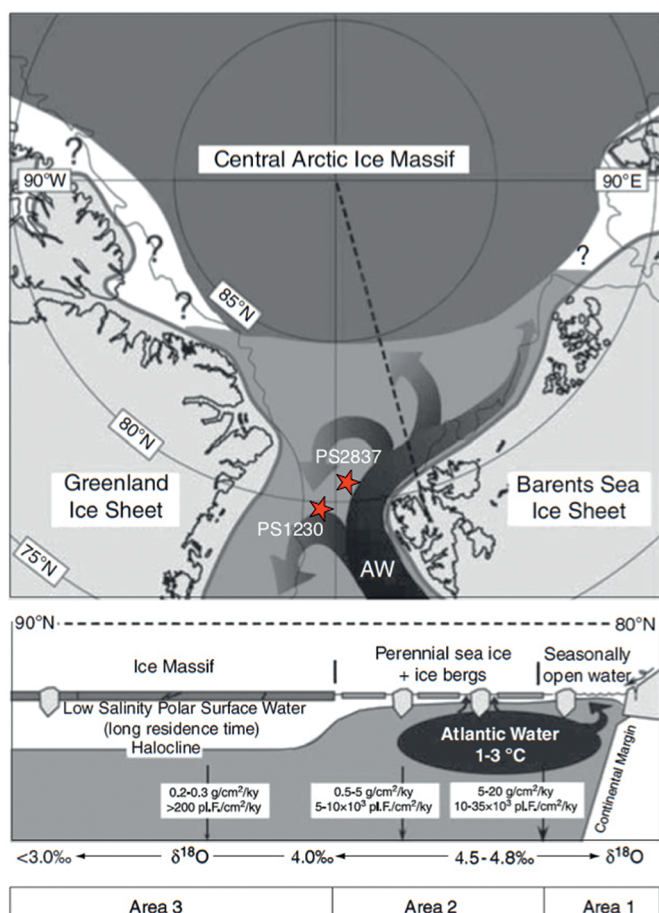


Fig. 11: Simplified model of sea-ice and surface-ocean characteristics in the Fram Strait to central Arctic Ocean region during the LGM (from NØRGAARD-PEDERSEN et al. 2003, supplemented). On the latitudinal transect from the northern Svalbard continental margin to the North Pole, related proxy data such as sedimentation rates, planktic foraminifer flux, planktic $\delta^{18}\text{O}$ values, and mean summer SST values of the Atlantic Water mass are shown. Advection and recirculation of relatively warm and saline Atlantic Water in the Fram Strait to southwestern Eurasian Basin caused an open ice cover and a relatively high flux of biogenic and lithic material. Polynyas probably occurred at the Barents Sea continental margin. From about 85°N and further into the interior Arctic, it is proposed that the sea-ice cover was permanently thick, resting upon cold, low-salinity halocline waters. This may explain the extreme low interior Arctic flux values. Red stars indicate locations of cores PS1230-1 and PS2837-5.

Abb. 11: Schematische Darstellung der Meereisverbreitung und Charakteristika des Oberflächenwassers im Bereich Framstraße/Arktischer Ozean während des Letzten Glazialen Maximums (ergänzt aus NØRGAARD-PEDERSEN et al. 2003). Auf dem Schnitt von Spitzbergen bis 90°N sind Proxydaten wie Sedimentations- und Akkumulationsraten, $\delta^{18}\text{O}$ -Werte planktischer Foraminiferen sowie der mittleren Temperaturen des Oberflächenwassers für drei unterschiedliche Gebiete angezeigt.

of planktic foraminifers (only a few hundred foraminifers g^{-1} sediment and $<0.2 \times 10^3$ specimens $\text{cm}^{-2} \text{ky}^{-1}$, respectively), and very low IRD ($>500 \mu\text{m}$) values $<1 \%$ (Fig. 11, NØRGAARD-PEDERSEN et al. 2003). These data suggest the existence of an extensive and thick sea-ice cover with low seasonal variation, limiting planktic productivity (“low productivity zone”) and minor IRD release in the eastern central Arctic during the LGM. Due to low temporal resolution, however, it has to be considered, that the data from the central Arctic Ocean are tentative and probably characterize average Marine Isotope Stage (MIS) 2 conditions rather than a specific LGM time slice (NØRGAARD-PEDERSEN et al. 2003).

MIS 2 (including the LGM) was already identified as a period of very limited bioproduction and extremely low sedimentation rates due to a massive sea-ice cover with limited seasonal variation from earlier studies of sediment cores from the eastern and western central Arctic Ocean (DARBY et al. 1997, NØRGAARD-PEDERSEN et al. 1998, POORE et al. 1999). Cores from the Northwind Ridge and the Chukchi Plateau (Amerasian Basin) are barren of foraminifers in the glacial interval (DARBY et al. 1997, PHILLIPS & GRANTZ 1997), suggesting an even thicker and more coherent sea-ice cover in the western central Arctic Ocean, which had a sufficient thickness to reduce solar irradiance to levels that precluded photosynthesis.

Grain-size distribution and IRD composition from this time period provides more detailed information on ice-sheet variability, ice export, and sea-ice versus iceberg transport. While there are very few icebergs calving into the Arctic Ocean, crossing the central basins, and exiting Fram Strait today (SUDGEN 1982), large quantities of glacial ice drifted across the central Arctic Ocean and finally through Fram Strait during the late Pleistocene. These pulses in IRD input during MIS 2 are mainly related to sudden, massive iceberg calving events in the North American Arctic ice sheets, as reconstructed by DARBY et al. (2002) from sedimentary records from the western central Arctic Ocean to Fram Strait (Fig. 12). In these cores, IRD composition $>250 \mu\text{m}$ and Fe oxides were used to trace the IRD in the glacial marine sediments back to its sources (see DARBY 2003 for background). A key core in their reconstruction is the AMS ^{14}C -dated core PS1230-1 located in 1235 m water depth at 78.9°N , 4.8°W , in the central Fram Strait (Fig. 12) where most of the Arctic sea ice is exported today (90 % of the modern sea-ice drifts through Fram Strait between 0 and 10°W , VINJE et al. 1998).

The record of core PS1230-1 representing the last 34 Cal. kyrs. BP (upper MIS 3 to MIS 1), shows significant, rapid fluctuations in the percentages of Fe oxide grains from different sources (Fig. 12, DARBY et al. 2002). Fe oxide maxima in the pre-Holocene probably represent primarily iceberg transport on the basis of the abundance of coarse IRD in the Pleistocene section and on the similarity of the IRD grain-size distribution to glacial tills (DARBY et al. 2002).

During the late Pleistocene (MIS 3 / MIS 2), a major source of IRD was the northwestern Laurentide Ice Sheet that calved into the Arctic Ocean. This source is identified by detrital Fe oxide grains in PS1230-1 that precisely match those in the tills of Banks Island and Victoria Island (source area 8 in Fig. 12). A northwestern Laurentide source is also supported by the presence of light-coloured detrital carbonate, which is rela-

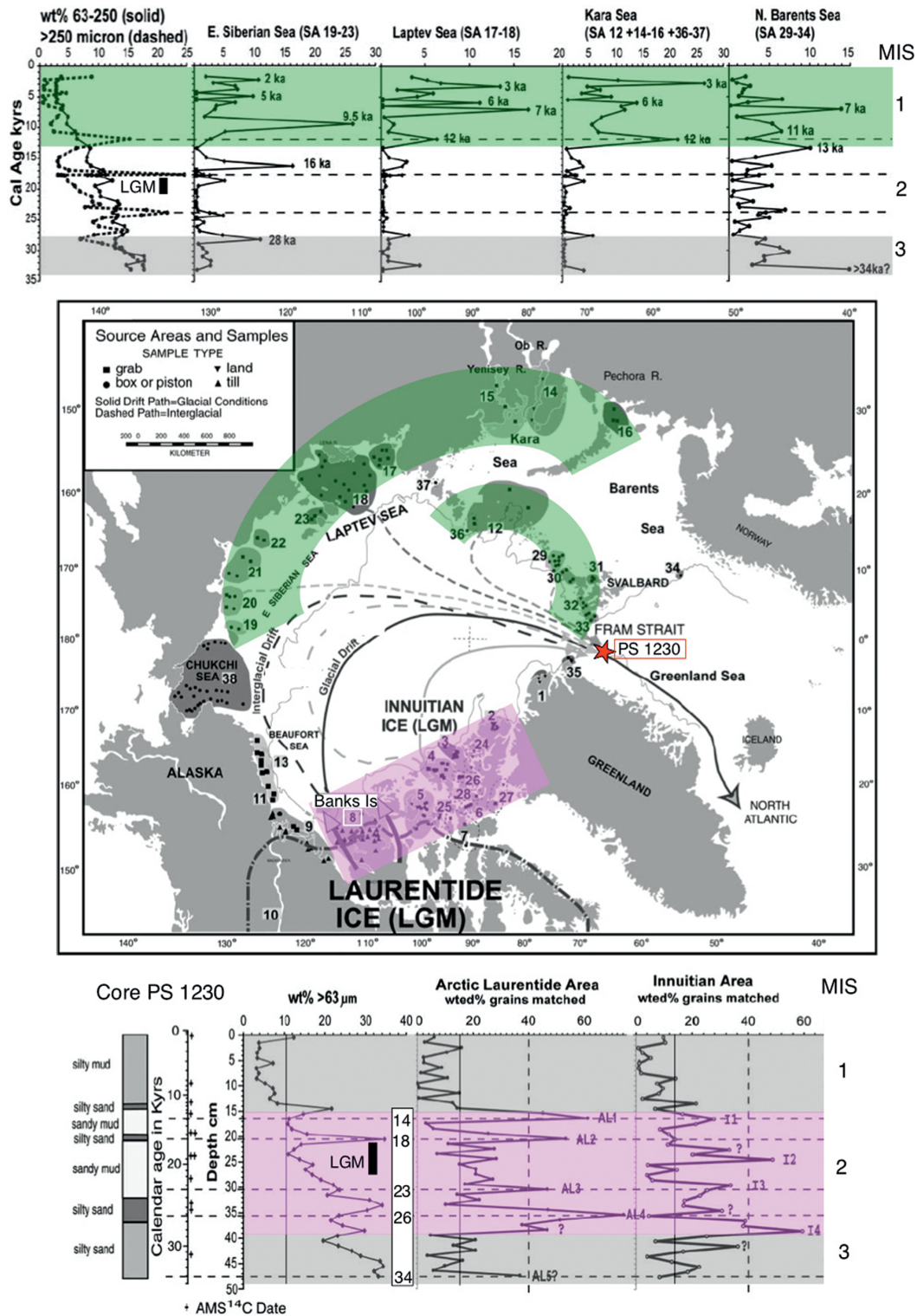


Fig. 12: Circum-Arctic source areas (samples 1-38) as defined by unique source compositions based on Fe oxide composition of sand-sized grains (DARBY 2003), drift paths of icebergs from Arctic Laurentide Ice Sheet and Innuitian Ice Sheet to Fram Strait (solid drift paths), and the location of core PS1230 (from DARBY et al. 2002, supplemented). Dashed drift paths of sea-ice in the Arctic show the influence of the Beaufort Gyre during warmer intervals like the Holocene by displacing North American ice drift paths westward. In green and pink, Eurasian and Canadian source areas, respectively, are highlighted. Graphs above and below the map show the amounts of terrigenous coarse fractions and Fe oxide grains from different circum-Arctic source areas determined in Fram Strait core PS1230 (from DARBY et al. 2002, supplemented). Bottom graphs: Arctic Laurentide (AL) and Innuitian (I) IRD events based on detrital Fe oxide mineral grain compositions matched to source area 8 (Banks Island) and source areas 2-7 plus 24-28, respectively, plotted *versus* core depth. Calendar years (kyrs. BP) and location of AMS¹⁴C datings (crosses) as well as major lithologies are indicated. Numbers 14 to 34 indicate ages of the main AL1 to AL 5 IRD events in Cal. kyrs. BP; bold black bar indicates the Last Glacial Maximum (LGM). Top graphs: IRD events originating from Siberian shelves, plotted *versus* age.

Abb. 12: Karte mit 38 unterschiedlichen, anhand von Fe-Oxiden in der Sandfraktion definierten, zirkum-arktischen Liefergebieten und Driftwegen von Eisbergen und Meereis. Die Kurven oberhalb und unterhalb der Karte zeigen Gehalte der terrigenen Grobfraktion und Fe-Oxide aus unterschiedlichen Liefergebieten im Kern PS1230. Abbildung ergänzt aus DARBY et al. (2002).

tively abundant in tills and derived from the extensive Paleozoic carbonates exposed on Victoria Island (e.g., BISCHOF et al. 1996). This is indicated by the coincidence of Fe oxide peaks in PS1230-1 with elevated detrital, light-coloured carbonate peaks of 4 to >8 % (Fig. 12). Another important but secondary source of Fe oxide grains in core PS1230-1 is the Innuitian ice sheet in the northern Canadian Islands (source areas 2 to 7 and 24 to 28 in Fig. 12; BISCHOF & DARBY 1999, DARBY et al. 2002).

The rapid onset and relatively short duration of the Fe oxide grain peaks suggest massive and fast deglaciation events in parts of the Laurentide and Innuitian ice sheets during MIS 2 (Fig. 12, at about 26, 23, 18 and 14 Cal. kyrs. BP), producing large armadas of icebergs, i.e., events probably similar to those recorded during Heinrich events in the North Atlantic. Indeed, the number of Arctic IRD events and their occurrence intervals over the last 34 ky are remarkably similar to those of Heinrich events, i.e., the events 1 to 4 seem to correspond to H0 to H3 (DARBY et al. 2002). The most prominent event seems to be the AL 2 event near 18 Cal. kyrs. BP, which coincides with a distinct IRD maximum, probably representing the decay of the LGM ice sheet (Fig. 12). Fe oxide peaks related to IRD input from the northwestern Laurentide Ice Sheet, occur at about the same time in cores from the Lomonosov,

Mendelev, and Northwind ridges (DARBY et al. 2002). These major collapses of the Laurentide Ice Sheet and iceberg discharge events through Fram Strait caused major pulses of fresh-water export into the Greenland-Iceland-Norwegian (GIN) seas (North Atlantic) where it may have been effective in arresting the deep-water formation and the global THC (cf., PELTIER 2007 and references therein).

During MIS 1, the weight percentages of the terrigenous sediment fraction >63 μm in Core PS1230-1 decreased significantly, reaching <4 % during the last 10 Cal. kyrs. BP (Fig. 12). The predominance of the silt and clay fractions suggests transport by sea ice rather than iceberg rafting (PFIRMAN et al. 1989, REIMNITZ et al. 1998, NÜRNBERG et al. 1994). The contemporaneous increase in Fe oxide grains from unglaciated Eurasian shelves such as the Kara, Laptev, and East Siberian seas (Fig. 12) supports sea-ice rafting as a most important transport process during the Holocene (DARBY et al. 2002, DARBY 2003).

Elevated IRD values during the LGM, decreasing during the deglaciation to minimum Holocene values were also recorded at near-by core PS2837-5 (Fig. 13, BIRGEL & HASS 2004, for locations of cores PS1230-1 and PS2837-5 see Fig. 11).

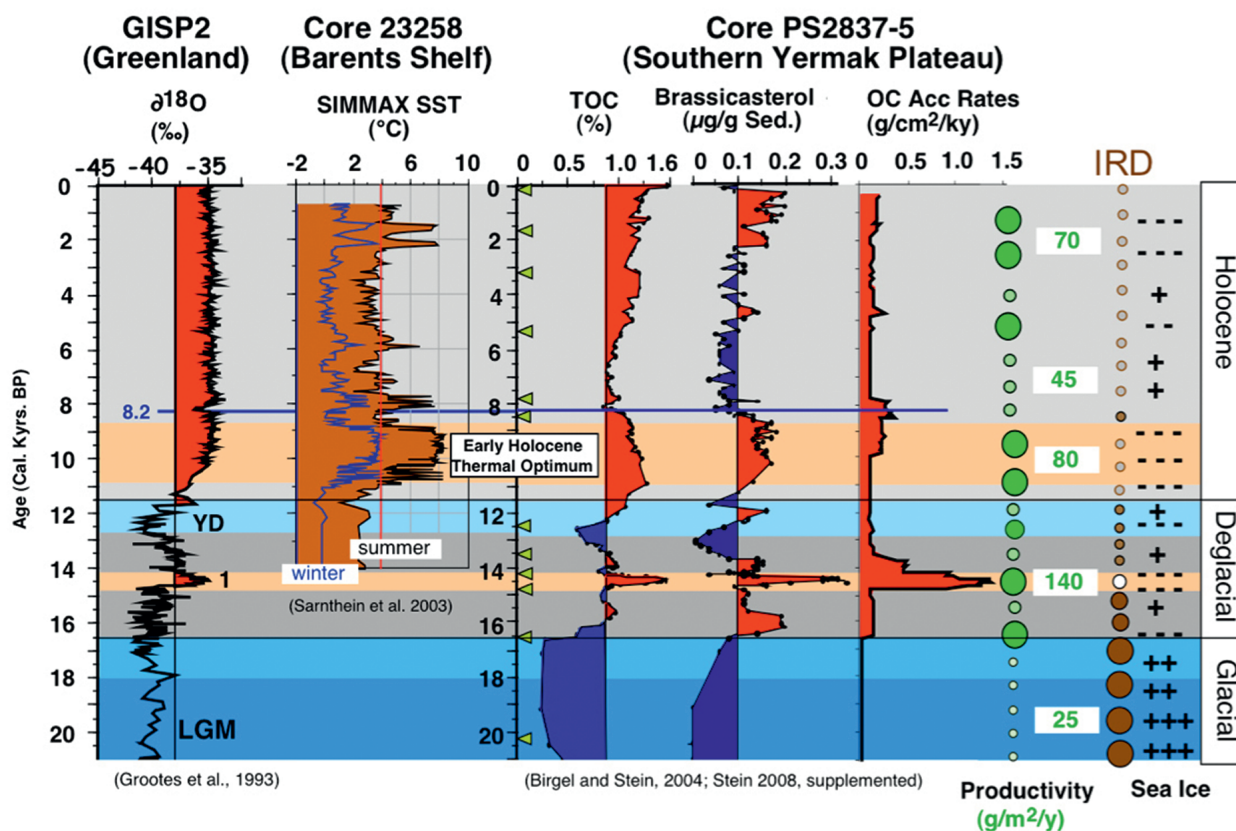


Fig. 13: Total organic carbon (%), brassicasterol ($\mu\text{g g}^{-1}\text{sed.}$) indicative for diatom productivity, and organic carbon accumulation rates ($\text{g C cm}^{-2}\text{ky}^{-1}$) of the last 20 ka at core PS2837-5; age scale in calendar years. Occurrence of ice-rafted debris (IRD; large/small brown circles = high/low amounts of IRD, white circle = absence of IRD (BIRGEL & HASS 2004). Primary productivity: large/small green circles = high/low productivity; calculation from organic carbon data following the approach of STEIN (1986), and general interpretation of data in terms of sea-ice cover (from +++ = very extended to --- = very reduced) are indicated. Records are related to the GISP2 ice core record and a sea-surface temperature record (based on foraminifera data) of core 23258 from the Barents Sea shelf. YD = Younger Dryas, 1 = Bølling interval. For location of cores see Figure 18.

Abb. 13: Organischer Kohlenstoffgehalt (TOC in %), Brassicasterol ($\mu\text{g g}^{-1}\text{Sed.}$) und Akkumulationsraten von organischem Kohlenstoff ($\text{g C cm}^{-2}\text{ky}^{-1}$) im Kernabschnitt der letzten 20.000 Jahre von Kern PS2837-5 sowie $\delta^{18}\text{O}$ -Kurve vom GISP2-Eiskern und aus Foraminiferendaten berechnete Oberflächenwassertemperatur in Kern M23258 vom Barentssee-Kontinentalrand. Weiterhin sind Vorkommen von IRD (BIRGEL & HASS 2004) und berechnete Paläoproduktivitäten (nach STEIN 1986) und deren Interpretation in Hinblick auf die Ausdehnung von Meereis dargestellt. Zur Lokation der Kerne siehe Abbildung 18.

Organic-carbon data determined at the same core provide additional qualitative information on the sea-ice cover in the Fram Strait at that time. Minimum total organic carbon (TOC) values and the near absence of the phytoplankton biomarker brassicasterol (indicative for very low diatom productivity) are interpreted to reflect a more or less closed sea-ice cover during the LGM (Fig. 13, BIRGEL & STEIN 2004, STEIN 2008). During the deglaciation, TOC and brassicasterol values as well as organic-carbon accumulation (flux) rates significantly increased, indicating a reduced sea-ice cover and increased primary productivity. An absolute maximum in productivity probably related to a minimum sea-ice cover occurred during the Bølling warm phase (Fig. 13). At that time, primary productivity may have reached $140 \text{ g C m}^{-2} \text{ y}^{-1}$ (following the approach by STEIN 1986), i.e., a value significantly higher than that recorded in this area today (about $50\text{--}100 \text{ g C m}^{-2} \text{ y}^{-1}$, JIN et al. 2012). A second maximum in TOC and brassicasterol was found between about 11 and 9 Cal. kyrs. BP, coinciding with the Early Holocene Thermal Optimum and maximum summer sea-surface temperatures of about $8 \text{ }^\circ\text{C}$ in core 23258 (Fig. 13, SARNTHEIN et al. 2003, BIRGEL & STEIN 2004, for location of core see Fig. 18). These data point again towards a reduced sea-ice cover. In order to get a more detailed and (semi-) quantitative record of sea-ice cover and its variability during glacial to Holocene times, a novel biomarker approach was used in the study of core PS2837-5 (MÜLLER et al. 2009, see below).

A NOVEL BIOMARKER APPROACH FOR SEA-ICE RECONSTRUCTIONS

Our ability to quantitatively reconstruct past sea-ice distributions is now greatly improved by a novel biomarker approach, which is based on the determination of a highly-branched isoprenoid (HBI) with 25 carbon atoms (C_{25} HBI monoene = "IP₂₅"), and developed by BELT et al. (2007). This biomarker is only biosynthesized by diatoms living in the Arctic ice, i.e., it seems to be an Arctic sea-ice diatom-specific biomarker and, as shown by these authors in their original study, seems to be a sensitive and stable proxy for sea-ice in sediments over at least the Holocene. The isotopically very heavy $\delta^{13}\text{C}$ signature of IP₂₅ determined in sea ice, sediment trap material and sediments further supports the use of IP₂₅ as sea-ice proxy (BELT et al., 2008). In sea-ice and sediment samples collected from various locations around Antarctica, on the other hand, no IP₂₅ was found. Instead, a HBI diene could be determined which co-occur in Arctic Ocean sediments together with IP₂₅ (MASSÉ et al. 2011). These authors propose that the presence of this also isotopically ^{13}C enriched HBI diene in Antarctic sediments might be a useful proxy indicator for organic matter derived from sea-ice diatoms. The analytical approach to identify and quantify the IP₂₅ biomarker (as well as the other relevant biomarkers) and currently used in our laboratory at the Alfred Wegener Institute, is summarized in Fig. 14 (cf., MÜLLER et al. 2011, FAHL & STEIN 2012).

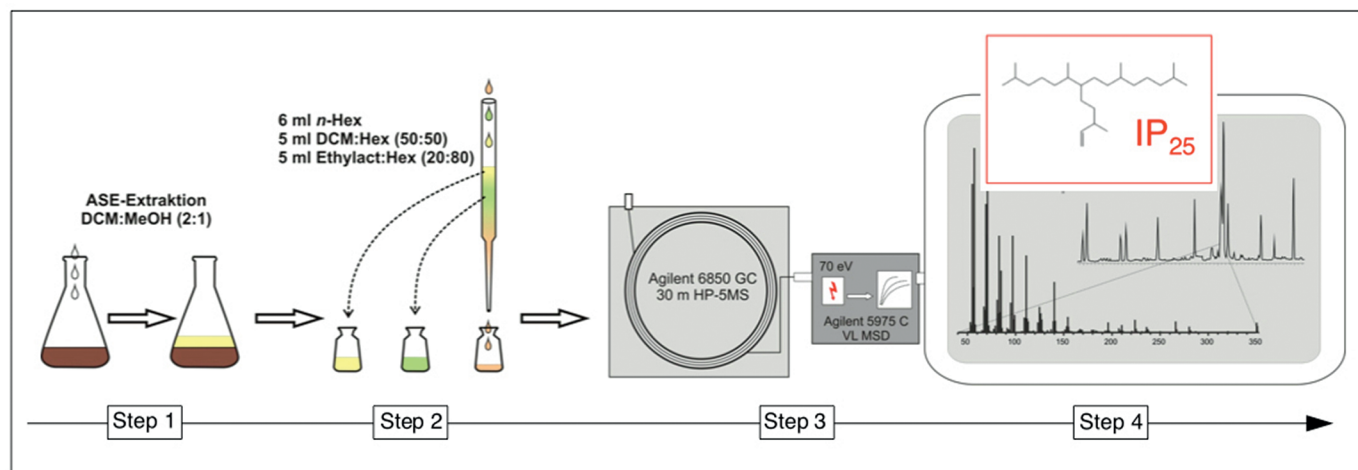


Fig. 14: Scheme summarizing the AWI analytical procedure for identification and quantification of IP₂₅ as well as sterols, developed by K. Fahl and J. Müller at the AWI (cf. MÜLLER et al. 2011; for more details see FAHL & STEIN 2012).

(1) For lipid biomarker analyses, the freeze-dried and homogenised sediments were extracted with an Accelerated Solvent Extractor (DIONEX, ASE 200; $100 \text{ }^\circ\text{C}$, 5 min, 1000 psi) using a dichloromethane/methanol mixture (2:1 v/v). Prior to this step, 7-hexylnonadecane, squalane, and cholesterol- d_6 (cholest-5-en-3 β -ol- d_6) were added as internal standards.

(2) Hydrocarbons and sterols were separated via open column chromatography (SiO_2) using *n*-hexane and methyl-acetate/*n*-hexane (20:80 v/v), respectively. Sterols were silylated with 500 μl BSTFA ($60 \text{ }^\circ\text{C}$, 2 h) (FAHL & STEIN 1999).

(3) Gas chromatography-mass spectrometry (GC-MS) compound analyses of both fractions were performed using an Agilent 6850 GC (30 m HP-5 ms column, 0.25 mm inner diameter, 0.25 μm film thickness) coupled to an Agilent 5975 C VL mass selective detector. The GC oven was heated from $60 \text{ }^\circ\text{C}$ to $150 \text{ }^\circ\text{C}$ at $15 \text{ }^\circ\text{C min}^{-1}$, and then at $10 \text{ }^\circ\text{C min}^{-1}$ to $320 \text{ }^\circ\text{C}$ (held 15 min) for the analysis of hydrocarbons (IP₂₅, C_{25} -HBI-diene, and *n*-alkanes) and at $3 \text{ }^\circ\text{C min}^{-1}$ to $320 \text{ }^\circ\text{C}$ (held 20 min) for sterols, respectively. Helium was used as carrier gas.

(4) Individual compound identification was based on comparisons of their retention times with that of reference compounds (applies to brassicasterol and *n*-alkanes) and on comparisons of their mass spectra with published data (for sterols see BOON et al. (1979) and VOLKMAN (1986), for IP₂₅ see BELT et al. (2007), and for C_{25} -HBI diene see JOHNS et al. 1999). The Kovats Index calculated for IP₂₅ is 2085. Biomarker concentrations were calculated on the basis of their individual GC-MS ion responses compared with those of respective internal standards.

(5) IP₂₅ and C_{25} -HBI diene were quantified using their molecular ion m/z 350 and m/z 348 in relation to the abundant fragment ion m/z 266 of 7-hexylnonadecane and by means of an external calibration curve ($R^2 = 0.9989$) to balance the different responses of the used ions (for further details see FAHL & STEIN, 2012). Brassicasterol (24-methylcholesta-5,22E-dien-3 β -ol) and dinosterol (4 α ,23,24-trimethyl-5 α -cholest-22E-en-3 β -ol) were quantified as trimethylsilyl ethers using the molecular ions m/z 470 and m/z 500, respectively, and m/z 464 for cholesterol- d_6 . Fragment ion m/z 57 was used to quantify the short-chain *n*-alkanes (*n*-C₁₅, *n*-C₁₇, *n*-C₁₉) via squalane. Finally, biomarker concentrations were corrected to the amount of extracted sediment.

Abb. 14: Zusammenstellung der am AWI benutzten und von K. Fahl und J. Müller aufgebauten GC- und GC/MS-Analytik zur Identifizierung und Quantifizierung von IP₂₅, Dien und Sterolen (FAHL & STEIN 1999, 2012, MÜLLER et al. 2011).

In follow-up studies, the identification of this new sea-ice proxy IP_{25} in marine surface sediments and sediment cores from the Canadian Arctic Archipelago (BELT et al. 2008, 2010, VARE et al. 2009), the shelf north off Iceland (MASSÉ et al. 2008), the Barents Sea (VARE et al. 2010), northern Fram Strait and off East Greenland (MÜLLER et al. 2009, 2011, 2012), the Kara and Laptev seas (XIAO et al. 2012) the Lomonosov Ridge (central Arctic Ocean, FAHL & STEIN 2012) as well as from the Bering Sea (MÉHEUST et al. 2012) allowed reconstructions of the ancient sea-ice variability in these regions during the last 30 Cal. kyrs. BP (see maps of Figs. 1, 3 and 15). Within this paper (see below), we demonstrate for the first time that IP_{25} is also preserved in Arctic Ocean sediments as old as 130 to 150 ka (MIS 6). For older (pre-MIS6) sediments, no IP_{25} determinations have been carried out so far (at least according to our knowledge), except for some test measurements in Eocene samples from the IODP-ACEX record (see discussion above and Fig. 1 for location) in which, however, no IP_{25} was found (Stein unpubl. data 2010), and a pilot study of samples from ODP site 912 (Fram Strait; see Fig. 15 for location), in which IP_{25} was even found in two million years old sediments (STEIN & FAHL 2012).

A one-year IP_{25} record is available from a sediment trap deployed in August 2004 at 200 m water depth in Franklin Bay, Arctic Canada (BELT et al. 2008, see Fig. 15, location ARC-6). This one-year proxy record with a prominent IP_{25} maximum in May/June 2005 represents the seasonal sea-ice variability with maximum sea-ice algae growth during spring. For the first time, such an IP_{25} data set was obtained from an array of two sediment traps deployed at the southern Lomonosov Ridge in the central Arctic Ocean at water depth of 150 m and 1550 m ("LOMO-2") and recording the seasonal variability of sea-ice cover in 1994/1995 (FAHL & STEIN 2012, for location see Figs. 1 and 15). The IP_{25} data, together with other biomarker proxies and abundances of different diatom species (FAHL & NÖTHIG 2007, FAHL & STEIN 2012), indicate a predominantly permanent sea-ice cover at the trap location between November 1995 und June 1996 (IP_{25} absent or insignificant), an ice-edge situation with maximum phytoplankton productivity and sea-ice algae input in July/August 1996 (maximum in IP_{25}), and the start of new-ice formation in late September (drop in IP_{25}) (Fig. 16). From these data it seems to be that the maximum August 1996 IP_{25} concentration decreased from about $12 \text{ ng m}^{-2} \text{ d}^{-1}$ to about $2 \text{ ng m}^{-2} \text{ d}^{-1}$ during its fall through the water column from 150 to 1550

Sediment traps

LOMO-2 (FAHL & STEIN 2012)
 Fram Strait; Laptev Sea, Kara Sea (continuing research FAHL et al.
 ARC-6 (BELT et al. 2008)

Surface sediments

Box 1 (MÜLLER et al. 2011)
 Box 2, 3, 4 (continuing PhD research, XIAO et al.
 Box 5 (BELT et al. 2007, 2010)

Deglacial-Holocene sediments

PS2837, MSM5/5-712, -723, PS2641
 (MÜLLER et al. 2009, 2012, unpublished)
 PS2458 (FAHL & STEIN 2012)
 PS72/350 (Stein et al. unpublished)
 BASICC-1, -8, -43 (VARE et al. 2010)
 ARC-3, -4, -5, -6 (BELT et al. 2008, 2010)
 MD99-2275 (MASSÉ et al. 2008)

MIS 3 to MIS 1

PS2185, PS2170, PS2163 (continuing PhD
 research, Xiao et al.)
 PS2767 (Stein et al. unpublished)
 Bering Sea (continuing PhD research;
 MÉHEUST et al.)

MIS 6 to MIS 5 (Saalian/Eemian transition)

PS2138, PS2200, PS2757, PS51/038, PS66/309
 (Stein et al. unpublished)

MIS 6 to MIS 1

PS72/340, PS51/038, PS66/309
 (continuing PhD research, XIAO et al.)

ODP Site 912 (0-2 Ma)

(STEIN & FAHL 2012)

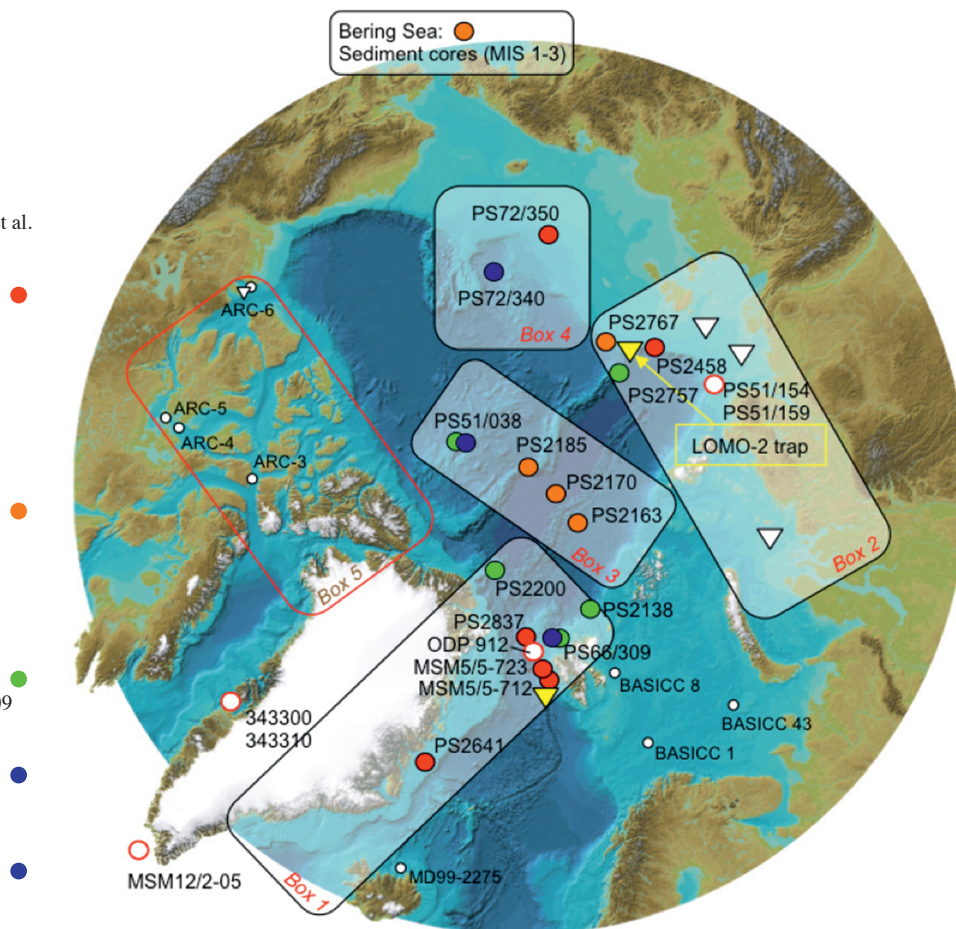


Fig. 15: Map showing locations/areas with published Arctic Ocean IP_{25} data/records and on-going IP_{25} studies at the AWI. In addition, cores selected for future IP_{25} studies in the Baffin Bay (343300 and 343310), south of Greenland (MSM12/2-05), the Laptev Sea (PS51/154 and PS51/159) and ODP Site 912 are shown.

Abb. 15: Übersichtskarte mit Lokationen von Arbeitsgebieten und Kernstationen, an denen Untersuchungen von IP_{25} -Messungen am AWI durchgeführt wurden oder kurzzeitig laufen bzw. geplant sind. Zusätzlich sind Gebiete mit publizierten IP_{25} -Daten anderer Arbeitsgruppen dargestellt. Zitate mit weiteren Details sind angegeben.

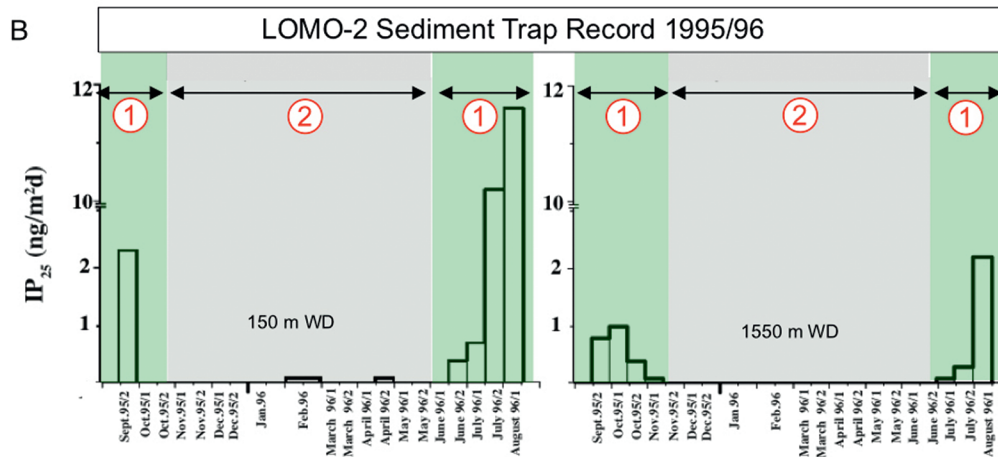
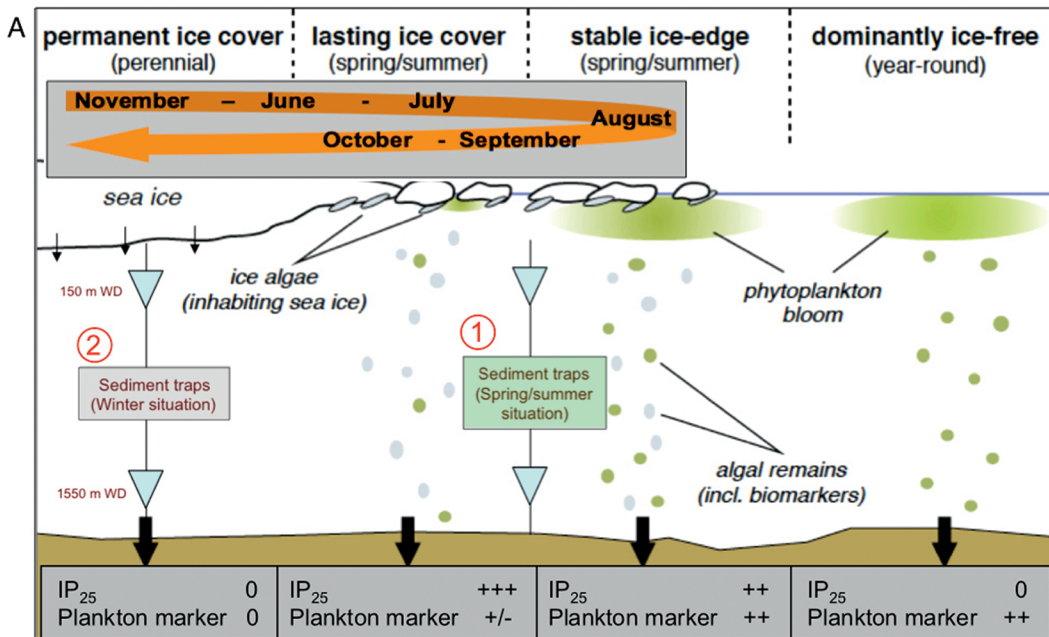


Fig. 16: (A) Generalized scheme of sea surface conditions and respective productivities of ice algae and phytoplankton, and sedimentary content of IP₂₅ and phytoplankton-derived biomarkers for each setting (MÜLLER et al. 2011, supplemented). This scheme indicates the seasonal variability of sea-ice cover in 1995/96 as well as summer/spring (1) and winter (2) situations at the sediment trap location on Lomonosov Ridge. (B) Seasonal variability of IP₂₅ fluxes in 1995/1996 as determined at the shallow (150 m) and deep (1550 m) sediment traps (FAHL & STEIN 2012). For location of trap see Figures 1 and 3.

Abb. 16: (A) Oberflächenwasser-Charakteristika und Schema der Eisalgen- und Phytoplankton-Produktion sowie der IP₂₅- und Phytoplankton-Sedimentdaten (MÜLLER et al. 2011). Skizziert wird die saisonale Meereis-Variabilität mit Sommer-/Frühjahrs-Situation (1) und Wintersituation (2) an der Sedimentfallenposition LOMO-2. B = Saisonale Variabilität von IP₂₅ in den Sedimentfallen aus 150 m bzw. 1550 m Wassertiefe (verändert nach FAHL & STEIN 2012). Zur Lokation der Sedimentfalle vgl. Abbildungen 1 oder 3.

m water depth, i.e., decreased by a factor of about six. This decrease in concentration during transfer through the water column may be related to decomposition and decay of the organic compounds (FAHL & STEIN 2012), a decomposition, which certainly will continue down-core with increasing core depth and age. One should have in mind this process when comparing and interpreting absolute IP₂₅ concentrations in sedimentary records of cores from different environments as well as samples from different core depth and age.

The one-year IP₂₅ record obtained from the LOMO-2 sediment traps also clearly show one known ambiguity in the interpretation of IP₂₅ data (cf., BELT et al. 2007, MÜLLER et al. 2009). IP₂₅ is absent under a permanent ice cover limiting light penetration and, thus, sea-ice algal growth, i.e., IP₂₅ = 0 as it also would be under totally ice-free conditions (Fig. 16). In other words, both extreme climatic situations, i.e., ice-free versus permanent sea-ice cover, would result in the same IP₂₅ value of about zero. Here, MÜLLER et al. (2009, 2011) recently succeeded in overcoming this difficulty of interpreting IP₂₅ data. These authors demonstrated that in surface sediments from the subpolar North Atlantic (cf., Fig. 17) and sediment cores from Fram Strait, the

ambiguity of the IP₂₅ signal can be circumvented by additional use of phytoplankton-derived, open-water biomarkers such as brassicasterol or dinosterol (e.g., VOLKMAN 2006). Under a thick sea-ice cover, both IP₂₅ and the phytoplankton-derived biomarker concentrations are about zero, under open-water conditions IP₂₅ is zero whereas the phytoplankton biomarker concentrations may reach maximum values, and under an ice-edge situation, both IP₂₅ and phytoplankton biomarker concentrations may reach very high values (Fig. 16).

In a next step, MÜLLER et al. (2011) have combined the environmental (sea surface) information carried by IP₂₅ and phytoplankton biomarkers in a phytoplankton-IP₂₅ index, the so-called “PIP₂₅ Index“. Since there is a significant concentration difference between IP₂₅ and phytoplankton-derived biomarkers (e.g., brassicasterol or dinosterol), MÜLLER et al. (2011) recommend using a concentration balance factor *c* (based on mean concentrations of IP₂₅ and the phytoplankton biomarker in a specific data set) for the calculation of the PIP₂₅ index:

$$PIP_{25} = IP_{25} / (IP_{25} + (\text{phytoplankton marker} \cdot c))$$

with $c = \text{mean IP}_{25} \text{ concentration} / \text{mean phytoplankton biomarker concentration}$

The “PIP₂₅ approach” was used successfully to reconstruct (spring) sea-ice coverage in the subpolar North Atlantic (Fig. 17, MÜLLER et al. 2011). The PIP₂₅ ratios shown together with satellite-based sea-ice distribution in Figure 17A, were calculated using brassicasterol as phytoplankton biomarker (“P_BIP₂₅”). Using dinosterol concentrations (instead of brassicasterol) for the calculation of respective PIP₂₅ indices (“P_DIP₂₅”) yields basically similar results for the study area, as pointed out by MÜLLER et al. (2011). For a more quantitative comparison of the biomarker and satellite data, IP₂₅ and PIP₂₅ values were plotted versus the sea-ice concentrations as they are displayed for the individual sediment sampling sites (Fig. 17B, MÜLLER et al. 2011). As expected, IP₂₅ concentrations correlate positively with ice coverage ($R^2 = 0.67$). This correlation, however, also highlights the fundamental ambiguity of the sea-ice proxy as relatively low IP₂₅ contents are observed not only for minimum but also maximum ice coverage. Thus, the sedimentary IP₂₅ content on its own should not be used as a direct measure for sea-ice

concentrations. This and also the slightly higher correlation of PIP₂₅ values with sea-ice concentrations (Fig. 17B, $R^2 = 0.74$) strengthen the argument that the coupling of IP₂₅ with a phytoplankton marker (e.g. brassicasterol) seems to be a valuable and more reliable approach for realistic sea-ice reconstructions (at least in the study area of the polar/subpolar North Atlantic). Furthermore, a comparison of this biomarker-based assessment of the sea-ice distribution in the study area with (1) modern remote-sensing data and (2) numerical-modelling results reveal a good agreement between organic geochemical, satellite and modelling observations (MÜLLER et al. 2011). The good correlation between modelled sea-ice parameters and the biomarker-based estimate of sea ice coverage substantiates that linking proxy and model data occurs to be a promising concept in terms of a cross-evaluation. This integrative data-model approach by MÜLLER et al. (2011) may provide a first step towards more quantitative sea-ice reconstructions by means of IP₂₅.

When using the PIP₂₅ index to distinguish between different sea-ice conditions, one should have in mind that coevally high amounts of both biomarkers (suggesting ice-edge conditions)

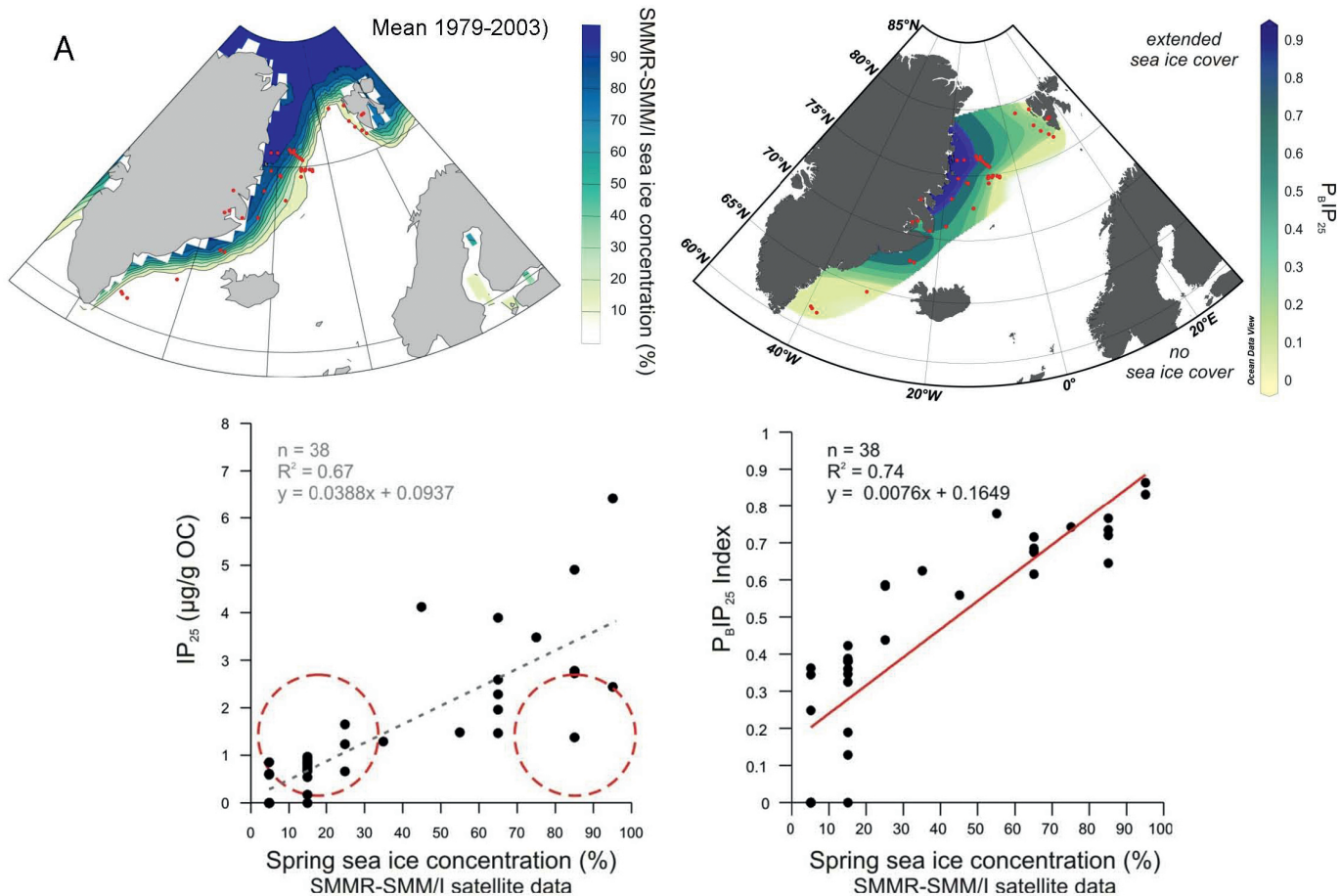


Fig. 17: Top: Comparison of the biomarker-based estimate of sea-ice coverage using the PIP₂₅ index (combination of IP₂₅ and brassicasterol data: P_BIP₂₅) with SMMR-SSM/I satellite derived mean spring (March-April-May) sea-ice concentrations. Red dots indicate location of studied surface sediment samples. Bottom: Correlation of spring (March-April-May) sea-ice concentrations ($\pm 5\%$) derived from satellite data (SMMR and SSM/I; averaged over the period of 1979-2003) with IP₂₅ contents and PIP₂₅ values (combination of IP₂₅ and brassicasterol data: P_BIP₂₅). Coefficients of determination (R^2) are given for the respective regression lines. Red dashed circles highlight low IP₂₅ concentrations, which misleadingly may be interpreted as indicative of low sea-ice concentrations though they result from severe sea-ice coverage limiting ice algae growth; (from MÜLLER et al. (2011)).

Abb. 17: Vergleich der mittels IP₂₅ und PIP₂₅ rekonstruierten Meereisverbreitung mit der auf SMMR-SSM/I-Satelliten-Daten basierenden gemessenen Meereisverbreitung (Frühjahr = März-April-Mai) im nördlichen Nordatlantik. Rote Punkte sind Lokationen der untersuchten Oberflächensedimentproben; (aus MÜLLER et al. 2001).

as well as coevally low contents (suggesting permanent-like ice conditions) would give a similar or even the same PIP_{25} value. Especially, for the latter situation of permanent sea-ice conditions both biomarker concentrations may approach values around zero and the calculation PIP_{25} index may become indeterminable (or misleading). That means, for a correct interpretation of the PIP_{25} data it requires essential awareness of the individual IP_{25} and phytoplankton biomarker concentrations to avoid misleading interpretations (MÜLLER et al. 2011). Although the “ PIP_{25} approach” still has its limitations and needs further development and verification using additional data from other Arctic areas, the main idea of pairing IP_{25} with a productivity measure to distinguish between multiple ice and ice-free conditions, both characterized by zero IP_{25} (as introduced by MÜLLER et al. 2009, 2011), remains an important further development of the original IP_{25} approach.

RECONSTRUCTIONS OF LATE QUATERNARY ARCTIC SEA-ICE VARIABILITY BASED ON IP_{25}

The high potential of the novel biomarker proxies for a more detailed reconstruction of paleo-sea-ice cover and its variability through time is demonstrated in three examples:

- Sea-ice variability in the Fram Strait over the last 30 Cal. kyrs. BP.
- Deglacial to Holocene variability of central Arctic sea-ice cover and the Younger Dryas Event.
- Comparison of historical sea ice and IP_{25} proxy records: The last millennium.

In addition first data from an IP_{25} pilot study of MIS 6 sediments from the northern Barents Sea continental margin, are shortly presented.

Sea-ice variability in the Fram Strait over the last 30 Cal. kyrs. BP

MÜLLER et al. (2009) determined the sedimentary abundance of the novel IP_{25} sea-ice proxy in core PS2837-5, recovered on the Yermak Plateau ($81^{\circ}13.99'N, 02^{\circ}22.85'E$, water depth of 1042 m) during “Polarstern” Expedition ARK-XIII/2 and located close to the modern summer sea-ice margin (Fig. 18, STEIN & FAHL 1997). The 8.76 m thick sedimentary sequence of the core represents the last Glacial to Holocene time interval (NØRGAARD-PEDERSEN et al. 2003). The main aim of the MÜLLER et al. (2009) study was to generate a record of sea-ice conditions in the northernmost Atlantic Ocean for the past 30,000 years, a study which was the first application of the novel sea-ice biomarker IP_{25} in determining Arctic sea-ice records prior to the Holocene.

At 29.6 Cal. kyrs. BP, during a short-lived event, and between 27 and 24 Cal. kyrs. BP, increased IP_{25} and brassicasterol concentrations and fluxes indicate favourable conditions for both sea-ice diatom and phytoplankton growth (Fig. 19). Since primary production is enhanced at the ice edge (SMITH et al. 1987), resulting in higher sedimentary concentrations of marine-derived biomarkers (BIRGEL et al. 2004), these elevated concentrations and fluxes of IP_{25} and brassicasterol probably reveal the occurrence of a fairly stationary ice margin (ca. $81^{\circ}N, 2^{\circ}E$) during this otherwise perennially ice-covered interval (Fig. 19, situation (a)). An ice-edge

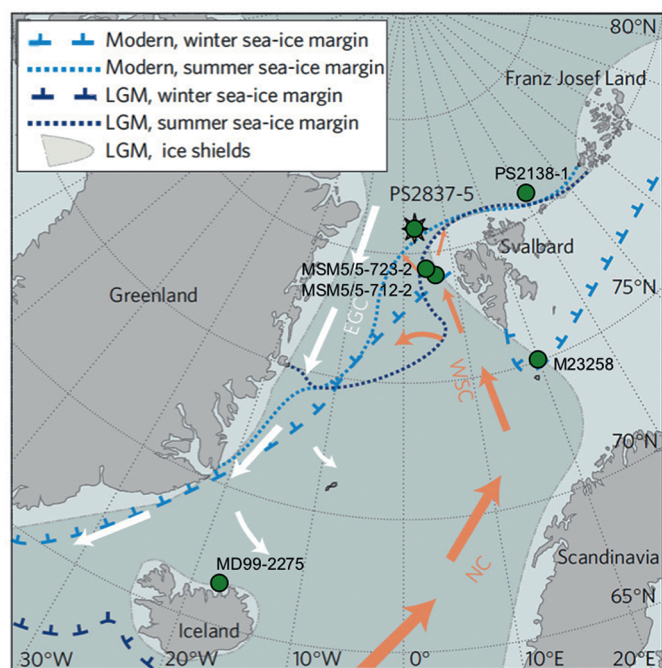


Fig. 18: Map showing the PS2837-5 core site in the northern Fram Strait, major ocean currents and sea-ice margins (from MÜLLER et al. 2009, supplemented). Light-shaded areas indicate the extent of the Greenland, Iceland and Scandinavian Ice Shields during the Last Glacial Maximum (LGM). Orange arrows refer to warm Atlantic Water inflow through the Norwegian (NC) and West Spitsbergen (WSC) currents; white arrows indicate cold polar water transported by the East Greenland Current (EGC). In addition, site locations of other cores discussed in the text, are indicated.

Abb. 18: Karte des Nordatlantiks mit Oberflächenströmungen, Meereisgrenze, und Ausdehnung der Eisschilde im Letzten Glazialen Maximum (LGM). Lokationen von Kern PS2837-5 sowie weiteren im Text genannten Sedimentkernen sind eingezeichnet (MÜLLER et al. 2009, ergänzt).

situation is also supported by PIP_{25} values around 0.5–0.6 (Fig. 19, cf., MÜLLER et al. 2011). For most of the interval between 30 and 17 Cal. kyrs. BP (Late Weichselian to early deglaciation), however, IP_{25} and brassicasterol concentrations (and fluxes) are almost zero, especially during the Last Glacial Maximum (LGM) and the early deglaciation (23.5–17 Cal. kyrs. BP) (Fig. 19). MÜLLER et al. (2009) interpreted the absence of both IP_{25} and brassicasterol as a period of permanently closed sea-ice cover, possibly resulting from an extension of the Svalbard-Barents Sea-Ice Sheet (SBIS) to the shelf edge during this time (ANDERSEN et al. 1996) and a distinct weakening of warm Atlantic water inflow into northern Fram Strait (Fig. 19, situation (b)). Under such conditions, sea-ice diatom and phytoplankton growth is limited since the presence of thick pack ice inhibits light penetration and enhanced stratification reduces nutrient availability. These observations suggest that the summer sea-ice margin during the LGM must have been located south of approx. $81^{\circ}N$.

Coincident with intensified Atlantic Water advection and the onset of the SBIS disintegration at about 17 Cal. kyrs. BP (ANDERSEN et al. 1996, KNIES et al. 1999), higher fluxes of IP_{25} occurred, likely as a result of reduced ice thickness and thus better light penetration and nutrient availability suitable for sea-ice diatom growth. An increase in brassicasterol concentrations lagged those observed for IP_{25} by about 400 yr (Fig. 19), consistent with a progressive retreat of the ice sheet

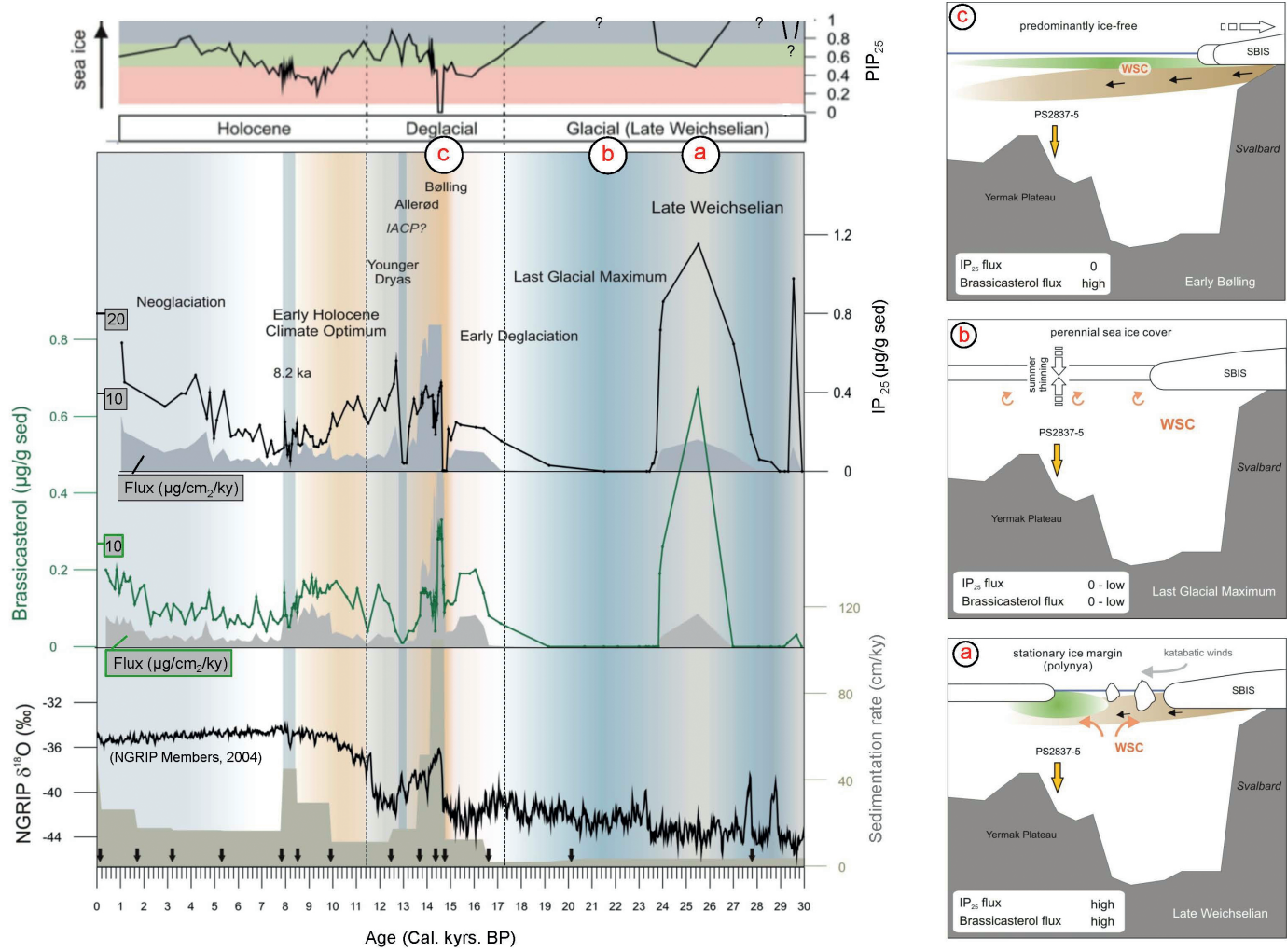


Fig. 19: Concentrations ($\mu\text{g g}^{-1}$ sediment) and accumulation (flux) rates ($\mu\text{g cm}^{-2} \text{ky}^{-1}$) of brassicasterol and IP_{25} , PIP_{25} ratios and sedimentation rates (cm ky^{-1}) of the last 30 Cal. kyrs. BP at core PS2837-5 ((BIRGEL & HASS 2004, MÜLLER et al. 2009) and $\delta^{18}\text{O}$ values from the NGRIP ice core (NGRIP MEMBERS 2004). Black arrows indicate depth of AMS^{14}C datings. Colour code in the PIP_{25} record highlights periods with reduced sea-ice cover (red = $\text{PIP}_{25} < 0.5$) marginal ice zone (green = PIP_{25} between 0.5 and 0.8) and extended ice-cover (grey, $\text{PIP}_{25} > 0.8$) (classification according to Müller et al., 2011). Different paleoenvironmental situations for three specific time intervals are presented in schematic models: (a) late Weichselian, (b) Last Glacial Maximum, and (c) the Bølling warm interval. Supplemented figure based on MÜLLER et al. (2009).

Abb. 19: Biomarkerdaten – IP_{25} , brassicasterol, und PIP_{25} – in Kern PS2837-5 (BIRGEL & HASS 2004, MÜLLER et al. 2009, 2011) sowie $\delta^{18}\text{O}$ -Kurve vom NGRIP-Eiskern. Drei Situationen mit unterschiedlichen Meereisausdehnungen sind dargestellt: (a) spätes Weichsel, (b) Letztes Glaziales Maximum (LGM) und (c) Bølling-Warmintervall (nach MÜLLER et al. 2009).

and more frequent summer ice melt and open water conditions. Close to the onset of the Bølling warm phase shortly after about 15 Cal. kyrs. BP, exceptionally high sedimentation rates resulting from huge deglacial meltwater plumes carrying high amounts of fine-grained terrigenous (Svalbard) material, led to extremely high flux and preservation of brassicasterol (Fig. 19, BIRGEL & HASS 2004, MÜLLER et al. 2009). Coeval with this rapid warming, a sudden drop in IP_{25} fluxes occurred for ca. 200 yr (14.8-14.6 Cal. kyrs. BP), reflecting a significantly reduced sea-ice cover. That means, open water phytoplankton has probably benefited dramatically from such essentially ice-free conditions (Fig. 19, situation (c)).

The Early Bølling was followed by an interval of variable sea-ice cover, probably close to the sea-ice edge (ca. 14.6-13 Cal. kyrs. BP), as reflected by the relatively high IP_{25} and brassicasterol values as well as PIP_{25} ratios between 0.5 and 0.8 (Fig. 19). With the onset of the Younger Dryas (YD) cooling

shortly after 13 Cal. kyrs. BP, IP_{25} and brassicasterol values drop drastically to almost zero, suggesting a distinct increase in sea-ice coverage. An almost identical evolution resulting in maximum sea-ice coverage at the beginning of the YD was recorded at Arctic Ocean core PS2458 (FAHL & STEIN 2012, see further discussion below). During the subsequent Mid-Late YD interval, sea-ice diatom and phytoplankton activity improved due to less severe sea-ice conditions (probably a sea-ice edge situation), as indicated by increased IP_{25} and brassicasterol concentrations and fluxes (Fig. 19). Such conditions probably resulted from a weak but constant inflow of warm water from the Atlantic via the West Spitsbergen Current, generating climate conditions also suitable for primary productivity (MÜLLER et al. 2009).

With the beginning of the Holocene, IP_{25} values decrease whereas at the same time brassicasterol values increase, suggesting diminishing sea-ice conditions. Minimum sea-ice

coverage probably occurs between about 10 and 6.5 Cal. kyrs. BP, i.e., during the Early Holocene Climate Optimum, as indicated by reduced IP₂₅ values and a minimum in PIP₂₅ ratios of <0.4 (Figs. 19 and 20). This is in agreement with multi-proxy compilations based on calcareous microfossils, drift wood, bowhead whale and IP₂₅ data from other Arctic sites (Fig. 21) as well as climate models indicating that early Holocene temperatures were higher than today and that the Arctic

contained less ice, consistent with a high intensity of orbitally-controlled spring and summer insolation that peaked about 10-11 Cal. kyrs. BP and gradually decreased thereafter (Fig. 21, e.g., CRUCIFIX et al. 2002, LASKAR et al. 2004, GOOSSE et al., 2007, JAKOBSSON et al. 2010a, POLYAK et al. 2010).

At about 8.2 Cal. kyrs. BP, i.e., contemporaneously with the prominent “8.2 ka cooling event” (e.g., ALLEY et al. 1997,

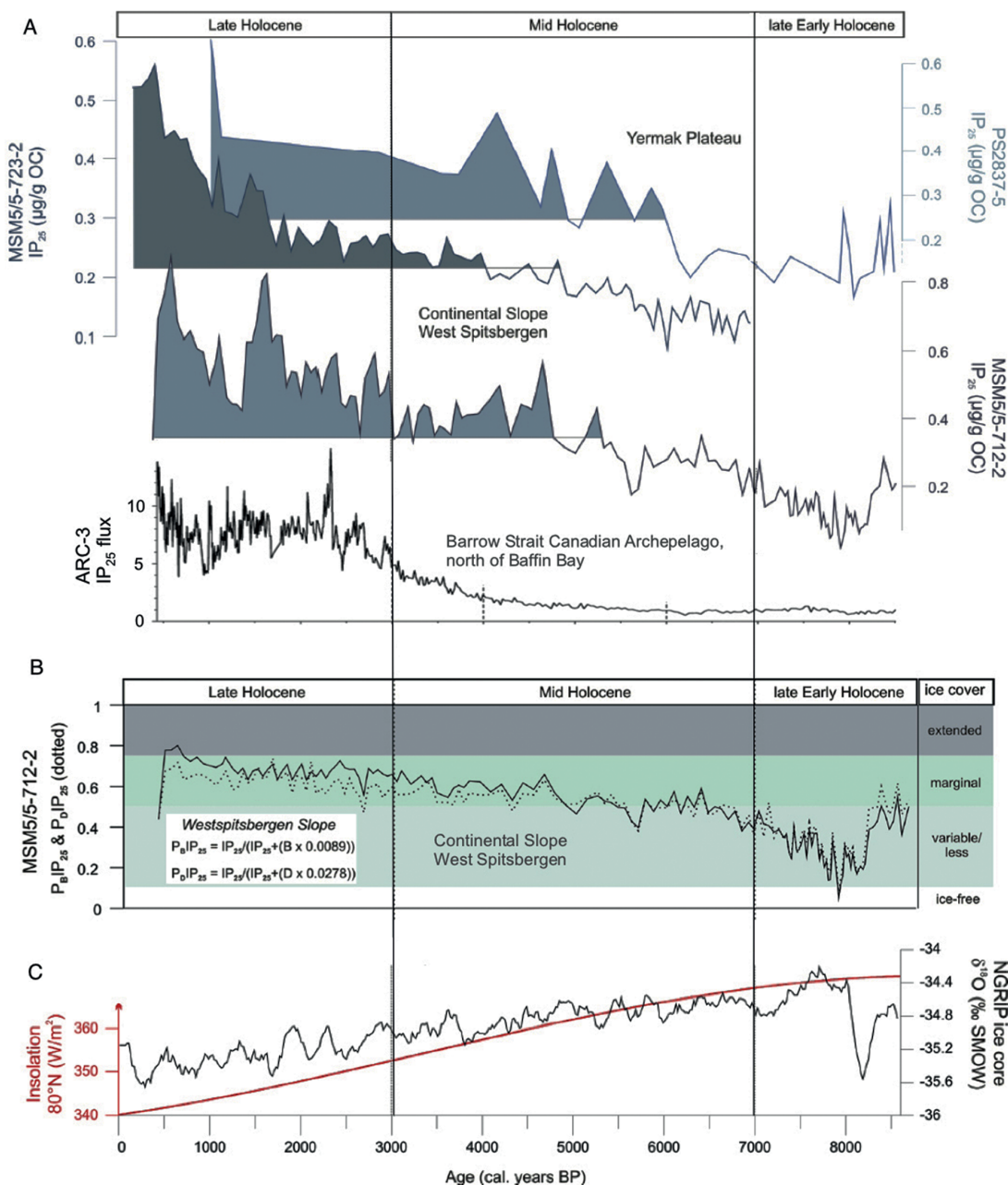


Fig. 20: A = Comparison of IP₂₅ concentrations (standardized to gram organic carbon) of sediment cores from the Yermak Plateau (core PS2837-5) and the eastern Fram Strait (MSM5/5-712-2 and MSM5/5-723-2) (MÜLLER et al. 2012), and IP₂₅ flux rates in core ARC-3 recovered in the Canadian Archipelago area (VARE et al. 2009). B = PIP₂₅ indices calculated for core MSM5/5-712-2, using IP₂₅ and brassicasterol (P_BIP₂₅; solid line) as well as IP₂₅ and dinosterol accumulation rates (P_DIP₂₅; dotted line) and respective balance factors following MÜLLER et al. (2011). Estimates of sea ice conditions (PIP₂₅ > 0.1 variable, PIP₂₅ > 0.5 marginal, PIP₂₅ > 0.75 extended ice cover are highlighted) (after MÜLLER et al. (2012)). C = Summer insolation for 80° N (red curve, LASKAR et al. 2004) and δ¹⁸O values from the NGRIP ice core (NGRIP MEMBERS 2004) strengthen a Holocene cooling. For core locations see figures 1 and 18.

Abb. 20: A = Konzentration von IP₂₅ in Sedimentkernen vom Yermak-Plateau und der Fram-Straße (PS2837-5, MSM5/5-712-2 und MSM5/5-723-2, MÜLLER et al. 2009, 2012) sowie IP₂₅-Fluxraten aus der kanadischen Arktis (ARC-3, VARE et al. 2009). B = PIP₂₅-Verhältnisse von Kern MSM5/5-712-2 (MÜLLER et al. 2012). C = Sommer-Insolationswerte für 80° N (LASKAR et al. 2004) und δ¹⁸O-Werte im NGRIP-Eiskern (NGRIP MEMBERS 2004). Für Kern-Lokationen vgl. Abbildungen 1 und 18.

CLARKE et al. 2004, KLEIVEN et al. 2008), a short-term, rapid decrease is observed in the brassicasterol and IP₂₅ records (Fig. 19). Values are low and similar to those determined for the Early YD and the LGM when near-permanent sea-ice coverage reduced not only the growth of phytoplankton but also that of ice algae. Similarly, MÜLLER et al. (2009) interpreted minimum fluxes of IP₂₅ and brassicasterol as indicative for a near-perennial sea-ice cover at the western Yermak Plateau (northern Fram Strait) at about 8.2 Cal. kyrs. BP.

Coinciding with a mid-late Holocene cooling trend observed in the subpolar North Atlantic domain (e.g., ANDERSEN et al., 2004, HALD et al. 2007, MILLER et al. 2010) and a long-term decrease in summer insolation, IP₂₅ values increased in Fram Strait cores PS2837-5 and, more clearly due to higher resolution record, MSM5/5-712-2 and MSM5/5-723-2 (see Fig. 18 for location), indicating an extension of sea-ice cover (Fig. 20, MÜLLER et al. 2009, 2012). Sustained oceanic surface cooling that stimulated the sea-ice formation during winter and retarded its retreat/melt during the late spring and early summer months is also supported by RASMUSSEN et al. (2007) and JENNINGS et al. (2002) who reconstruct increasingly cooler

conditions along the West Spitsbergen shelf and an increased sea-ice export through Fram Strait by means of benthic and planktic foraminifera and IRD records.

During the last 3-2 Cal. kyrs. BP, the increase in sea-ice coverage as well as amplitude of variability becomes even more pronounced (Fig. 20). Maximum IRD release and a sustained increase in the accumulation of IP₂₅ during the past 3,000 years – a period that is widely acknowledged as Neoglacial cooling phase (for recent review see MILLER et al. 2010) – point to an extended sea-ice cover at the West Spitsbergen continental margin (MÜLLER et al. 2012). Further reconstructions of gradually cooled sea surface temperatures, lowered productivity, and a higher polar water outflow to the Nordic Seas during the past 3,000 years BP support this general increase in sea-ice coverage (KOC et al. 1993, ANDREWS et al. 2001, JENNINGS et al. 2002, ANDERSEN et al. 2004). A very similar and more or less contemporaneous increase in sea-ice cover was also recorded in Barrow Strait, Canadian Archipelago north of Baffin Bay (Fig. 20, VARE et al. 2009, see Figs. 1 and 15 for location), as well as in the Bering Sea (MÉHEUST et al. 2012). The general increase in sea-ice cover and cooling

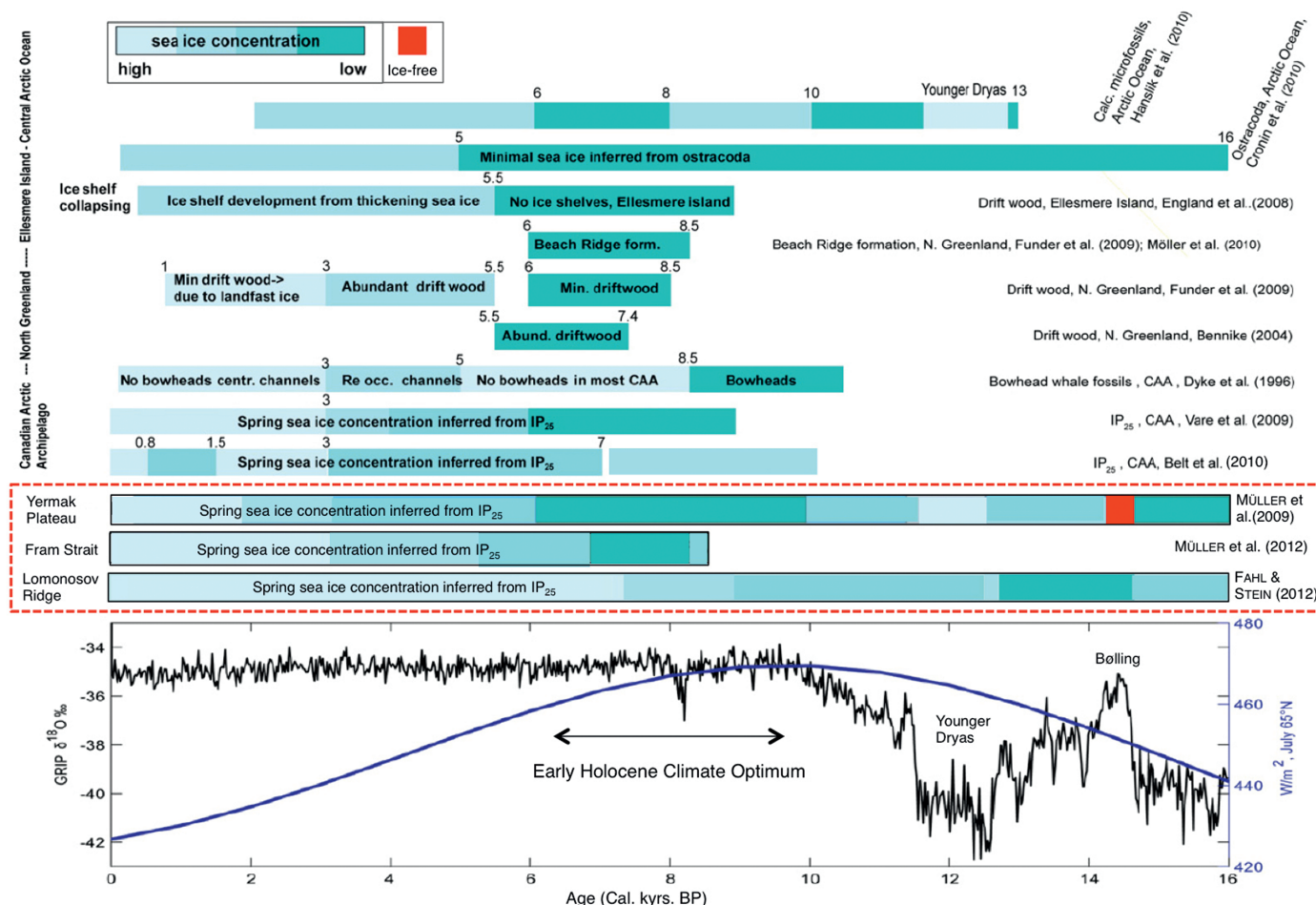


Fig. 21: Summary of results on the Arctic Ocean sea-ice variations throughout the last 15 Cal. kyrs. BP based on different proxy reconstructions (from JAKOBSSON et al. 2010a, supplemented). The inferred scale of sea-ice concentration is a highly qualitative scale in order to compare the results from the different studies. Recent own studies using the novel IP₂₅ biomarker approach are added and highlighted. References are listed at the right margin. The GRIP δ¹⁸O record is from JOHNSEN et al. (2001) and the solar insolation from BERGER & LOUÏRE (1991).

Abb. 21: Übersichtsdarstellung zur Meereisverbreitung im Arktischen Ozean nach verschiedenen Proxydaten während der letzten 15.000 Jahre vor Heute (JAKOBSSON et al. 2010a, ergänzt durch weitere eigene IP₂₅-Datensätze). GRIP δ¹⁸O-Kurve von JOHNSEN et al. (2001), Insulationskurve nach BERGER & LOUÏRE (1991).

of surface waters in the northpolar region during this Neoglac-
 ial cooling phase occur more or less contemporaneously with an advance of glaciers in western Norway (NESJE et al. 2001), a decrease in temperature and precipitation in Siberia (ANDREEV & KLIMONOV 2000), and a decrease in Siberian river discharge into the Arctic Ocean (STEIN et al. 2004). This variability may reflect natural cyclic climate variations to be seen in context with the interannual and interdecadal environmental changes recorded in the High Northern Latitudes over the last decades, such as the North Atlantic Oscillation/Arctic Oscillation (NAO/AO) pattern (e.g., DICKSON et al. 2000). That means, for example, the reduced Siberian river discharge during the past 2-3 Cal. kyrs. BP and vegetation changes in northeast European Russia, indicating the development of a colder and dryer climate in the Eurasian Arctic, may be related to negative NAO-like conditions (STEIN et al. 2004, SALONEN et al. 2011, see MÜLLER et al. 2012 for more detailed discussion).

Deglacial/Holocene variability of central Arctic sea-ice cover and the Younger Dryas Event

In order to study the deglacial/Holocene variability of central Arctic sea-ice cover, core PS2458-4 has been studied in detail for its biomarker composition, focussing on IP₂₅ and brassicasterol data (FAHL & STEIN 2012). The core was recovered from the upper eastern Laptev Sea continental slope (78°09.95' N, 133°23.86' E, water depth 983 m, see Fig. 15 for location) during "Polarstern" Cruise ARK-IX/4 and consists of a 8 m long sedimentary sequence of dominantly very dark olive-gray silty clay of mainly terrigenous origin (FÜTTERER 1994). Based on several AMS-¹⁴C datings carried out on bivalves, a very reliable chronology is available for the sediment section between about 250 and 650 cm core depth (Figs. 22 and 23), representing a time interval between about 14.7 and 9.3 Cal. kyrs. BP (SPIELHAGEN et al. 2005). That means, very prominent cold and warm phases such as the Bølling/Allerød warm period and the Younger Dryas (YD) Cooling Event are represented within the studied sediment section. The base of the core has an extrapolated age of about 16.5 ka, i.e., Heinrich Event 1 (HE 1) was probably recovered in the lowermost part of the core (Fig. 22, FAHL & STEIN 2012).

Looking at the long-term trend of the IP₂₅ record of Core PS2458-4, an increase in IP₂₅ from the Bølling-Allerød warm period towards the Modern is obvious, interpreted as long-term increase in sea-ice cover near the core location (FAHL & STEIN 2012). With the long-term increase in sea ice during deglacial-Holocene times, the HBI diene (C_{25:2}) decreases. This decrease is even more pronounced if the diene/IP₂₅ ratio is used

(Fig. 22). A very similar trend was described by VARE et al. (2009) in a sediment core from the Canadian Arctic Archipelago (see Fig. 15 for location). Following ROWLAND et al. (2001) who found that the more unsaturated HBI isomers (i.e., the diene in comparison to the monoene) are formed at higher diatom growth temperatures, we as well as VARE et al. (2009) postulate warmer climatic conditions during periods characterized by higher relative concentrations of the diene over the IP₂₅, i.e., higher diene/IP₂₅ ratios. That means, the diene/IP₂₅ ratio might be indicative for higher sea-surface temperatures (SSTs). Our interpretation is also supported by the generally positive correlation between diene/IP₂₅ ratios determined in surface sediments from the Kara and Laptev seas and mean summer SST from the same area extracted from the World Ocean Atlas (XIAO et al., 2012).

In Figure 23, the biomarker records of the well-dated core section between 250 and 650 cm core depth are plotted versus age to have a closer look at the short-term variability. Within the Bølling-Allerød warm interval, minimum IP₂₅ and PIP₂₅ values were found. In detail, PIP₂₅ values display three minimum values at 14.6, 13.5, and 13.1 Cal. kyrs. BP (Fig. 23), indicating a minimum sea-ice cover during these events. Further support for warmer, more ice-free climate conditions during that period also comes from the elevated HBI diene concentrations determined in the core PS2458-4 section (FAHL & STEIN 2012). Whereas in the Holocene interval the diene/IP₂₅ ratio is around 3 and shows a low variability, the diene/IP₂₅ ratios are distinctly higher in the Bølling-Allerød period

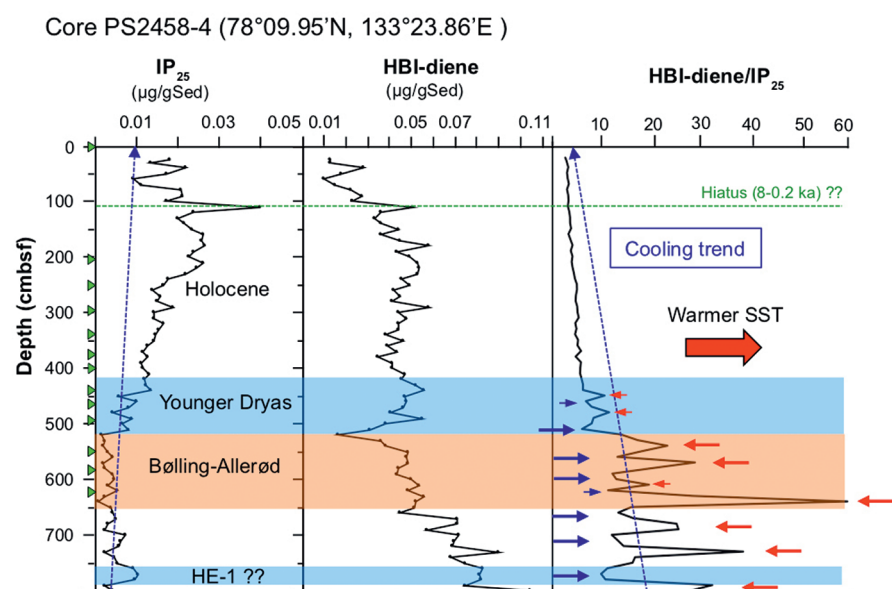


Fig. 22: Concentrations of IP₂₅ and HBI-diene (μg g⁻¹ sed.) and diene/IP₂₅ ratios determined in sediments from core PS2458-4, plotted versus core depth (data from FAHL & STEIN 2012). Bølling-Allerød, Younger Dryas and Holocene intervals are indicated. Green triangles mark depth of AMS-¹⁴C datings, stippled horizontal green line marks a possible hiatus at about 100 cm core depth (for age model see SPIELHAGEN et al. 2005). Heinrich Event 1 (HE 1) is probably represented in the lowermost part of the section if using the extrapolated age of 16.4 Cal. kyrs. BP. Small blue arrows highlight colder intervals, small red arrows highlight warmer intervals. Stippled blue arrows indicate long-term increase in sea ice and cooling trend, respectively. Based on these biomarker records, sea ice and SST display a high-amplitude, centennial-scale variability during deglacial times, whereas towards the Holocene climate became more stable.

Abb. 22: Konzentrationen von IP₂₅ und HBI-Dien (in μg g⁻¹ Sed.) sowie Dien/IP₂₅-Verhältnisse im Kern PS2458-4 (FAHL & STEIN 2012). Die Zeitabschnitte Heinrich-Event 1 (HE-1, extrapoliertes Alter), Bølling-Allerød, Jüngere Dryas und Holozän sind angezeigt. Kleine blaue (rote) Pfeile markieren kalte (warme) Zeitabschnitte.

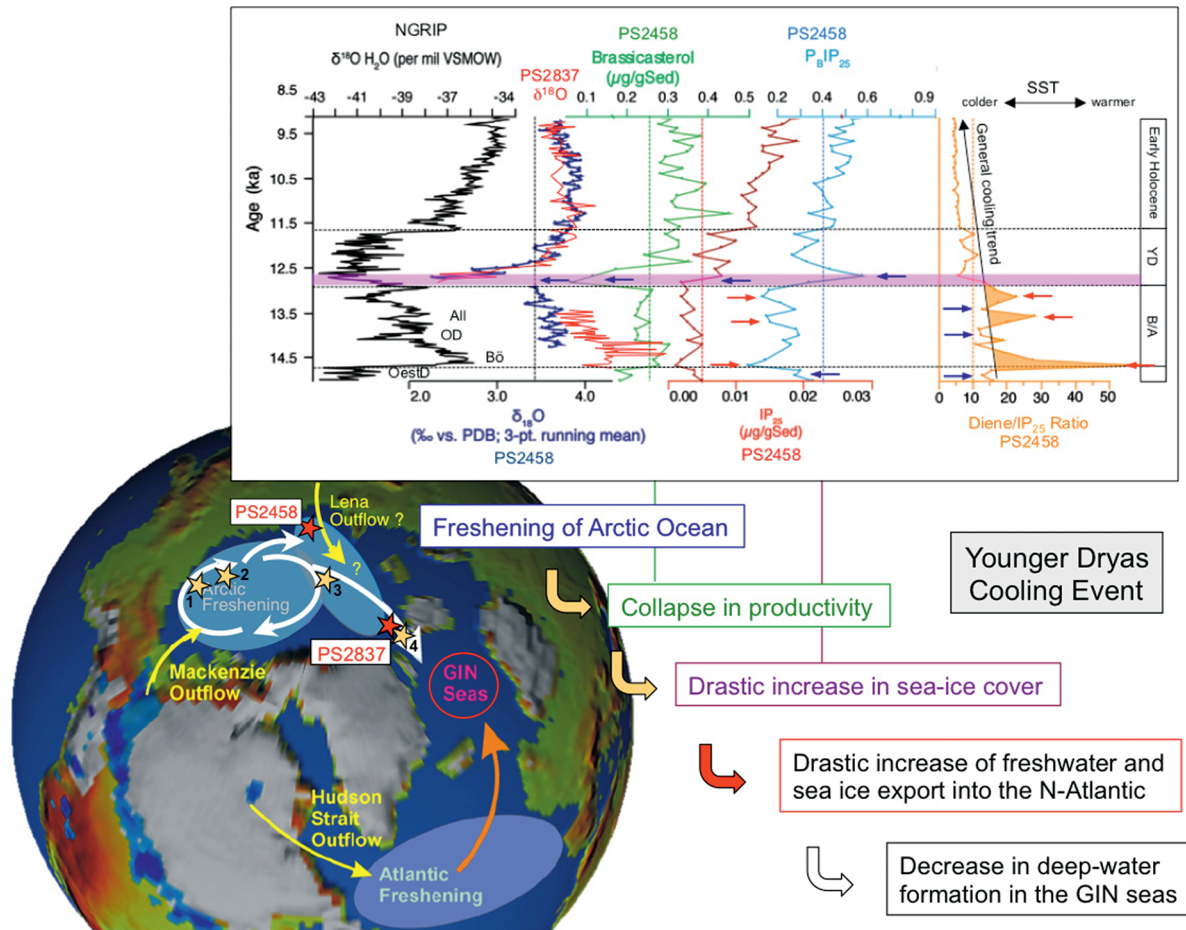


Fig. 23: Oxygen isotopes of planktic foraminifer *Neogloboquadrina pachyderma* sin. (SPIELHAGEN et al. 2005), concentrations of brassicasterol and IP₂₅, diene/IP₂₅ ratio, and PIP₂₅ index (combination of IP₂₅ and brassicasterol data: P_BIP₂₅) determined in the AMS-¹⁴C dated interval 14.7 to 9.3 Cal. kyrs. BP of core PS2458-4, and paleoenvironmental interpretation. In addition, the NGRIP δ¹⁸O record (NGRIP MEMBERS, 2004) as well as a δ¹⁸O record of planktic foraminifer *N. pachyderma* sin. determined at core PS2837-5 (red curve, NØRGAARD-PEDERSEN et al. 2003), are shown. Small blue arrows highlight colder intervals, small red arrows highlight warmer intervals. The long black arrow indicates long-term cooling trend. All = Allerød; OD = Older Dryas; Bø = Bølling; OesD = Oldest Dryas; YD = Younger Dryas; B/A = Bølling/Allerød. (from FAHL & STEIN 2012, supplemented). In the map of the Northern Hemisphere, areas in which intense freshwater forcing likely occurred, and distribution of land ice (light grey) and pro-glacial lakes (blue) at the beginning of the Younger Dryas (12.9 Cal. kyrs. BP) are shown (PELTIER et al. 2006, supplemented). As possible additional (more local) source for freshwater supply into the Arctic Ocean, Lena discharge into the Laptev Sea was added (according to SPIELHAGEN et al. 2005). Locations of cores showing distinct deglacial meltwater events in δ¹⁸O and δ¹³C records of planktic foraminifers near the Younger Dryas Event, are indicated: 1 = Chukchi margin (POLYAK et al. 2007); 2 = Mendeleev Ridge (POORE et al. 1999); 3 = Eurasian Basin (STEIN et al. 1994a, 1994b, NØRGAARD-PEDERSEN et al. 1998, 2003); 4 = Fram Strait (BAUCH et al. 2001a) as well as Yermak Plateau core PS2837-5 (NØRGAARD-PEDERSEN et al. 2003).

Abb. 23: δ¹⁸O-Kurve von planktischen Foraminiferen (SPIELHAGEN et al. 2005), Konzentrationen von Brassicasterol und IP₂₅, Dien/IP₂₅ und PIP₂₅-Verhältnisse (FAHL & STEIN 2012) im Kern PS2458-4 und δ¹⁸O-Kurve von planktischen Foraminiferen im Kern PS2837-5 (NØRGAARD-PEDERSEN et al. 2003) für den Zeitabschnitt 14.7 bis 9.3 ka sowie Interpretation der Proxydaten in Hinblick auf Süßwassereintrag, Meereisbildung, Meereisexport und Tiefenwasserbildung im Nordatlantik (ergänzt nach FAHL & STEIN 2012). Die Karte zeigt Gebiete mit verstärktem Süßwassereintrag zum Beginn der Jüngerer Dryas (ergänzt nach PELTIER et al. 2006). Lokationen von Sedimentkernen mit starkem Süß-/Schmelzwassersignal zum Beginn der Jüngerer Dryas sind eingetragen (Ziffern 1 bis 4)

and vary between about 10 and 60 (Fig. 23), i.e., the more unsaturated HBIs become more predominant in comparison to IP₂₅, suggesting significantly warmer but also more variable climate conditions during this time interval. The absolute maximum in the diene/IP₂₅ ratio of 60, coinciding with the absolute PIP₂₅ minimum of 0.05, supports minimum sea-ice (probably almost ice-free) conditions during the peak Bølling warm interval (Fig. 23, FAHL & STEIN 2012). Such extreme ice-free conditions during the Bølling peak warm interval were also described in core PS2837-5 from Fram Strait, contemporaneously with a distinct maximum in phytoplankton productivity (Figs. 19 and 21, MÜLLER et al. 2009).

At the end of the Bølling-Allerød interval, i.e., towards the transition to the YD cold interval, major changes in fresh-

water discharge, primary productivity, and sea-ice cover were recorded in the sedimentary section of core PS2458-4. With the onset of the YD, a strong freshwater signal was determined by a very prominent minimum in δ¹⁸O of planktic foraminifers (Fig. 23, SPIELHAGEN et al. 2005). The exact onset of the rapid outburst of freshwater is somewhat critical as directly below the δ¹⁸O minimum at 12.7 Cal. kyrs. BP foraminifers are absent in the sediments, interpreted as a drop in salinity below critical limit for foraminifer growth. That means that probably at this time (about 13 Cal. kyrs. BP) the maximum freshwater discharge occurred (SPIELHAGEN et al. 2005). Parallel to the distinct freshwater event, phytoplankton productivity seems to be drastically decreased, followed by a sudden increase in sea-ice cover, as reflected in the abrupt drop in brassicasterol concentrations and the very prominent PIP₂₅ increase,

respectively (Fig. 22, FAHL & STEIN 2012). These data may indicate that enhanced freshwater flux related to a local Lena river input (SPIELHAGEN et al. 2005) and/or contributions from other (Canadian?) freshwater sources (FAHL & STEIN 2012) may have increased sea-ice formation in the southern Lomonosov Ridge area close to the Laptev Sea continental margin at the beginning of the YD (for further discussion see FAHL & STEIN 2012).

Some evidence for a distinct freshwater event near the beginning of the YD was also found in sediment cores from other Arctic Ocean areas. For example, during the last deglaciation, strong meltwater signals are recorded in sharp depletions in $\delta^{18}\text{O}$ as well as $\delta^{13}\text{C}$ values determined in planktic foraminifers in sediment cores from the Mendeleev Ridge and Makarov Basin through the Lomonosov Ridge and Amundsen Basin to the eastern Gakkel Ridge/Nansen Basin region (STEIN et al. 1994a, 1994b, NØRGAARD-PEDERSEN et al., 1998, 2003, POORE et al. 1999, ANDERSSON et al. 2003, POLYAK et al. 2007). Very low sedimentation rates, however, make it difficult to clearly identify the YD Event in these cores. "Marine" evidence for a major Mackenzie drainage event in the Canadian Arctic related to the decay of the Laurentide Ice Sheet, and increased sea-ice formation at the onset of the YD was proposed from elevated IRD with a mineralogical (dolomite) signature indicative for a Canadian origin, found in a sediment core from Lomonosov Ridge close to the North Pole (NOT & HILLAIRE-MARCEL 2012). Finally, a strong contemporaneous meltwater input from the Arctic Ocean into the North Atlantic was also deduced due to the distinct decrease in planktic $\delta^{18}\text{O}$ identified in the Fram Strait core PS1230-1 (BAUCH et al. 2001a; see Fig. 11 for location) as well as in the Yermak Plateau core PS2837 (Fig. 23, NØRGAARD-PEDERSEN et al. 2003) at the beginning of the YD interval. Thus, the described deglacial freshwater and sea-ice event (probably) coinciding

with the YD Cooling Event, seems to be a basin-wide event having influenced the entire Arctic Ocean.

The importance and consequences of such a major Arctic Ocean freshwater and sea-ice event has to be seen in context with the ongoing discussion of trigger mechanisms for the onset of the YD cooling event, e.g., an extraterrestrial impact hypothesis (ISRADE-ALCÁNTARA et al. 2011 and references therein) and a paleoceanography-driven hypothesis (e.g., BROECKER et al. 1989, MCMANUS et al. 2004, BROECKER 2006). Most recently BROECKER et al. (2010) concluded that, based on the study of Terminations IV to I in Antarctic ice-core records, there is perhaps even no need for a one-time catastrophic event to explain the YD and similar YD-like events accompanied previous deglacial periods as well. In the paleoceanography community, there is still broad support for the hypothesis that the YD cooling event was probably a response to a slowdown in Atlantic Meridional Overturning Circulation (AMOC) due to a huge meltwater input into the North Atlantic, related to the deglacial decay of the Laurentide Ice Sheet (e.g., BROECKER et al. 1989, MCMANUS et al. 2004, BROECKER 2006). Here, almost contemporaneously with the onset of the YD, a huge outflow event of $9.5 \cdot 10^3 \text{ km}^3$ freshwater (or a flux of 0.30 Sv if assuming a release within one year) from the North American glacial Lake Agassiz into the North Atlantic has been proposed (e.g., TELLER et al. 2002), which may have weakened the deep-water formation in the Greenland, Icelandic, Norwegian seas and, thus, the global THC during this interval (BROECKER et al. 1989, CLARK et al. 2002, TELLER et al. 2002, MCMANUS et al. 2004). There is, however, an ongoing debate about the origin and pathways of freshwater (Fig. 23, e.g., BROECKER 2006, BROECKER et al. 2010), i.e., whether the freshwater/meltwater was directly supplied (via Hudson Bay) into the Atlantic Ocean (BROECKER et al. 1989) or whether the drainage of Lake Agassiz was towards the

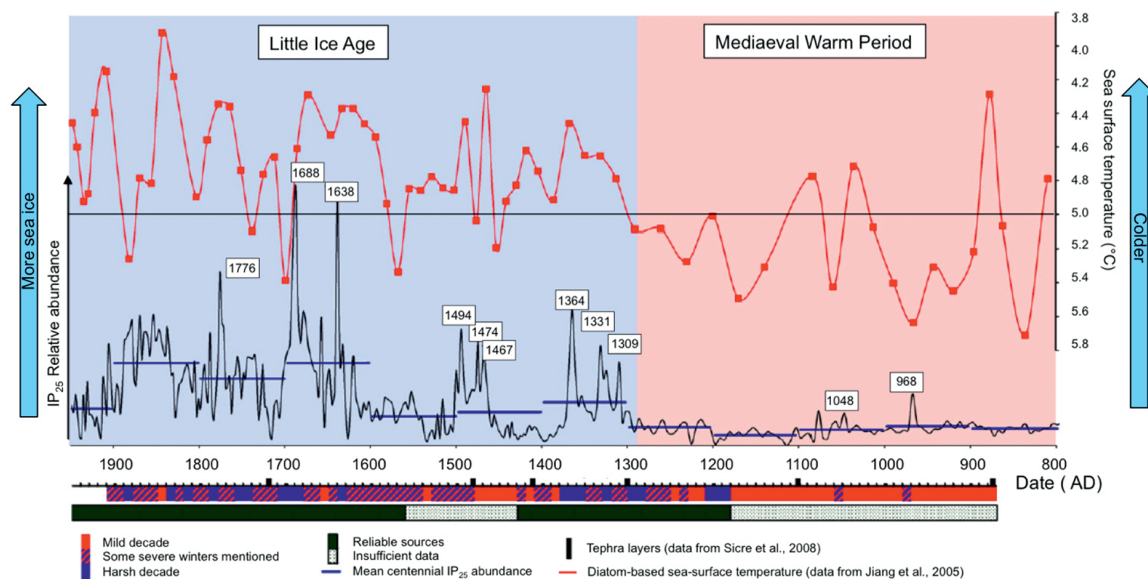


Fig. 24: Relative abundances of IP_{25} determined in core MD99-2275 for the period 800-1950 AD in comparison to historical records of Icelandic sea ice (according to OGILVIE 1992 and OGILVIE & JÓNSSON 2001) and diatom-based sea surface temperature. Note the reversed scale of the sea surface temperature. Six tephra layers were used to constrain the (AMS^{14}C -dated) age model (SICRE et al. 2008). Figure from MASSÉ et al. (2008), supplemented.

Abb. 24: Relative Konzentrationen von IP_{25} in Kern MD99-2275 für den Zeitabschnitt 800-1950 (MASSÉ et al. 2008) im Vergleich zu historischen Aufzeichnungen der Meereisverbreitung um Island (OGILVIE 1992 und OGILVIE & JÓNSSON 2001) und rekonstruierten Oberflächenwassertemperaturen nach Diatomeenverteilungen. Abbildung ergänzt aus MASSÉ et al. (2008).

Arctic Ocean with a subsequent export of freshwater through Fram Strait into the Atlantic (TARASOV & PELTIER 2005, PELTIER et al. 2006). PELTIER et al. (2006), for example, could show that such freshening of the surface of the Arctic Ocean would have been as efficient for shutting down the Atlantic THC as would direct Atlantic freshening. A third option, of course, could be that both hypotheses are right.

As stated by BROECKER (2006), a clear proof of the path taken by the flood was still missing. MURTON et al. (2010) could identify such a missing flood path, evident from gravels and a regional erosion surface, running through the Mackenzie River system in the Canadian Arctic Coastal Plain. From optically stimulated luminescence (OSL) dating, these authors have determined the approximate age of this Mackenzie River flood into the Arctic Ocean to be shortly after 13 Cal. kyrs. BP, supporting the hypothesis that a trigger of the YD Event may have been along the Arctic route. Our new data from core PS2458 certainly cannot prove or disprove this hypothesis. However, these data (Fig. 23), especially in combination with the other $\delta^{18}\text{O}$ records of planktic foraminifers from the central Arctic Ocean towards the Fram Strait (see above), point at least to increased, wide-spread freshening and sea-ice formation in the Arctic and related freshwater and sea-ice export through Fram Strait near the beginning of the YD. That means, these observations are in line with the hypothesis that freshwater (and ice) export from the Arctic into the North Atlantic may have played an important trigger role during the onset of the YD cold reversal, as proposed by TARASOV & PELTIER (2005).

Comparison of historical sea ice and IP_{25} proxy records: The last millennium

MASSÉ et al. (2008) have measured the sea-ice proxy IP_{25} to obtain a complete and continuous, high resolution (ca. 2–5 yr!) record of sea-ice distribution for the last millennium, using a well-dated sediment core recovered from the area directly north of Iceland and characterized by very high sedimentation rates (core MD99-2275: 66° 33.06' N, 17° 41, 59' W, 410 m water depth, for location see Fig. 18). This unique high-resolution proxy record was compared with historical data documenting past sea ice over the last about one thousand years (i.e., going back to the early days of Icelandic colonization, OGILVIE 1992 and OGILVIE & JÓNSSON 2001) and with diatom-based sea surface temperature reconstructions, indicating a strong correlation between these data sets on both longer and shorter time scales (JIANG et al. 2005) (Fig. 24). That means, during the Warm Mediaeval Period (MWP) between 800 and 1300 AD the Icelandic climate was relatively mild and sea ice extension was reduced. During the time interval between 1300 and 1900 AD, a period corresponding to the Little Ice Age (LIA), on the other hand, the climatic conditions around northern Iceland deteriorated, i.e., this period is characterized by a significant cooling of surface water and an increase in sea ice. Even on shorter-time scales, partly excellent correlations between historical observations and IP_{25} values are obvious, indicating abrupt climate changes around Iceland. For example, the IP_{25} record displays strong peaks in sediments dated to 1776, 1688, 1638, 1364, 1331 and 1309, corresponding to decades where large amounts of sea ice have been described around Iceland (OGILVIE & JÓNSSON 2001) and colder diatom-based sea

surface temperatures have been determined (JIANG et al. 2005) (Fig. 24, MASSÉ et al. 2008). With this high-resolution study, MASSÉ et al. (2008) could demonstrate very well that IP_{25} is a reliable proxy for historical sea ice reconstructions.

Pilot study of core PS2138-1: IP_{25} found in MIS 6 sediments

So far, IP_{25} could be detected in sediments no older than 30 Cal. kyrs. BP (MÜLLER et al. 2009). However, in order to test whether IP_{25} can also be found in sediments older than 30 ka (MÜLLER et al., 2009), we carried out a pilot study, using a set of samples taken from core PS2138-1 representing the last 150 Cal. kyrs. BP (i.e., MIS 6 to MIS 1, for core location see Fig. 18). In previous studies of this well-dated sediment core, detailed sedimentological, organic geochemical and micropaleontological investigations were performed for reconstruction of the late Quaternary history of the Svalbard-Barents Sea Ice Sheet and related paleoceanographic circulation patterns in the Arctic Ocean along the Barents Sea continental margin (KNIES et al. 1999, 2000, MATTHIESSEN & KNIES 2001, WOLLENBURG et al. 2001, 2004).

Using a transfer function approach to estimate paleoproductivity from relative abundance data of benthic foraminiferal species, WOLLENBURG et al. (2001, 2004) determined the paleoproductivity and its change during the last about 150 Cal. kyrs. BP in core PS2138-1 (Fig. 25). From this record it is obvious that calculated paleoproductivity values generally correlate with the growth and decay of the Svalbard Ice Sheet (ELVERHØI et al. 1995, KNIES et al. 1998, MANGERUD et al. 1998). The highest paleoproductivity occurred in interglacial period MIS 5.5 and at the termination of interstadials to stadials within MIS substages 6.3(?), 5.3, 5.1, 3.2, and Termination Ia. These productivity maxima are related to distinct ice retreat and partly coincide with the increased inflow of temperate and saline Atlantic Water into the Arctic Ocean (WOLLENBURG et al. 2001). During glacial periods, on the other hand, productivity was significantly reduced, suggesting increased sea-ice cover. During the latter intervals, also significant concentrations of the sea-ice proxy IP_{25} were found, in accordance with the interpretation by Wollenburg et al. (2001) (Fig. 25).

Although only a limited number of samples have been studied for IP_{25} here and also large gaps exist in the record of core PS2138-1, these preliminary results are very promising. Our qualitative IP_{25} data indicate that IP_{25} may also occur in sediments as old as MIS 6, i.e., the IP_{25} approach can also be used for the reconstruction of sea-ice cover during glacials significantly older than MIS 2. A more detailed IP_{25} study of MIS 5 and MIS 6 sedimentary sections from several Arctic Ocean cores is underway (see Fig. 15, STEIN et al. unpublished).

CONCLUSIONS AND OUTLOOK

Arctic Ocean sea-ice cover and its change through Cenozoic times

The Cenozoic history of Arctic Ocean sea-ice cover can be reconstructed by different sedimentological, mineralogical, micropaleontological, and organic-geochemical proxies, as

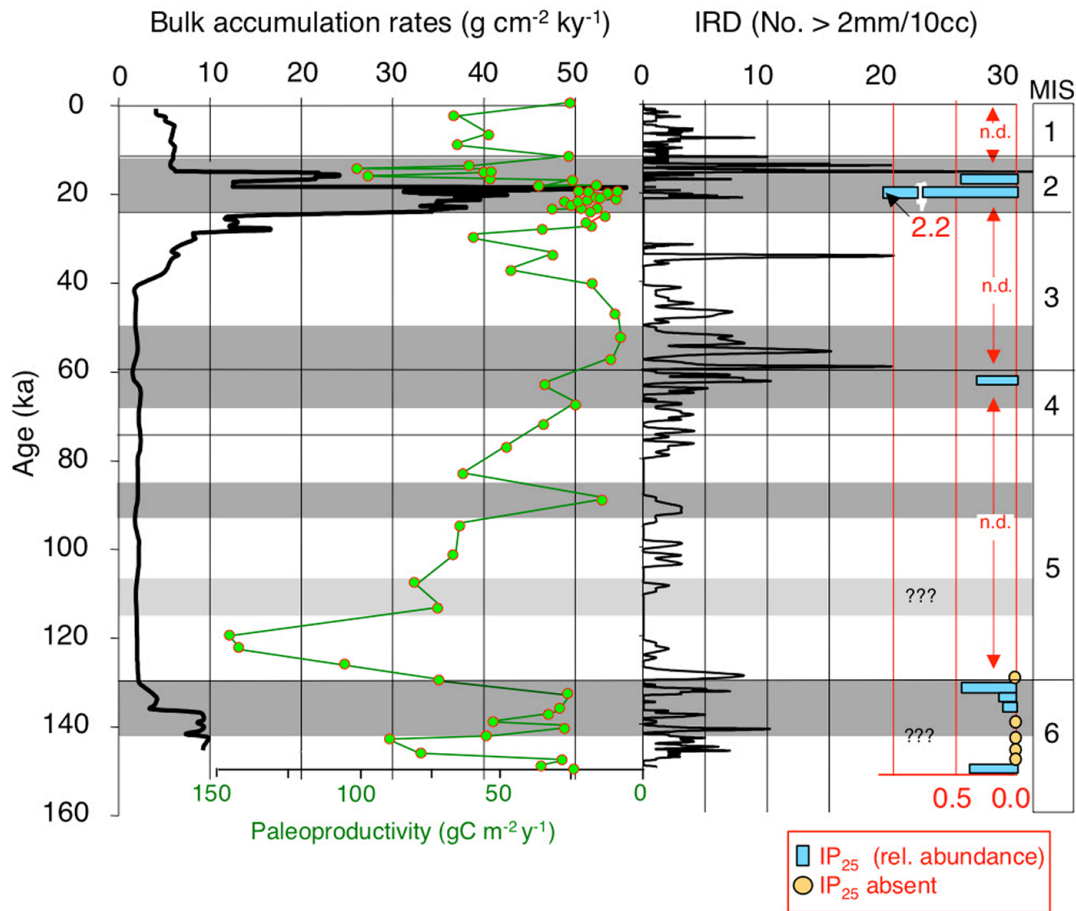


Fig. 25: Relative abundance of IP₂₅ (this study), bulk accumulation rates and IRD variability (KNIES et al. 2000) and a paleoproductivity record based on benthic foraminifers (WOLLENBURG et al. 2001) determined for core PS2138-1 (for location see Fig. 18) and plotted *versus* age. Within our pilot study the first IP₂₅ measurements were carried-out in a selected set of samples, proving that IP₂₅ is even preserved in sediments as old as about 150 ka (MIS 6); n.d. = no data so far. Grey bars indicate time intervals of an extended ice sheet on Svalbard (MANGERUD et al. 1998). According to WINKELMANN et al. (2008), the extension of the ice sheet was much smaller around 110 ka (MIS 5.4) than originally proposed by MANGERUD et al. (1998) (light grey bar).

Abb. 25: Relative Konzentration von IP₂₅ (diese Arbeit), Gesamtakkumulationsraten und IRD-Verteilungen (KNIES et al. 2000) und aus benthischen Foraminiferenvergesellschaftungen berechnete Paläoproduktivitäten (WOLLENBURG et al. 2001) im Kern PS2138-1 für den Zeitabschnitt der letzten 150 ka (MIS 6 bis MIS 1). Graue Balken zeigen Zeitabschnitte mit ausgedehnter Vereisung auf Svalbard (MANGERUD et al. 1998).

presented and discussed for a selected set of examples in this review paper.

- Records of ice-rafted debris (IRD), specific sea-ice related needle-shaped diatoms, and mineralogical composition of the terrigenous sediment fraction determined in the ACEX drill core recovered on Lomonosov Ridge during IODP Expedition 302, give information about the first onset of Arctic Ocean seasonal sea-ice cover at about 47 Ma, the development of first perennial (?) sea-ice cover near 14 Ma, and the variability of sea-ice cover through Neogene-Pleistocene times (e.g., DARBY 2008, KRYLOV et al. 2008, ST. JOHN 2008, STICKLEY et al. 2009, O'REGAN et al. 2010).
- Records of IRD and its mineralogy, in combination with abundances of planktic foraminifers, allowed reconstruction of glacial and interglacial variability of sea-ice cover and ice-sheet fluctuations during late Quaternary times, i.e., MIS 6 to MIS 1 (e.g., SPIELHAGEN et al. 1997, 2004, STEIN 2008). These data, however, also raise new interesting questions about pre-MIS 6 variations that need to be studied more carefully (e.g., POLYAK et al. 2009, 2010, O'REGAN et al. 2010).

- Fluxes of planktonic foraminifers and $\delta^{18}\text{O}$ records determined in well-dated sediment cores from the Eurasian sector of the Arctic Ocean constrained sea-ice distribution during the Last Glacial Maximum (LGM) (e.g., NØRGAARD-PEDERSEN et al. 2003).
- Abundances of specific Fe oxides determined in a sediment core from the central Fram Strait were used to identify the circum-Arctic source areas of the terrigenous sediment fraction (IRD), providing insights into the LGM, deglacial to Holocene Arctic Ocean sea-ice cover and ice-sheet decay (DARBY et al. 2002).
- The "IP₂₅" sea-ice proxy in combination with phytoplankton biomarkers (BELT et al. 2007, MÜLLER et al. 2009, 2011) determined in sediment cores from the Fram Strait and from the southern Lomonosov Ridge close to the Laptev Sea continental margin, allowed reconstructions of the Arctic Ocean sea-ice cover and its variability over the last 30 ka, suggesting extended sea-ice cover during the LGM, minimum sea-ice cover (to ice-free conditions) during the Bølling as well as the Early Holocene Climate Optimum, and significantly increased sea-ice cover at the onset of the Younger Dryas (YD) Cooling Event and during the late

Holocene “Neoglacial” period (MÜLLER et al. 2009, 2012, FAHL & STEIN 2012).

- The freshening of the Arctic Ocean, coinciding with a prominent increase in sea-ice cover at the onset of the YD may support the hypothesis that Arctic Ocean freshwater and sea-ice export might have been an important mechanism for shutting down the North Atlantic Deep Water (NADW) formation, triggering the YD cooling event (BROECKER 2006, NOT & HILLAIRE-MARCEL 2012, FAHL & STEIN 2012).
- The diene/IP₂₅ ratio – possibly a new proxy for SST reconstruction – reached maximum values during the Bølling-Allerød warm period and decreased during the Holocene cooling trend (FAHL & STEIN 2012).
- Observations of historical sea ice records off northern Iceland during the last millennium demonstrates a strong correlation between documented sea ice occurrences and the IP₂₅ proxy record (MASSÉ et al. 2008).
- For the first time, IP₂₅ could be identified in Arctic Ocean sediments older than 30 ka, i.e., IP₂₅ was found 150 ka old (MIS 6) in sediments from core PS2138-1 recovered at the Barents Sea continental margin.

IP₂₅, PIP₂₅, and diene/IP₂₅: challenges for future paleoenvironmental reconstructions

The novel IP₂₅ approach (BELT et al. 2007) is certainly a very promising proxy approach that may allow more detailed reconstructions of past Arctic Ocean sea-ice cover. The combination of IP₂₅ with a phytoplankton marker (in terms of a phytoplankton marker-IP₂₅ index “PIP₂₅”, MÜLLER et al. 2011) proves highly valuable to properly interpret the sea-ice proxy signal as an under- or over-estimation of sea-ice coverage can be circumvented and more quantitative estimates of paleo-sea-ice coverage seem to be possible. Although the “PIP₂₅ approach” still has its limitations and needs further development and verification by additional data from other Arctic areas, the fundamental idea of pairing IP₂₅ with a phytoplankton productivity measure to distinguish between multiple ice conditions characterized by zero IP₂₅ (as introduced by MÜLLER et al. 2009, 2011), remains an important development of the original IP₂₅ approach. Based on the new biomarker data from core PS2458-4 (FAHL & STEIN 2012, and this paper) as well as surface sediments from the Kara-Laptev seas (XIAO et al. 2012), we propose that the diene/IP₂₅ ratios might have a potential for becoming a new temperature proxy for low-SST environments (cf. ROWLAND et al. 2001, SACHS et al. 2008). To prove this hypothesis, however, certainly more ground-truth data are needed.

In order to establish the IP₂₅ approach as key proxy for the reconstruction of past Arctic Ocean sea-ice conditions, however, more basic data from sea ice and sediment traps (i.e., algae abundances, IP₂₅, phytoplankton biomarkers, IRD) as well as surface sediments and sediment cores (IP₂₅, phytoplankton biomarkers, IRD) with large spatial coverage from different environments of the entire Arctic Ocean (i.e., permanently ice-covered central Arctic Ocean, marginal seas with seasonally open-water conditions, polynyas, etc.) are still needed. Concerning the temporal applicability of IP₂₅ as paleo-sea-ice proxy, it has to be tested how old the sediment could be for using this approach. In our pilot study we could show that

IP₂₅ may occur in Arctic Ocean sediment as old as MIS 6, and STEIN & FAHL (2012) even found IP₂₅ in two million years old sediments from the Fram Strait area. The IP₂₅ approach can also be used for the reconstruction of sea-ice cover during glacials significantly older than MIS 2. However, what about Pleistocene, Neogene or even older sediments? In a few test measurements we carried-out on ACEX sediments of Eocene age, no IP₂₅ was found.

When interpreting IP₂₅ and PIP₂₅ records and comparing absolute numbers, determined in different studies and/or in material from different areas and with different sample storage times and temperature (i.e., old versus fresh material and deep-frozen versus storage under plus temperatures), possible differences in biomarker decomposition/degradation within the water column, at the seafloor and within the sediments as well as IP₂₅ losses during sample storage, have to be considered. Here, improved knowledge of production, degradation and preservation/burial of the IP₂₅ signal is urgently needed.

A correct identification of IP₂₅ in extracts by GC-MS and a correct quantification of IP₂₅, which requires some understanding of instrumental response factors between IP₂₅ and the internal standard, are essential in this approach (see BROWN 2011, MÜLLER et al. 2011, BELT et al. 2012a, 2012b, FAHL & STEIN 2012). In this context, an analytical standard protocol should be developed in order to allow a direct comparison of IP₂₅ data obtained in different laboratories.

The challenge of future scientific drilling

Considering the importance of the Arctic Ocean for the global ocean circulation and the climate system, more high-resolution paleoceanographic data sets from key areas are needed to reconstruct the climatically important parameters such as sea-ice cover – the major focus of this paper – but also sea-surface temperature, salinity, inflow of Atlantic Water, and river discharge. This kind of data sets going back beyond the time scale of direct measurements can be used to determine the natural variability of these parameters as a background for an assessment of anthropogenically influenced changes in the last 100 to 150 years. For studying the (sub-)millennial climate variability on longer time scales, i.e., under different boundary conditions during pre-Quaternary times, as well as for studying the long-term climate change from Greenhouse to Icehouse conditions during Mesozoic-Cenozoic times, however, new drill cores from the Arctic Ocean are needed (Fig. 26). That means, undisturbed and complete sedimentary sequences have to be drilled on depth transects across the major ocean ridge systems, i.e., the Lomonosov Ridge, the Alpha-Mendelev Ridge, and the Chukchi Plateau and Northwind Ridge. High-resolution records allowing to study climate variability on Milankovich and millennial to sub-millennial time scales can be drilled along the continental margins characterized by high sedimentation rates. Here, key areas are the Arctic Ocean marginal seas characterized by variable sea-ice cover and strong river discharge. Key location for studying the history of exchange of the Arctic Ocean with the world’s oceans are the Fram Strait, Yermak Plateau and Chukchi Plateau areas. Part of these drilling campaigns will hopefully become reality within the new phase of the International Ocean Discovery Program (IODP) post 2013 (COAKLEY & STEIN 2010, STEIN

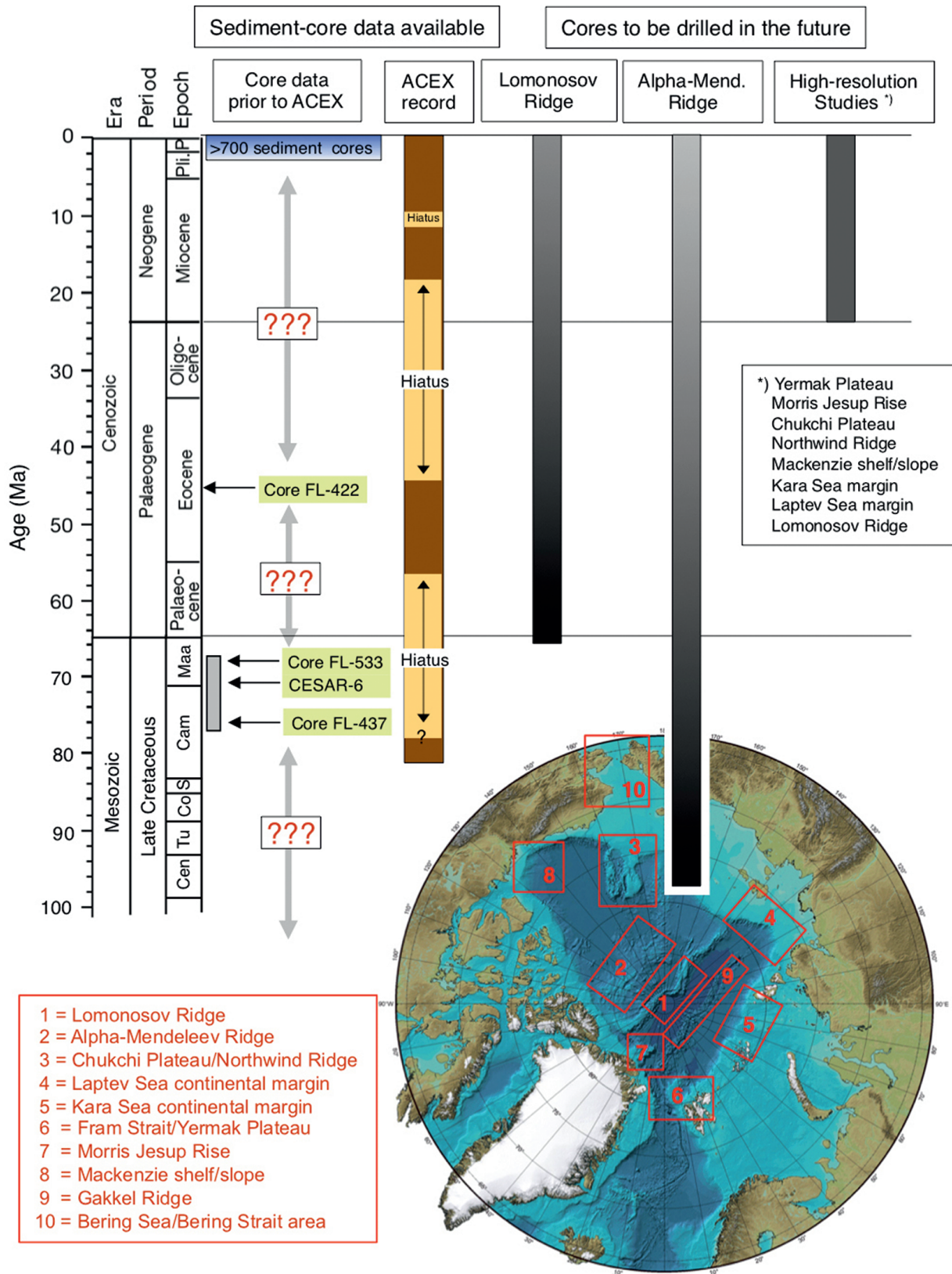


Fig. 26: Stratigraphic coverage of existing sediment cores in the central Arctic Ocean prior to IODP-ACEX (based on THIEDE et al. 1990) and the section recovered during the ACEX drilling expedition (BACKMAN et al. 2006, BACKMAN et al. 2008), and stratigraphic coverage and key areas for future scientific drilling campaigns in the Arctic Ocean. The middle Eocene sediments recovered at core FL-422 are arbitrarily placed at 45 Ma, the three Late Cretaceous (Maastrichtian/Campanian) cores are arbitrarily placed on the time axis as well. Each of these four cores (all recovered on Alpha Mendeleev Ridge) documents a time period of at the most a few hundred kyrs (BACKMAN et al. 2008). Figure from Stein (2011) and further references therein.

Abb. 26: Stratigraphie der bislang verfügbaren Sedimentkerne im Arktischen Ozean (ergänzt nach THIEDE et al. 1990) und Stratigraphie der ACEX-Bohrung (BACKMAN et al. 2008) sowie Stratigraphie und Lokationen möglicher zukünftiger wissenschaftlicher Bohrungen im Arktischen Ozean (aus STEIN 2011).

2011 and further references therein; for details see also New IODP Science Plan (BICKLE et al. 2012; also online available at <http://www.iodp.org/science-plan-for-2013-2023>).

ACKNOWLEDGMENTS

This paper focusses on the proxy reconstructions of the long- and short-term history of Arctic Ocean sea-ice cover, summarizing major aspects presented by the first author in an overview talk at the “20 year North Pole Anniversary Symposium” on 07 September 2011 at GEOMAR Kiel, Germany. On September 07, 1991, 10:35 UTC, the Swedish Icebreaker “Oden” (with Leif Anderson, Gothenburg University, as chief scientist) and the German Research Icebreaker “Polarstern” (with Dieter Fütterer, AWI Bremerhaven, as chief scientist) reached the North Pole as first non-nuclear powered surface vessels during their joint ARCTIC 91 Expedition. At the Symposium in Kiel, scientists and crewmembers from both ships convened, followed by a ferry trip from Kiel to Gothenburg with a joint social event onboard the ferry and in Gothenburg on September 07/08. We would like to thank especially Dieter Fütterer, main organizer of this North Pole Anniversary Event in Kiel and Gothenburg.

Many thanks goes to the three reviewers of this paper, to Matthias Forwick (Tromsø University), Jens Matthiessen (AWI Bremerhaven), and Matt O’Regan (Stockholm University), for numerous constructive suggestions improving the manuscript.

References

ACIA (2004): Impacts of a Warming Arctic: Arctic Climate Impact Assessment.- Cambridge University Press, Cambridge, 1-139, <http://www.acia.uaf.edu>

ACIA (2005): Arctic Climate Impact Assessment.- Cambridge University Press, 1-1042.

Alley, R.B., Mayewski, P.A., Sowers, T., Stuiver, M., Taylor, K.C., Clark, P.U. (1997): Holocene climatic instability: a prominent, widespread event 8200 yr ago.- *Geology* 25: 483-486

Andersen, E.S., Dokken, T.M., Elverhøi, A., Solheim, A., Fossen, I. (1996): Late Quaternary sedimentation and glacial history of the western Svalbard margin.- *Mar. Geol.* 133: 123-156.

Andersen, C., Koç, N., Jennings, A. & Andrews, J.T. (2004): Nonuniform response of the major surface currents in the Nordic Seas to insolation forcing: implications for the Holocene climate variability.- *Paleoceanography* 19: PA 2003.

Andersson, C., Risebrobakken, B., Jansen, E. & Dahl, S.O. (2003): Late Holocene surface ocean conditions of the Norwegian Sea (Vøring Plateau).- *Paleoceanography* 18(2): 1044.

Andreev, A.A. & Klimanov, V.A. (2000): Quantitative Holocene climatic reconstruction from Arctic Russia.- *J. Paleolimnol.* 24: 81-91.

Andrews, J.T., Helgadottir, G., Geirsdottir, A. & Jennings, A.E. (2001): Multi-century-scale records of carbonate (hydrographic?) variability on the northern Iceland margin over the last 5000 years.- *Quat. Res.* 56: 199-206.

Backman, J., Jakobsson, M., Frank, M., Sangiorgi, F., Brinkhuis, H., Stickley, C., O’Regan, M., Løvlie, R., Pälike, H., Spofforth, D., Gattaceca, J., Moran, K., King, J. & Heil, C. (2008): Age model and core-seismic integration for the Cenozoic Arctic Coring expedition sediments from the Lomonosov Ridge.- *Paleoceanography* 23: PA1S03.

Backman, J. & Moran, K. (2008): Introduction to special section on Cenozoic paleoceanography of the central Arctic Ocean.- *Paleoceanography* 23: PA1S01, doi: 10.1029/2007PA001516.

Backman, J., Moran, K., McInroy, D.B., Mayer, L.A., and the Expedition 302 Scientists (2006): Proceedings IODP, 302.- College Station, Texas (Integrated Ocean Drilling Program Management International, Inc.). doi:10.2204/iodp.proc.302.104.2006.

Barry, R.G. (1996): The parameterization of surface albedo for sea ice and its snow cover.- *Prog. Phys. Geogr.* 20: 63-79.

Bauch, H.A., Erlenkeuser, H., Spielhagen, R.F., Struck, U., Matthiessen, J., Thiede, J. & Heinemeier, J. (2001a): A multiproxy reconstruction of the evolution of deep and surface waters in the subarctic Nordic seas over the last 30,000 yr.- *Quat. Sci. Rev.* 20: 659-678.

Behrends, M. (1999): Reconstruction of sea-ice drift and terrigenous sediment supply in the Late Quaternary: heavy-mineral associations in sediments of the Laptev-Sea continental margin and the central Arctic Ocean.- *Reports Polar Res.* 310: 1-167.

Behrends, M., Hoops, E. & Peregovich, B. (1999): Distribution patterns of heavy minerals in Siberian rivers, the Laptev Sea and the eastern Arctic Ocean: an approach to identify sources, transport and pathways of terrigenous matter.- In: H. KASSENS, H. BAUCH, I. DMITRENKO, H. EICKEN, H.W. HUBBERTEN, M. MELLES, J. THIEDE & L. TIMOKHOV (eds), *Land-Ocean Systems in the Siberian: Dynamics and History*. Springer-Verlag, Heidelberg, 265-286.

Belt, S.T., Massé, G., Rowland, S.J., Poulin, M., Michel, C., LeBlanc, B. (2007): A novel chemical fossil of palaeo sea ice: IP₂₅.- *Org. Geochem.* 38: 16-27.

Belt, S.T., Massé, G., Vare, L.L., Rowland, S.J., Poulin, M., Sicre, M.-A., Sampei, M. & Fortier, L. (2008): Distinctive ¹³C isotopic signature distinguishes a novel sea ice biomarker in Arctic sediments and sediment traps.- *Mar. Chemistry* 112(3-4): 158-167.

Belt, S.T., Vare, L.L., Massé, G., Manners, H.R., Price, J.C., MacLachlan, S.E., Andrews, J.T. & Schmidt, S. (2010): Striking similarities in temporal changes to spring sea ice occurrence across the central Canadian Arctic Archipelago over the last 7000 years.- *Quat. Sci. Rev.* 29 (25-26): 3489-3504.

Belt, B.T., Brown, T.A., Cabedo Sanz, P. & Navarro Rodriguez, A. (2012): Structural confirmation of the sea ice biomarker IP₂₅ found in Arctic marine sediments.- *Environmental Chemistry Letters* DOI: 10.1007/s10311-011-0344-0.

Belt, B.T., Brown, T.A., Navarro Rodriguez, A., Cabedo Sanz, P., Tonkin, A. & Ingle, R. (2012b): A reproducible method for the extraction, identification and quantification of the Arctic sea ice proxy IP₂₅ from marine sediments.- *Analytical Methods*, DOI: 10.1039/c2ay05728j.

Bennike, O. (2004): Holocene sea-ice variations in Greenland: onshore evidence.- *The Holocene* 14: 607-613.

Berger, A. & Loutre, M.F. (1991): Insolation values for the climate of the last 10 million years.- *Quat. Sci. Rev.* 10: 297-317.

Bickle, M. et al. (eds) (2012): *Illuminating Earth’s Past, Present, and Future.- The International Ocean Discovery Program – Exploring the Earth under the Sea*. Science Plan for 2013-2023: 1-84.

Birgel, D. & Hass, C. (2004): Oceanic and atmospheric variations during the last deglaciation in the Fram Strait (Arctic Ocean): a coupled high-resolution organic-geochemical and sedimentological study.- *Quat. Sci. Rev.* 23: 29-47.

Birgel, D. & Stein, R. (2004): Northern Fram Strait und Yermak Plateau: distribution, variability and burial of organic carbon and paleoenvironmental implications.- In: R. STEIN & R.W. MACDONALD (eds), *The Organic Carbon Cycle in the Arctic Ocean*. Springer Verlag, Heidelberg, 279-295.

Birgel, D., Stein, R. & Hefter, J. (2004): Aliphatic lipids in recent sediments of the Fram Strait/Yermak Plateau (Arctic Ocean): composition, sources and transport processes.- *Mar. Chemistry* 88: 127-160.

Bischof, J.F., Clark, D.L. & Vincent, J.S. (1996): Pleistocene paleoceanography of the central Arctic Ocean: the sources of ice rafted debris and the compressed sedimentary record.- *Paleoceanography* 11: 743-756.

Bischof, J.F. & Darby, D.A. (1999): Quaternary ice transport in the Canadian Arctic and extent of late Wisconsinan glaciation in the Queen Elizabeth Islands.- *Can. J. Earth Sci.* 36: 2007-2022.

Boon, J.J., Rijpstra, W.I.C., de Leeuw, J.W., Yoshioka, M. & Shimizu, Y. (1979): The Black Sea sterols - A molecular fossil for dinoflagellate blooms.- *Nature* 277: 125-127.

Broecker, W.S. (1997): Thermohaline circulation, the Achilles heel of our climate system: will man-made CO₂ upset the current balance?- *Science* 278: 1582-1588.

Broecker, W.S. (2006): Was the Younger Dryas triggered by a flood?- *Science* 312: 1146-1148.

Broecker, W.S., Denton, G.H., Edwards, R.L., Cheng, H., Alley, R.B. & Putnam, A.E. (2010): Putting the Younger Dryas cold event into context.- *Quat. Sci. Rev.* 29: 1078-1081.

Broecker, W.S., Kennett, J.T., Flower, B.P., Teller, J.T., Trumbore, S., Bonani, G. & Wolfli, W. (1989): Routing of meltwater from the Laurentide Ice Sheet during the Younger Dryas cold episode.- *Nature* 341: 318-320.

Brown, T.A. (2011): Production and preservation of the Arctic sea ice diatom biomarker IP₂₅.- Petroleum and Environmental Geochemistry Group, School of Geophysics, Earth and Environmental Sciences, Plymouth, University of Plymouth, 1-291; <http://hdl.handle.net/10026.1/314>.

Carstens, J. & Wefer, G. (1992): Recent distribution of planktonic foraminifera in the Nansen Basin, Arctic Ocean.- *Deep-Sea Res.* 30: 507-524.

- Clark, D.L. & Hanson, A. (1983): Central Arctic Ocean sediment texture: A key to ice transport mechanism.- In: B.F. MOLNIA (ed), Glacial-marine sedimentation. Plenum Press, New York, 301-330.
- Clarke, G.K.C., Leverington, D.W., Teller, J.T. & Dyke, A.S. (2004): Paleohydraulics of the last outburst flood from glacial Lake Agassiz and the 8200 BP cold event.- *Quat. Sci. Rev.* 23(3-4): 389-407.
- Clark, P.U., Pisias, N.G., Stocker, T.F. & Weaver, A.J. (2002): The role of the thermohaline circulation in abrupt climate change.- *Nature* 415: 863-869.
- Coakley, B. & Stein, R. (2010): Arctic Ocean Scientific Drilling: the next frontier.- *Sci. Drilling* 9: 45-49; doi:10.2204/iodp.sd.9.09.2010.
- Colony, R. & Thorndike, A.S. (1985): Sea ice motion as a drunkard's walk.- *J. Geophys. Res.* 90: 965-974.
- Coxall, H.K., Wilson, P.A., Pälike, H., Lear, C.H. & Backman, J. (2005): Rapid stepwise onset of Antarctic glaciation and deeper calcite compensation in the Pacific Ocean.- *Nature* 433: 53-57.
- Cronin, T.M., Gemery, L., Briggs Jr., W.M., Jakobsson, M., Polyak, L. & Brouwers, E.M. (2010): Quaternary Sea-ice history in the Arctic Ocean based on a new Ostracode sea-ice proxy.- *Quat. Sci. Rev.* doi:10.1016/j.quascirev.2010.05.024.
- Cronin, T.M., Smith, S.A., Eynaud, F., O'Regan, M. & King, J. (2008): Quaternary paleoceanography of the central Arctic based on Integrated Ocean Drilling Program Arctic Coring Expedition 302 foraminiferal assemblages.- *Paleoceanography* 23: PA1S18. doi: 10.1029/2007PA001484.
- Crucifix, M., Loutre, M.-F., Tulkens, P., Fichefet, T. & Berger, A. (2002): Climate evolution during the Holocene: a study with an Earth system model of intermediate complexity.- *Climate Dyn.* 19: 43-60.
- Darby, D.A. (2003): Sources of sediment found in sea ice from the western Arctic Ocean, new insights into processes of entrainment and drift patterns.- *J. Geophys. Res.* 108, C8, 3257, doi:10.1029/2002JC001350.
- Darby, D.A. (2008): The Arctic perennial ice cover over the last 14 million years.- *Paleoceanography*, doi:10.1029/2007PA001479.
- Darby, D.A., Bischof, J.F. & Jones, G.A. (1997): Radiocarbon chronology of depositional regimes in the western Arctic Ocean.- *Deep-Sea Res. II* 44(8): 1745-1757.
- Darby, D.A., Bischof, J.F., Spielhagen, R.F., Marshall, S.A. & Herman, S.W. (2002): Arctic ice export events and their potential impact on global climate during the late Pleistocene.- *Paleoceanography* 17, doi: 10.1029/2001PA000639.
- De Angeles, H. & Kleman J. (2005): Palaeo-ice streams in the northern Keewatin sector of the Laurentide Ice Sheet.- *Annals Glaciol.* 42: 135-144.
- Dethleff, D. (2005): Entrainment and export of Laptev Sea ice sediments, Siberian Arctic.- *J. Geophys. Res.* 110(C07009). doi:10.1029/2004JC002740.
- Dethleff, D., Rachold, V., Tintelnot, T. & Antonow, M. (2000): Sea-ice transport of riverine particles from the Laptev Sea to Fram Strait based on clay mineral studies.- *Internat. J. Earth Sci.* 89: 496-502.
- Dickson, R.R., Osborn, T.J., Hurrell, J.W., Meincke, J., Blindheim, J., Adlandsvik, B., Vinje, T., Alekseev, G. & Maslowski, W. (2000): The Arctic Ocean response to the North Atlantic Oscillation.- *J. Clim.* 13(15): 2671-2696.
- Dokken, T.M. & Hald, M. (1996): Rapid climatic shifts during isotope stages 2-4 in the Polar North Atlantic.- *Geology* 24: 599-602.
- Dyke, A.S., Andrews, J.T., Clark, P.U., England, J.H., Miller, G.H., Shaw, J. & Veillette, J.J. (2002): The Laurentide and Innuitian ice sheets during the Last Glacial Maximum.- *Quat. Sci. Rev.* 21: 9-31.
- Dyke, A.S., England, J., Reimnitz, E. & Jetté, H. (1997): Changes in driftwood delivery to the Canadian Arctic archipelago: the hypothesis of postglacial oscillations of the Transpolar Drift.- *Arctic* 50: 1-16.
- Dyke, A.S., Hooper, J. & Savelle, J.M. (1996): A history of sea ice in the Canadian Arctic Archipelago based on postglacial remains of the bowhead whale (*Balaena mysticetus*).- *Arctic* 49: 235-255.
- Eicken, H., Gradinger, R., Graves, A., Mahoney, A. & Rigor, I. (2005): Sediment transport by sea ice in the Chukchi and Beaufort Seas: Increasing importance due to changing ice conditions?- *Deep-Sea Res. (II)* 52: 3281-3302.
- Eicken, H., Reimnitz, E., Alexandrov, V., Martin, T., Kassens, H. & Viehoff, T. (1997): Sea-ice processes in the Laptev Sea and their importance for sediment export.- *Cont. Shelf Res.* 17: 205-233.
- Eldrett, J.S., Harding, I.C., Wilson, P.A., Butler, E. & Roberts, A.P. (2007): Continental ice in Greenland during the Eocene and Oligocene.- *Nature*, doi:10.1038/nature05591.
- Elverhøi, A., Svensen, J.I., Solheim, A., Andersen, E.S., Milliman, J., Mangerud, J. & Hooke, R.L. (1995b): Late Quaternary sediment yield from the High Arctic Svalbard Area.- *J. Geol.* 103: 1-17.
- England, J.H., Lakeman, T.R., Lemmen, D.S., Bednarski, J.M., Stewart, T.G. & Evans, D.J.A. (2008): A millennial-scale record of Arctic Ocean sea ice variability and the demise of the Ellesmere Island ice shelves.- *Geophys. Res. Lett.* 35: xx-xx.
- Fahl, K. & Nöthig, E.-M. (2007): Lithogenic and biogenic particle fluxes on the Lomonosov Ridge (central Arctic Ocean) and their relevance for sediment accumulation: vertical vs. lateral transport.- *Deep-Sea Res. I*, 54(8): 1256-1272.
- Fahl, K. & Stein, R. (2012): Modern seasonal variability and deglacial / Holocene change of central Arctic Ocean sea-ice cover: new insights from biomarker proxy records.- *Earth Planet. Sci. Lett.*, doi: 10.1016/j.epsl.2012.07.009.
- Fahl, K. & Stein, R. (1999): Biomarkers as organic-carbon-source and environmental indicators in the Late Quaternary Arctic Ocean: "problems and perspectives"- *Mar. Chem.* 63: 293-309.
- Flower, B. & Kennett, J. (1995): Middle Miocene deepwater paleoceanography in the Southwest Pacific; relations with East Antarctic ice sheet development.- *Paleoceanography* 10: 1095-1112.
- Francis, J.A., Hunter, E., Key, J.R. & Wang, X. (2005): Clues to variability in Arctic minimum sea ice extent.- *Geophys. Res. Lett.* 32, L21501, doi:10.1029/2005GL024376.
- Frank M., Backman, J., Jakobsson, M., Moran, K., O'Regan, M., King, J., Haley, B., Kubik, P. & Garbe-Schönberg, D. (2008): Beryllium isotopes in central Arctic Ocean sediments over the past 12.3 million years: stratigraphic and paleoclimatic implications.- *Paleoceanography* 23: PA1S01, doi:10.1029/2007PA001478.
- Fronval, T. & Jansen, E. (1996): Late Neogene paleoclimates and paleoceanography in the Iceland Norwegian Sea: evidence from the Iceland and Vøring Plateaus.- In: J. THIEDE, A.M. MYHRE, J.V. FIRTH, G.L. JOHNSON, W.F. RUDDIMAN (eds), Proc. ODP, Sci. Results, 151, College Station, Texas (Ocean Drilling Program), 455-468.
- Funder, S., Kjør, K.H., Linderson, H., Lyså, A. & Olsen, J. (2009): Driftwood and Ice - a sketchy history of Holocene multiyear sea ice in the Arctic Ocean.- Third Conf. Arctic Paleoclimate and its Extremes. APEX, Copenhagen, Denmark, p. 27.
- Fütterer, D.K. (ed) (1994): The Expedition ARCTIC'93 Leg ARK IX/4 of RV "Polarstern" 1993.- *Reports Polar Res.* 149: 1-244.
- Gloersen, P.W. Campbell, J., Cavalieri, D.J., Comiso, J.C., Parkinson, C.L., Zwally, H.J. (1992): Arctic and Antarctic sea ice, 1978-1987: Satellite passive-microwave observations and analysis.- *NASA SP-511*, 1-290.
- Goosse, H., Driesschaert, E., Fichefet, T. & Loutre, M.-F. (2007): Information on the early Holocene climate constrains the summer sea ice projections for the 21st century.- *Climate of the Past Discussions* 2: 999-1020
- Groote, P.M., Stuiver, M., White, J.W.C., Johnsen, S. & Jouzel, J. (1993): Comparison of oxygen isotope records from the GISP2 and GRIP Greenland ice cores.- *Nature* 366: 552-554.
- Hald, M., Andersson, C., Ebbesen, H., Jansen, E., Klitgaard-Kristensen, D., Risebrobakken, B.R., Salomonsen, G.R., Sarntheim, M., Sejrup, H.P. & Telford, R.J. (2007): Variations in temperature and extent of Atlantic Water in the northern North Atlantic during the Holocene.- *Quat. Sci. Rev.* 26: 3423-3440.
- Hanslik, D., Jakobsson, M., Backman, J., Björck, S., Sellén, E., O'Regan, M., Fornaciari, E. & Skog, G. (2010): Quaternary Arctic Ocean sea ice variations and radiocarbon reservoir age corrections.- *Quat. Sci. Rev.* 29: 3430-3441.
- Hass, H.C. (2002): A method to reduce the influence of ice-rafted debris on a grain-size record from the northern Fram Strait, Arctic Ocean.- *Polar Res.* 21: 299-306.
- Hebbeln, D., Dokken, T., Andersen, E.S., Hald, M. & Elverhøi, A., (1994): Moisture supply for northern ice-sheet growth during the Last Glacial Maximum.- *Nature* 370: 357-360.
- Hebbeln, D. & Wefer, G. (1991): Effects of ice coverage and ice-rafted material on sedimentation in the Fram Strait.- *Nature* 350: 409-411.
- Hovland, M. (ed), 2001. The High-Arctic Drilling Challenge.- Final Report Arctic's Role in Global Change Program Planning Group (APPG), Ocean Drilling Program, 1-38.
- Israde-Alcántara, I., James L. Bischoff, J.L., Domínguez-Vázquez, G., Lid, H.-C., DeCarli, P.S., Bunch, T.E., Witke, J.H., Weaver, J.C., Firestone, R.B., West, A., Kennett, J.P., Mercer, C., Xie, S., Richman, E.K., Kinzie, C.R., Wendy S. & Wolbach, W.S. (2011): Evidence from central Mexico supporting the Younger Dryas extraterrestrial impact hypothesis.- *PNAS*, doi/10.1073/pnas.1110614109.
- Jakobsson, M., Løvlie, R., Al-Hanbali, H., Arnold, E., Backman, J. & Mörth, M. (2000): Manganese color cycles in Arctic Ocean sediments constrain Pleistocene chronology.- *Geology* 28: 23-26.
- Jakobsson, M., Løvlie, R., Arnold, E., Backman, J., Polyak, L., Knudsen, J. & Musatov, E. (2001) Pleistocene stratigraphy and paleoenvironmental variation from Lomonosov Ridge sediments, central Arctic Ocean.- *Global Planet. Change* 31: 1-22.
- Jakobsson, M., Macnab, R., Mayer, L., Anderson, R., Edwards, M., Hatcky, J., Schenke, H.-W. & Johnson, P. (2008): An improved bathymetric portrayal of the Arctic Ocean: Implications for ocean modeling and geological, geophysical and oceanographic analyses.- *Geophys. Res. Lett.* 35, L07602, doi:10.1029/2008GL033520.
- Jakobsson, M., Long, A., Ingolfsson, O., Kjør, K.H. & Spielhagen, R.F. (2010a): New insights on Arctic Quaternary climate variability from palaeo-records and numerical modelling.- *Quat. Sci. Rev.* 29: 3349-3358.
- Jakobsson, M., Nilsson, J., O'Regan, M., Backman, J., Löwemark, L., Dowdeswell, J.A., Mayer, L., Polyak, L., Colleoni, F., Anderson, L.G.,

- Björk, G., Darby, D., Eriksson, B., Hanslik, D., Hell, B., Marcussen, C., Sellén, E. & Wallin, A. (2010b): An Arctic Ocean ice shelf during MIS 6 constrained by new geophysical and geological data.- *Quat. Sci. Rev.* 29: 3505-3517.
- Jennings, A.E., Knudsen, K.L., Hald, M., Hansen, C.V. & Andrews, J.T. (2002): A mid-Holocene shift in Arctic sea-ice variability on the East Greenland Shelf.- *The Holocene* 12: 49-58.
- Jin, M., Deal, C., Lee, S.H., Elliott, S., Hunke, E., Maltrud, M. & Jeffery, N. (2012): Investigation of Arctic sea ice and ocean primary production for the period 1992–2007 using a 3-D global ice–ocean ecosystem model.- *Deep-Sea Res.* in press, doi: 10.1016/j.dsr2.2011.06.003.
- Jiang, H., Eiriksson, J., Schultz, M., Knudsen, K.L. & Seidenkrantz, M.S. (2005): Evidence for solar forcing of sea surface temperature on the North Icelandic Shelf during the late Holocene.- *Geology* 33: 73-76.
- Johannessen, O.M., Bengtsson, L., Miles, M.W., Kuzmina, S.L., Semenov, V.A., Alekseev, G.V., Nagurnyi, A.P., Zakharov, V.F., Bobylev, L.P., Pettersson, L.H., Hasselmann, K. & Cattle, H.P. (2004): Arctic climate change, observed and modelled temperature and sea-ice variability.- *Tellus* 56A: 328-341.
- Johannessen, O.M., Shalina, E.V. & Miles, M.W. (1999): Satellite evidence for an Arctic sea ice cover in transformation.- *Science* 286: 1937-1939.
- Johns, L., Wraige, E.J., Belt, S.T., Lewis, C.A., Masse, G., Robert, J.M. & Rowland, S.J. (1999): Identification of a C-25 highly branched isoprenoid (HBI) diene in Antarctic sediments, Antarctic sea-ice diatoms and cultured diatoms.- *Org. Geochem.* 30: 1471-1475.
- Johnsen, S.J., Dahl-Jensen, D., Gundestrup, N., Steffensen, J.P., Clausen, H.B., Miller, H., Masson-Delmotte, V., Sveinbjörnsdóttir, A.E. & White, J. (2001): Oxygen isotope and palaeotemperature records from six Greenland ice core stations: Camp Century, Dye-3, GRIP, GISP2, Renland and NorthGRIP.- *J. Quat. Sci.* 16: 299-307.
- Kerr, R.A. (2007): Is battered Arctic sea ice down for the count? - *Science* 318: 33-34.
- Kleiven, H.F., Kissel, C., Laj, C., Ninnemann, U.S., Richter, T.O. & Cortijo, E. (2008): Reduced North Atlantic Deep Water coeval with the glacial Lake Agassiz freshwater outburst.- *Science* 319: 60-64.
- Kleman, J. & Glasser, N.F. (2007): The subglacial thermal organisation (STO) of ice sheets.- *Quat. Sci. Rev.* 26: 585-597.
- Knies, J. & Gaina, C. (2008): Middle Miocene ice sheet expansion in the Arctic: views from the Barents Sea.- *Geochem. Geophys. Geosyst.* 9: Q02015, doi:10.1029/2007GC001824.
- Knies, J., Müller, C., Nowaczyk, N., Vogt, C. & Stein, R. (2000): A multiproxy approach to reconstruct the environmental changes along the Eurasian continental margin over the last 150 kyr.- *Mar. Geol.* 163: 317-344.
- Knies, J. & Stein, R. (1998): New aspects of organic carbon deposition and its paleoceanographic implications along the northern Barents Sea margin during the last 30,000 years.- *Paleoceanography* 13: 384-394.
- Knies, J., Vogt, C. & Stein, R. (1999): Late Quaternary growth and decay of the Svalbard-Barents-Sea Ice Sheet and paleoceanographic evolution in the adjacent Arctic Ocean.- *GeoMar. Lett.* 18: 195-202.
- Knies, J., Kleiber, H.P., Matthiessen, J., Müller, C. & Nowaczyk, N. (2001): Marine ice-rafted debris records constrain maximum extent of Saalian and Weichselian ice-sheets along the northern Eurasian margin.- *Global Planet. Change* 31: 45-64.
- Koç, N., Jansen, E. & Hafliðason, H. (1993): Paleoceanographic reconstructions of surface ocean conditions in the Greenland, Iceland and Norwegian seas through the last 14 ka based on diatoms.- *Quat. Sci. Rev.* 12: 115-140.
- Krause, G. (1969): Ein Beitrag zum Problem der Erneuerung des Tiefenwassers im Arkona-Becken.- *Kieler Meeresforsch.* 25: 268-271.
- Krylov, A.A., Andreeva, I.A., Vogt, C., Backman, J., Krupskaya, V.V., Griukurov, G.E., Moran, K. & Shoji, H. (2008): A Shift in heavy and clay mineral provenance indicates a Middle Miocene onset of a perennial sea-ice cover in the Arctic Ocean.- *Paleoceanography* 23: PA1S06, doi: 10.1029/2007PA001497.
- Kruglikova, S.B., Björklund, K.R., Hammer, Ø. & Anderson, O.R. (2009): Endemism and speciation in the polycystine radiolarian genus *Actinomma* in the Arctic Ocean: description of two new species *Actinomma georgii* n. sp. and *A. turidae* n. sp.- *Mar. Micropal.* 72: 26-48.
- Kwok, R. & Rothrock, D.A. (2009): Decline in Arctic sea ice thickness from submarine and ICESat records: 1958-2008.- *Geophys. Res. Lett.* 36: L15501, doi:10.1029/2009GL039035.
- Laskar, J., Robutel, P., Joutel, F., Gastineau, M., Correia, A.C.M. & Levrard, B. (2004): A long-term numerical solution for the insolation quantities of the Earth.- *Astronomy Astrophys.* 428: 261-285.
- Levi, B.G. (2000): The decreasing Arctic ice cover.- *Physics Today* Jan. 2000: 19-20.
- Lowenstein, T.K. & Demicco, R.V. (2006): Elevated Eocene atmospheric CO₂ and its subsequent decline.- *Science* 313: 1928.
- Macdonald, R.W., Sakshaug, E. & Stein, R. (2004): The Arctic Ocean: modern status and recent climate change.- In: R. STEIN & R.W. MACDONALD (eds), *The Organic Carbon Cycle in the Arctic Ocean*, Springer-Verlag, Berlin, 6-21.
- Mangerud, J., Dokken, T., Hebbeln, D., Heggen, B., Ingolfsson, O., Landvik, J.Y., Meydahl, V., Svendsen, J.I. & Vorren, T.O. (1998): Fluctuations of the Svalbard-Barents Sea ice sheet during the last 150,000 years.- *Quat. Sci. Rev.* 17: 11-42.
- Manighetti, B. & McCave, I.N. (1995): Late glacial and Holocene palaeocurrents through South Rockall Gap, NE Atlantic Ocean.- *Paleoceanography* 10: 611-626.
- Maslanik, J.A., Serreze, M.C. & Barry, R.G. (1996): Recent decreases in Arctic summer ice cover and linkages to atmospheric circulation anomalies.- *Geophys. Res. Lett.* 23: 1677-1680.
- Massé, G., Belt, S.T., Crosta, X., Schmidt, S., Snape, I., Thomas, D.N. & Rowland, S.J. (2011): Highly branched isoprenoids as proxies for variable sea ice conditions in the Southern Ocean. *Antarctic Science* 23, 487-498.
- Massé, G., Rowland, S.J., Sicre, M.-A., Jacob, J., Jansen, E. & Belt, S.T. (2008): Abrupt climate changes for Iceland during the last millennium: Evidence from high resolution sea ice reconstructions. *Earth Planet. Sci. Lett.* 269: 565-569.
- Matthiessen, J., Brinkhuis, H., Poulsen, N. & Smelror, M. (2009): *Dcahedrella martinheadii* Manum 1997 – a stratigraphically and paleoenvironmentally useful Miocene acritarch of the high northern latitudes.- *Micropaleontology* 55: 171-186.
- Matthiessen, J. & Knies, J. (2001): Dinoflagellate cyst evidence for warm interglacial conditions at the northern Barents Sea margin during marine oxygen isotope stage 5.- *J. Quat. Sci.* 16: 727-738.
- Matthiessen, J., Knies, J., Nowaczyk, N.R. & Stein, R. (2001): Late Quaternary dinoflagellate cyst stratigraphy at the Eurasian continental margin, Arctic Ocean: indications for Atlantic water inflow in the past 150,000 years.- *Global Planet. Change* 31: 65-86.
- Maurer, J. (2007): Atlas of the cryosphere.- Boulder, Colorado USA, Nation. Snow Ice Data Center, digital media; <http://nsidc.org/data/atlas/>.
- McManus, J.F., Francois, R., Gherardi, J.-M., Keigwin, L.D. & Brown-Lager, S. (2004): Collapse and rapid resumption of Atlantic meridional circulation linked to deglacial climate changes.- *Nature* 428: 834-837.
- Méheust, M., Stein, R. & Fahl, K. (2012): Deglacial-Holocene variability of sea ice and surface water temperature in the Bering Sea: reconstruction based on IP₂₅ and alkenone data.- *Geophys. Res. Abstracts* 14: EGU2012-3319-3, EGU General Assembly
- Miller, K.G., Mountain, G.S., Browning, J.V., Kominz, M., Sugarman, P.J., Christie-Blick, N., Katz, M.E. & Wright, J.D. (1998): Cenozoic global sea-level, sequences, and the New Jersey transect: results from coastal plain and slope drilling.- *Rev. Geophys.* 36: 569-601.
- Miller, G.H., Brigham-Grette, J., Alley, R.B., Anderson, L., Bauch, H.A., Douglas, M.S.V., Edwards, M.E., Elias, S.A., Finney, B.P., Fitzpatrick, J.J., Funder, S.V., Herbert, T.D., Hinzman, L.D., Kaufman, D.S., Macdonald, G.M., Polyak, L., Robock, A., Serreze, M.C., Smol, J.P., Spielhagen, R., White, J.W.C., Wolfe, A.P. & Wolff, E.W. (2010): Temperature and precipitation history of the Arctic.- *Quat. Sci. Rev.* 29: 1679-1715.
- Möller, P., Larsen, N.K., Kjær, K.H., Funder, S., Schomacker, A., Linge, H. & Fabel, D. (2010): Early to middle Holocene valley glaciations on northernmost Greenland.- *Quat. Sci. Rev.* doi:10.1016/j.quascirev.2010.06.044.
- Moran, K., Backman, J., Brinkhuis, H., Clemens, S.C., Cronin, T., Dickens, G.R., Eynaud, F., Gattacceca, J., Jakobsson, M., Jordan, R.W., Kaminski, M., King, J., Koc, N., Krylov, A., Martinez, N., Matthiessen, J., McInroy, D., Moore, T.C., Onodera, J., O'Regan, A.M., Pälike, H., Rea, B., Rio, D., Sakamoto, T., Smith, D.C., Stein, R., St. John, K., Suto, I., Suzuki, N., Takahashi, K., Watanabe, M., Yamamoto, M., Frank, M., Jokat, W. & Kristoffersen, Y. (2006): The Cenozoic palaeoenvironment of the Arctic Ocean.- *Nature* 441: 601-605.
- Müller, J., Massé, G., Stein, R. & Belt, S. (2009): Extreme variations in sea ice cover for Fram Strait during the past 30 ka.- *Nature Geoscience*. DOI: 10.1038/NNGEO665.
- Müller, J., Wagner, A., Fahl, K., Stein, R., Prange, M. & Lohmann, G. (2011): Towards quantitative sea ice reconstructions in the northern North Atlantic: a combined biomarker and numerical modelling approach.- *Earth Planet. Sci. Lett.* 306: 137-148.
- Müller, J., Werner, K., Stein, R., Fahl, K., Moros, M. & Jansen, E. (2012): Holocene cooling culminates in sea ice oscillations in Fram Strait.- *Quat. Sci. Rev.* 47: 1-14, doi:10.1016/j.quascirev.2012.04.024.
- Murton, J.B., Bateman, M.D., Dallimore, S.R., Teller, J.T. & Yang, Z. (2010): Identification of Younger Dryas outburst flood path from Lake Agassiz to the Arctic Ocean.- *Nature* 464: 740-743.
- Nesje, A., Matthews, J.A., Dahl, S.O., Berrisford, M.S. & Andersson, C. (2001): Holocene glacier fluctuations of Flatebreen and winter-precipitation changes in the Jostedalbreen region, western Norway, based on glaciolacustrine sediment records.- *The Holocene* 11: 267-280.
- Nghiem, S.V., Rigor, I.G., Perovich, D.K., Clemente-Colón, P., Weatherly, J.W. & Neumann, G. (2007): Rapid reduction of Arctic perennial sea ice.- *Geophys. Res. Lett.* 34, L19504, doi:10.1029/2007GL031138.

- NGRIP Members (2004): High-resolution record of Northern Hemisphere climate extending into the last interglacial period.- *Nature* 431: 147-151.
- Nørgaard-Pedersen, N., Mikkelsen, N., Lassen, S.J., Kristoffersen, Y. & Sheldon, E. (2007): Reduced sea ice concentrations in the Arctic Ocean during the last interglacial period revealed by sediment cores off northern Greenland.- *Paleoceanography* 22: PA1218.
- Nørgaard-Pedersen, N., Spielhagen, R.F., Erlenkeuser, H., Grootes, P.M., Heinemeier, J. & Knies, J. (2003): The Arctic Ocean during the Last Glacial Maximum: atlantic and polar domains of surface water mass distribution and ice cover.- *Paleoceanography* 18: 1-19.
- Nørgaard-Pedersen, N., Spielhagen, R.F., Thiede, J. & Kassens, H. (1998): Central Arctic surface ocean environment during the past 80,000 years.- *Paleoceanography* 13: 193-204. doi:10.1029/2006PA001283.
- Not, C. & Hillaire-Marcel, C. (2012): Enhanced sea-ice export from the Arctic during the Younger Dryas.- *Nature Communications* 3:647. Doi:10.1038/ncomms1658.
- Nürnberg, D., Wollenburg, I., Dethleff, D., Eicken, H., Kassens, H., Letzig, T., Reimnitz, E. & Thiede, J. (1994): Sediments in Arctic sea ice: implications for entrainment, transport and release.- In: J. THIEDE, T. VORREN & R.F. SPIELHAGEN (eds), *Mar. Geol.* 119: 185-214.
- Ogilvie, A.E.J. (1992): Documentary evidence for changes in the climate of Iceland AD 1500 to 1800.- In: R.S. BRADLEY & P.D. JONES (eds), *Climate since AD 1500*, London New York, 92-117.
- Ogilvie, A.E.J. & Jónsson, T. (2001): "Little ice Age" research: a perspective from Iceland.- *Clim. Change* 48: 9-52.
- O'Regan, M. (2011): Late Cenozoic paleoceanography of the central Arctic Ocean.- *IOP Conf. Series, Earth and Environmental Sci.* 14, doi:10.1088/1755-1315/14/1/012002.
- O'Regan, M., King, J., Backman, J., Jakobsson, M., Pälike, H., Moran, K., Heil, C., Sakamoto, T., Cronin, T., Jordan, R. (2008): Constraints on the Pleistocene chronology of sediments from the Lomonosov Ridge.- *Paleoceanography* 23: PA1S19.
- O'Regan, M., St. John, K., Moran, K., Backman, K., King, J., Haley, B.A., Jakobsson, M., Frank, M. & Röhl, U. (2010): Plio-Pleistocene trends in ice rafted debris on the Lomonosov Ridge.- *Quat. Internat.* 219: 168-176, doi:10.1016/j.quaint.2009.08.010.
- Pagani, M., Pedentchouk, N., Huber, M., Sluijs, A., Schouten, S., Brinkhuis, H., Sinninghe Damsté, J.S., Dickens, G.R. & the IODP Expedition 302 Scientists (2006): The Arctic's hydrologic response to global warming during the Palaeocene-Eocene thermal maximum.- *Nature* 442: 671-675.
- Parkinson, C.L., Cavalieri, D.J., Gloersen, P., Zwally, J.H., Comiso, J.C. (1999): Arctic sea ice extents, areas, and trends, 1978-1996.- *J. Geophys. Res.* 104: 20837-20856.
- Peltier, W.R. (2007): Rapid climate change and Arctic Ocean freshening.- *Geology* 35: 1147-1148.
- Pearson, P.N. & Palmer, M.R. (2000): Atmospheric carbon dioxide concentrations over the past 60 million years.- *Nature* 406: 695-699.
- Peltier, W.R., Vettoretti, G. & Stastna, M. (2006): Atlantic meridional overturning and climate response to Arctic Ocean freshening.- *Geophys. Res. Lett.* 33, doi:10.1029/2005GL025251.
- Pfirman, S.L., Colony, R., Nürnberg, D., Eicken, H. & Rigor, I. (1997): Reconstructing the origin and trajectory of drifting Arctic sea ice.- *J. Geophys. Res.* 102(C6): 12575-12586.
- Pfirman, S., Gascard, J.-C., Wollengurg, I., Mudie, P. & Abelmann, A. (1989): Particle-laden Eurasian Arctic sea ice: observations from July and August 1987.- *Polar Res.* 7: 59-66.
- Pflaumann, U., Sarntheim, M., Chapman, A.L., Funnell, B., Huels, M., Kiefer, T., Maslin, M., Schulz, H., Swallow, J., van, K.S., Vautravens, M., Vogel-sang, E. & Weinelt, M. (2003): Glacial North Atlantic sea-surface conditions reconstructed by GLAMAP 2000.- *Paleoceanography* 18: 1065, doi:10.1029/2002PA000774.
- Phillips, R.L. & Grantz, A. (1997): Quaternary history of sea ice and paleo-climate in the Amerasia Basin, Arctic Ocean, as recorded in the cyclical strata or Northwind Ridge.- *Geol. Soc. Amer. Bull.* 109: 1101-1115.
- Phillips, R.L. & Grantz, A. (2001): Regional variations in provenance and abundance of ice-rafted clasts in Arctic Ocean sediments: Implications for the configuration of Late Quaternary oceanic and atmospheric circulation in the Arctic. *Mar. Geol.* 172, 91-115.
- Poirier, A. & Hillaire-Marcel, C. (2011): Improved Os-isotope stratigraphy of the Arctic Ocean.- *Geophys. Res. Lett.* 38, doi: 10.1029/2011GL047953.
- Polyak, L., Alley, R.B., Andrews, J.T., Brigham-Grette, J., Cronin, T.M., Darby, D.A., Dyke, A.S., Fitzpatrick, J.J., Funder, S., Holland, M., Jennings, A.E., Miller, G.H., O'Regan, M., Saville, J., Serreze, M., St. John, K., White, J.W.C. & Wolff, E. (2010): History of sea ice in the Arctic. *Quat. Sci. Rev.* 29: 1757-1778.
- Polyak, L., Bischof, J., Ortíz, J., Darby, D., Channell, J., Xuan, C., Kaufman, D., Lovlie, R., Schneider, D. & Adler, R. (2009): Late Quaternary stratigraphy and sedimentation patterns in the western Arctic Ocean.- *Global Planet. Change* 68: 5-17.
- Polyak, L.V., Curry, W.B., Darby, D.A., Bischof, J. & Cronin, T.M. (2004): Contrasting glacial/interglacial regimes in the western Arctic Ocean as exemplified by a sedimentary record from the Mendeleev Ridge.- *Palaeogeogr. Palaeoclim. Palaeoecol.* 203: 73-93.
- Polyak, L.V., Darby, D.A., Bischof, J.F. & Jakobsson, M. (2007): Stratigraphic constraints on late Pleistocene glacial erosion and deglaciation of the Chukchi margin, Arctic Ocean.- *Quat. Res.* 67: 234-245.
- Polyakov, I.V., Johnson, M.A., Colony, R.L., Bhatt, U. & Alekseev, G.V. (2002): Observationally based assessment of polar amplification of global warming.- *Geophys. Res. Lett.* 29: 1878 (doi:10.2929/2002GL011111).
- Polyakov, I.V. & Johnson, M.A. (2000): Arctic decadal and interdecadal variability.- *Geophys. Res. Lett.* 27: 4097-4100.
- Poore, R.Z., Osterman, L., Curry, W.B. & Phillips, R.L. (1999): Late Pleistocene and Holocene meltwater events in the western Arctic Ocean.- *Geology* 27: 759-762.
- Rasmussen, T.L., Thomsen, E., Slubowska, M.A., Jessen, S., Solheim, A. & Kog, N. (2007): Paleoclimatological evolution of the SW Svalbard margin (76° N) since 20,000 ¹⁴C yr BP.- *Quat. Res.* 67: 100-114.
- Reimnitz, E., McCormick, M., McDougall, K. & Brouwers, E. (1993): Sediment export by ice rafting from a coastal polynya, Arctic Alaska, U.S.A.- *Arct. Alpine Res.* 25: 83-98.
- Reimnitz, E., McCormick, M., Bischof, J. & Darby, D. (1998): Comparing sea-ice sediment load with Beaufort Sea shelf deposits: is entrainment selective?- *J. Sed. Res.* 68: 777-787.
- Rigor, I.G., Wallace, J.M. & Colony, R. (2002): Response of sea ice to the Arctic Oscillation.- *J. Clim.* 15: 2648-2663.
- Rothrock, D.A., Yu, Y. & Maykut, G.A. (1999): Thinning of the Arctic sea-ice cover.- *Geophys. Res. Lett.* 26: 3469-3472.
- Rowland, S.J., Belt, S.T., Wraige, E.J., Massé, G., Roussakis, C. & Robert, J.-M. (2001): Effects of temperature on polyunsaturation in cytosolic lipids of *Haslea ostrearia*.- *Phytochemistry* 56: 597-602.
- Sachs, J.P., Pahnke, K., Smittenberg, P. & Zhang, Z. (2008): In: S. ELIAS (ed), *Encyclopedia of Quaternary Science*, Elsevier, Amsterdam, QUAT 00313.
- Sakshaug, E. (2004): Primary and secondary production in the Arctic Seas.- In: R. STEIN, R.W. MACDONALD (eds), *The organic carbon cycle in the Arctic Ocean*. Springer Verlag, Heidelberg, 57-82.
- Salonen, J.S., Seppö, H., Väiliranta, M., Jones, V.J., Self, A., Heikkilä, M., Kultti, S. & Yang, H. (2011): The Holocene thermal maximum and late-Holocene cooling in the tundra of NE European Russia. *Quat. Res.* 75: 501-511.
- Sarntheim, M., Pflaumann, U. & Weinelt, M. (2003a): Past extent of sea ice in the northern North Atlantic inferred from foraminiferal paleotemperature estimates.- *Paleoceanography* 18: 25-1 - 25-8.
- Sarntheim, M., van Kreveld, S., Erlenkeuser, H., Grootes, P.M., Kucera, M., Pflaumann, U., Schulz, M. (2003c): Centennial-to-millennial-scale periodicities of Holocene climate and sediment injections off the Barents shelf, 75° N.- *Boreas* 32: 447-461.
- Schlüter, M., Sauter, E.J., Schäfer, A. & Ritzrau, W. (2000): Spatial budget of organic carbon flux to the seafloor of the northern North Atlantic (60° N - 80° N).- *Global Biogeochem. Cycles* 14: 329-340.
- Serreze, M.C., Holland, M.M. & Stroeve, J. (2007): Perspectives on the Arctic's shrinking sea-ice cover.- *Science* 315: 1533-1536.
- Sicre, M.-A., Jacob, J., Ezat, U., Rousse, S., Kissel, K., Eiriksson, J., Knudsen, K.-L., Jansen, E., & Turon, J.L. (2008): Decadal variability of sea surface temperatures off North Iceland over the last 200 yrs.- *Earth Planet. Sci. Lett.* 268: 137-142.
- Smith, D. (1998): Recent increase in the length of the melt season of perennial Arctic sea ice.- *Geophys. Res. Lett.* 25: 655-658.
- Smith, W.O.Jr, Baumann, M.E.M., Wilson, D.L. & Alekseev, L. (1987): Phytoplankton biomass and productivity in the marginal ice zone of the Fram Strait during summer 1984.- *J. Geophys. Res.* 92: 6777-6786.
- Spielhagen, R.F., Baumann, K.-H., Erlenkeuser, H., Nowaczyk, N.R., Nørgaard-Pedersen, N., Vogt, C. & Weiel, D. (2004): Arctic Ocean deep-sea record of Northern Eurasian ice sheet history.- *Quat. Sci. Rev.* 23: 1455-1483.
- Spielhagen, R.F., Bonani, G., Eisenhauer, A., Frank, M., Frederichs, T., Kassens, H., Kubik, P.W., Mangini, A., Nørgaard-Pedersen, N., Nowaczyk, N.R., Schäper, S., Stein, R., Thiede, J., Tiedemann, R., Wahsner, M. (1997): Arctic Ocean evidence for Late Quaternary initiation of northern Eurasian ice sheets.- *Geology* 25: 783-786.
- Spielhagen, R.F., Erlenkeuser, H. & Siebert, C. (2005): History of freshwater runoff across the Laptev Sea (Arctic) during the last deglaciation.- *Global Planet. Change* 48: 187-207.
- St. John, K. (2008): Cenozoic ice-rafting history of the central Arctic Ocean: terrigenous sands on the Lomonosov Ridge.- *Paleoceanography* 23, doi:10.1029/2007PA001483.
- St. John, K. & Krissek, L.A. (2002): The late Miocene to Pleistocene ice-rafting history of southeast Greenland.- *Boreas* 31: 28-35.
- Stabeno, P. & Overland, J.E. (2001): Bering Sea shifts toward an earlier spring transition.- *EOS Transactions AGU* 82: 317, 32.
- Stein, R. (1986): Surface-water paleo-productivity as inferred from sediments

- deposited in oxic and anoxic deep-water environments of the Mesozoic Atlantic Ocean.- In: E.T. DEGENS et al. (eds), *Biochemistry of Black Shales*, *Mittel. Geol. Paläont. Inst. Univ. Hamburg* 60: 55-70.
- Stein, R. (1991): Organic carbon accumulation in Baffin Bay and paleoenvironment in High-Northern Latitudes during the past 20 m.y.- *Geology* 19: 356-359.
- Stein, R. (2008): Arctic Ocean sediments: processes, proxies, and paleoenvironment.- *Developments in Marine Geology*, Vol. 2, Elsevier, Amsterdam, 1-587.
- Stein, R. (2011): The great challenges in Arctic Ocean paleoceanography. *IOP Conf. Series Earth Environ. Sci.* 14, doi: 10.1088/1755-1315/14/1/012001.
- Stein, R. & Fahl, K. (1997): Scientific cruise report of the Arctic Expedition ARK-XIII/2 of RV "Polarstern" in 1997.- *Reports Polar Res.* 255: 1-235.
- Stein, R. & Fahl, K. (2012): Biomarker proxy IP25 shows potential for studying entire Quaternary Arctic sea-ice history.- *Org. Geochem.* doi: 10.1016/j.orggeochem.2012.11.005.
- Stein, R., Nam, S.-I., Schubert, C., Vogt, C., Fütterer, D. & Heinemeier, J. (1994a): The last deglaciation event in the eastern central Arctic Ocean. *Science* 264: 692-696.
- Stein, R., Schubert, C.J., Vogt, C. & Fütterer, D. (1994b): Stable isotope stratigraphy, sedimentation rates, and salinity changes in the Latest Pleistocene to Holocene eastern central Arctic Ocean.- *Mar. Geol.* 119: 333-355.
- Stein, R., Dittmers, K., Fahl, K., Kraus, M., Matthiessen, J., Niessen, F., Pirrung, M., Polyakova, Ye., Schoster, F., Steinke, T. & Fütterer, D.K. (2004): Arctic (Palaeo) river discharge and environmental change: evidence from Holocene Kara Sea sedimentary records.- *Quat. Sci. Rev.* 23: 1485-1511.
- Stein, R., Boucsein, B. & Meyer, H. (2006): Anoxia and high primary production in the Paleogene central Arctic Ocean: first detailed records from Lomonosov Ridge.- *Geophys. Res. Lett.* 33, L18606, doi: 10.1029/2006GL026776.
- Stein, R., Matthiessen, J. & Niessen, F. (2010a): Re-Coring at Ice Island T3 Site of Key Core FL-224 (Nautilus Basin, Amerasian Arctic): Sediment characteristics and stratigraphic framework.- *Polarforschung* 79: 81-96.
- Stein, R., Matthiessen, J., Niessen, F., Krylov, R., Nam, S. & Bazhenova, E. (2010b): Towards a better (litho-) stratigraphy and reconstruction of Quaternary paleoenvironment in the Amerasian Basin (Arctic Ocean).- *Polarforschung* 79: 97-121.
- Steinsund, P.I. & Hald, M. (1994): Recent calcium carbonate dissolution in the Barents Sea: Paleooceanographic applications.- *Mar. Geol.* 117: 303-316.
- Stickley, C.E., John, K.S., Koc, N., Jordan, R.W., Passchier, S., Pearce, R.B. & Kearns, L.E. (2009): Evidence for middle Eocene Arctic sea ice from diatoms and ice-rafted debris.- *Nature* 460: 376-380.
- Stroeve, J., Holland, M.M., Meier, W., Scambos, T. & Serreze, M. (2007): Arctic sea ice decline: faster than forecast.- *Geophys. Res. Lett.* 34, L09501, doi:10.1029/2007GL029703.
- Sudgen, D. (1982): Arctic and Antarctic - A modern geographical synthesis. Blackwell Publ., Oxford, 1-472.
- Svensen, J.I., Alexanderson, H., Astakhov, V.I., Demidov, I., Dowdeswell, J.A., Funder, S., Gataullin, V., Henriksen, M., Hjort, C., Houmark-Nielsen, M., Hubberten, H.-W., Ingólfsson, O., Jakobsson, M., Kjær, K.H., Larsen, E., Lokrantz, H., Lunkka, J.P., Lyså, A., Mangerud, J., Matushkov, A., Murray, A., Möller, P., Niessen, F., Nikolskaya, O., Polyak, L., Saarnisto, M., Siegert, C., Siegert, M.J., Spielhagen, R.F. & Stein, R. (2004): Late Quaternary ice sheet history of Northern Eurasia.- *Quat. Sci. Rev.* 23: 1229-1272.
- Tarasov, L. & Peltier, W.R. (2005): Arctic freshwater forcing of the Younger Dryas cold reversal.- *Nature* 435: 662-665.
- Teller, J.T., Leverington, D.W. & Mann, J.D. (2002): Freshwater outbursts to the oceans from glacial Lake Agassiz and their role in climate change during the last deglaciation.- *Quat. Sci. Rev.* 21: 879-887.
- Thiede, J., Clark, D.L. & Hermann, Y. (1990): Late Mesozoic and Cenozoic paleoceanography of the northern polar oceans.- In: *The Geology of North America*, Vol. L, The Arctic Ocean Region, 427-458.
- Thiede, J., Janssen, C., Knutz, P., Kuijpers, A., Mikkelsen, N., Nørgaard-Pedersen, N. & Spielhagen, R.F. (2011): Millions of years of Greenland ice sheet history recorded in ocean sediments.- *Polarforschung* 80: 141-159.
- Thiede, J., Winkler, A., Wolf-Welling, T., Eldholm, O., Myhre, A., Baumann, K.-H., Henrich, R. & Stein, R. (1998): Late Cenozoic history of the polar North Atlantic: results from ocean drilling.- In: A. ELVERHØI, J. DOWDESWELL, S. FUNDER, J. MANGERUD & R. STEIN (eds), *Glacial and Oceanic History of the Polar North Atlantic Margins*. *Quat. Sci. Rev.* 17: 185-208.
- Thomas, E. (2008): Descent into the Icehouse.- *Geology* 36: 191-192.
- Thorndike, A.S. (1986): Kinematics of sea ice.- In: N. UNTERSTEINER (ed), *The Geophysics of Sea Ice*, *Nato ASI Ser. B Physics* 146: 489-549.
- Tripati, A., Backman, J., Elderfield, H. & Ferretti, P. (2005): Eocene bipolar glaciation associated with global carbon cycle changes.- *Nature* 436: 341-346.
- Tripati, A.K., Eagle, R.A., Morton, A., Dowdeswell, J.A., Atkinson, K.L., Bahé, Y., Dawber, C.F., Khadun, E., Shaw, R.M.H., Shorttle, O. & Thanabalasundaram, L. (2008): Evidence for glaciation in the Northern Hemisphere back to 44 Ma from ice-rafted debris in the Greenland Sea.- *Earth Planet. Sci. Lett.* 265: 112-122.
- Vare, L.L., Massé, G. & Belt, S.T. (2010): A biomarker-based reconstruction of sea ice conditions for the Barents Sea in recent centuries.- *The Holocene*, doi:10.1177/0959683609355179.
- Vare, L.L., Massé, G., Gregory, T.R., Smart, C.W. & Belt, S.T. (2009): Sea ice variations in the central Canadian Arctic Archipelago during the Holocene. *Quat. Sci. Rev.* 28: 1354-1366.
- Vinje, T., Nordlund, N. & Kvambekk, A. (1998): Monitoring ice thickness in Fram Strait.- *J. Geophys. Res.* C 103:10437-10449.
- Vinnikov, K.Ya., Robock, A., Stouffer, R.J., Walsh, J.E., Parkinson, C.L., Cavalieri, D.J., Mitchell, J.F.B., Garrett, D. & Zakharov, V.F. (1999): Global warming and Northern Hemisphere sea ice extent.- *Science* 286: 1934-1936.
- Vogt, C. (1997): Regional and temporal variations of mineral assemblages in Arctic Ocean sediments as climatic indicator during glacial/interglacial changes.- *Report. Polar Res.* 251: 1-309.
- Vogt, C. (2004): Mineralogy of sediment core PS2185-6.- PANGAEA, doi:10.1594/PANGAEA.138270
- Volkman, J.K. (1986): A review of sterol markers for marine and terrigenous organic matter.- *Org. Geochem.* 9: 83-99.
- Volkman, J.K. (2006): Lipid markers for marine organic matter.- In: J.K. VOLKMAN (ed), *Handbook of Environmental Chemistry*. Springer-Verlag, Berlin, Heidelberg, 27-70.
- Wahsner, M., Müller, C., Stein, R., Ivanov, G., Levitan, M., Shelekova, E. & Tarasov, G. (1999): Clay mineral distributions in surface sediments from the central Arctic Ocean and the Eurasian continental margin as indicator for source areas and transport pathways: a synthesis.- *Boreas* 28: 215-233.
- Wassmann, P., Bauerfeind, E., Fortier, M., Fukuchi, M., Hargrave, B., Moran, B., Noji, T., Nöthig, E.M., Olli, K., Peinert, R., Sasaki, H. & Shevchenko, V.P. (2004): Particulate organic carbon flux to the Arctic Ocean seafloor.- In: R. STEIN & R.W. MACDONALD (eds), *The Organic Carbon Cycle in the Arctic Ocean*, Springer Verlag, Heidelberg, 101-138.
- Wassmann, P. (2011): Arctic marine ecosystems in an era of rapid climate change.- *Progress Oceanogr.* 90: 1-17.
- Weller, P. & Stein, R. (2008): Paleogene biomarker records from the central Arctic Ocean (IODP Expedition 302): organic-carbon sources, anoxia, and sea-surface temperature.- *Paleoceanography* 23, PA1S17, doi:10.1029/2007PA001472.
- Wheeler, P.A., Gosselin, M., Sherr, E., Thiebault, D., Benner, R. & Whitedge, T.E. (1996): Active cycling of organic carbon in the central Arctic Ocean.- *Nature* 380: 697-699.
- Winkelmann, D., Schäfer, C., Stein, R. & Mackensen, A. (2008): Terrigenous events and climate history of the Sophia Basin, Arctic Ocean.- *Geochem. Geophys. Geosyst.* 9, doi:10.1029/2008GC002038.
- Wolf, T.C.W. & Thiede, J. (1991): History of terrigenous sedimentation during the past 10 m.y. in the North Atlantic (ODP Legs 104, 105, and DSDP 81).- *Mar. Geol.* 101: 83-102.
- Wolf-Welling, T.C.W., Cremer, M., O'Connell, S., Winkler, A. & Thiede, J. (1996): Cenozoic Arctic gateway paleoclimate variability: indications from changes in coarse-fraction compositions (ODP Leg 151).- In: J. THIEDE, A.M. MYHRE, J. FIRTH et al., *Proceedings ODP, Sci. Results* 151, College Station, Texas (Ocean Drilling Program) 515-525.
- Wollenburg, J.E., Knies, J. & Mackensen, A. (2004): High-resolution paleo-productivity fluctuations during the past 24 kyr as indicated by benthic foraminifera in the marginal Arctic Ocean.- *Palaeogeogr. Palaeoclimatol. Palaeoecol.* 204: 209-238.
- Wollenburg, J.E., Kuhnt, W. & Mackensen, A. (2001): Changes in Arctic Ocean palaeoproductivity and hydrography during the last 145 kyr: the benthic foraminiferal record.- *Paleoceanography* 16: 65-77.
- Wright, J.D., Miller, K.G. & Fairbanks, R.G. (1992): Early and middle Miocene stable isotopes: implications for deep water circulation and climate.- *Paleoceanography* 7: 357-389.
- Wüst, G. & Brögmus, W. (1955): Ozeanographische Ergebnisse einer Untersuchungsfahrt mit Forschungskutter "Südfall" durch die Ostsee Juni/Juli 1954 (anlässlich der totalen Sonnenfinsternis auf Öland).- *Kieler Meeresforsch.* 11: 3-21.
- Xiao, X., Fahl, K. & Stein, R. (2012): Modern spatial (seasonal) variability in sea ice cover of the Kara and Laptev seas: reconstruction from new biomarker data determined in surface sediments. *Quat. Sci. Rev.*, submitted.
- Zachos, J., Pagani, M., Sloan, L., Thomas, E. & Billups, K. (2001): Trends, rhythms, and aberrations in global climate 65 Ma to Present.- *Science* 292: 868-693.
- Zachos, J.C., Dickens, G.R. & Zeebe, R.E. (2008): An early Cenozoic perspective on greenhouse warming and carbon-cycle dynamics.- *Nature* 451: 281-283.